Design, fabrication and evaluation of an online intelligent machine for trout beheading and gutting

March 2021

Electronic Engineering Doctoral Program

Department of Mechanical Engineering of Agricultural Machinery

Author: Hossein Azarmdel[a,b]

Supervisors: Alfredo Rosado Munoz[a]; Seyed Saeid Mohtasebi[b]

Advisors: Ali Jafary[b]; Hossein Behfar[c]

a: Department of Electronics Engineering -University of Valencia-Spain

b: Department of Mechanical Engineering of Agricultural Machinery-University of Tehran-Iran

c: Department of Biosystems engineering-University of Tabriz-Iran

Abstract

Today, due to the increase of industrial automation, the need to design and manufacture automated devices with high capabilities in the fish and aquaculture industries is felt obviously. Considering the importance of trout consumption in the food basket and increasing the production efficiency with high quality, designing and developing the systems with higher capabilities compared to previous types is essential. Due to the slippery skin of the fish and the low friction coefficient, it is difficult to control the fish while processing. Since the fish processing operation is done step by step, in addition to providing fish stability, it is necessary that the grippers enable simultaneous operations along the system. Therefore, an automatic system with the ability of belly cutting, beheading, gutting and cleaning stages on different trout sizes is designed and manufactured based on the fish dimensions and cutting point extraction using machine vision. To reach the optimal system, the final model was simulated in Adams software. By performing the simulation, all the necessary forces and torques of the motors and pneumatic jacks were extracted at three input rates of four, seven and 10 fish per minute. To enable the system to process the fish in all capacities, the motors and pneumatic jacks were selected based on the maximum working capacity. Under these conditions, the maximum required force to provide this speed calculated as 332.45 N. Also in the belly cutting subsystem, the required torque for the stepper motor resulted in 1.79-2.145 Nm. The maximum required torque for the gutting stepper motor was calculated as 0.69 Nm in tested processing capacities (4, 7, and 10 fish per minute). The maximum required force of the cleaning jack resulted in 38.76 N. In order to extract the cutting points, the position of the fish fins was extracted by machine vision. To justify the processing method in the fin detection stage the identification of the fin regions resulted in 86.54%, 99.96% and 99.87 for sensitivity, specificity and total accuracy, respectively. By correcting the possible errors, the cutting points (fins) were identified in all fish samples. The controlling algorithm was written in TIA portal software compiled on the programmable logic control (PLC). Thus, the extracted data was sent to the controlling unit using the TCP/IP protocol for precise fish processing.

Keywords: trout; fish cleaning machine; image processing; fish processing; machine automation

Table of Contents

Tabla de contenido

Summary

Resumen

La clasificación y procesado de pescado empleando máquinas automáticas reduce costes e incrementa el volumen de procesado. Después de su llegada a los mercados de distribución mayorista y minorista, el tamaño de los ejemplares suele ser muy variado para la mayoría de las especies (trucha, caballa, dorada, lubina, etc.). Debido a ello, la limpieza y corte de pescado se realiza habitualmente de forma manual. Este proceso involucra diferentes pasos y a menudo se corta en función de la demanda del usuario: sin cabeza, sin vísceras, sin cabeza ni vísceras, fileteado, etc.

Combinando diferentes elementos tecnológicos, hoy en día es posible el desarrollo de sistemas automáticos capaces de mejorar los procesos de corte de pescado y el número de unidades procesadas. En cambio, las máquinas automáticas existentes actualmente son muy complejas y costosas, estando únicamente al alcance de las grandes empresas. La disponibilidad de máquinas automáticas en los pequeños mercados o comercio minorista facilitará el procesado de pescado que se sirve a los clientes, reduciendo el tiempo de espera para el cliente, con mayor calidad en el producto entregado y facilitando el consumo de pescado para la población.

Debido a la piel escurridiza del pescado, que posee un bajo coeficiente de fricción, la sujeción del pescado para la ejecución de los procesos de corte y limpieza es una labor que debe realizarse cuidadosamente y con sistemas de agarre específicamente diseñados. Este sistema de agarre debe sujetar el pescado a lo largo de todo el proceso y permitir la actuación de las diferentes herramientas, así como permitir el agarre de piezas de diferente tamaño. Este trabajo realiza la investigación necesaria para el adecuado procesamiento de la trucha (*Oncorhynchus mykiss),* perteneciente a la familia de los salmónidos.

Para permitir que la máquina propuesta se adapte a diferentes tamaños en las piezas de pescado, es necesario un sistema de visión artificial junto con los adecuados algoritmos para obtener las medidas fisiológicas de cada pieza y así poder establecer los puntos de actuación de las herramientas de corte y limpieza. El análisis del pescado se realiza en movimiento mientras éste circula por la máquina, siendo analizado antes de su llegada al primer punto de corte para poder realizar su aplicación en los puntos extraídos por el algoritmo.

Adicionalmente, todo el proceso debe ser controlado por un sistema integral de automatización. El sistema será responsable de sincronizar el sistema de visión, el algoritmo de extracción de puntos característicos, la actuación de los elementos de corte y limpieza, así como de gestionar los sistemas de seguridad para evitar que el operario pueda dañarse durante el manejo de la máquina.

1.1. Objetivos

El principal objetivo de esta Tesis Doctoral es el de diseñar, fabricar y evaluar una máquina automática para la limpieza y corte de truchas. La investigación se llevará a cabo en diferentes campos, con el objetivo de alcanzar los siguientes resultados:

1. Diseñar y fabricar todos los elementos mecánicos del Sistema, incluyendo el chasis, pinzas, elementos de corte y limpieza.
2. Diseño de elementos eléctricos y programación de los equipos de automatización para el control del sistema de visión artificial y las herramientas de corte y limpieza.
3. Desarrollar un algoritmo para adquirir, procesar y extraer los puntos de actuación de las herramientas en función de las características morfológicas de cada pieza de pescado.
4. Evaluar el correcto funcionamiento de los algoritmos y sistemas de corte y limpieza. Se emplearán elementos comparativos para establecer la precisión del sistema desarrollado.
5. Evaluar el tiempo de respuesta de los algoritmos para establecer una valoración de la velocidad máxima de procesado de pescado en función de la velocidad de los sistemas de actuación mecánica y el tiempo necesario por el algoritmo para obtener los puntos característicos.
6. Evaluar la calidad final del pescado procesado, con especial atención en la adecuada eliminación de los elementos indeseados (cabeza, vísceras, etc.) así como en la reducción al máximo en la eliminación de zonas útiles habitualmente comestibles y que en caso de eliminarse causarían pérdidas indeseadas.

De forma general, la máquina propuesta consiste en las siguientes partes y subsistemas:

1. Cámara de visión y cámara oscura para control de iluminación en la adquisición de imágenes.
2. Diseño del chasis de la máquina, en acero inoxidable para las partes en contacto con el agua y zonas húmedas, y en acero pintado para el resto de la estructura.
3. Sistema de transporte individualizado de piezas con el empleo de pinzas de agarre.
4. Sistema de corte y limpieza de vísceras, compuesto del sistema rotativo de corte y su motor eléctrico de giro, sistema de motor paso a paso para el control preciso de movimiento, y elementos mecánicos necesarios.
5. Sistema de corte de cabeza, con sistema neumático, cuchillas rotativas y sus elementos mecánicos.
6. Sistema de limpieza del pescado. Tras el corte, es necesaria la limpieza para eliminar restos de partes no deseadas que puedan haber quedado.
7. Sistemas de eliminación de las partes cortadas y extraídas del pescado, utilizando sistemas de succión por aire y aplicación de agua para limpieza.
8. Diseño del sistema neumático necesario para los elementos que funcionan con aire comprimido.
9. Elementos de automatización y control para el funcionamiento sincronizado de la máquina.

A lo largo de este documento se detallan todos los elementos diseñados, cálculos que apoyan la validez de las propuestas, y su verificación experimental tanto a nivel mecánico, eléctrico y algorítmico.

1.2. Metodología

El proceso investigativo de esta Tesis Doctoral se ha dividido en función de los elementos que deben componer la máquina, partiendo de un análisis morfológico de la especie de pescado a la que se destinará su uso (trucha). Una vez realizado el análisis, se obtienen las necesidades de la máquina a diseñar y, por tanto, se procederá a la definición de los elementos necesarios y al desarrollo pormenorizado de cada una de las partes.

1.2.1. Análisis inicial de muestras.

Se tomó una muestra de 97 piezas de trucha de modo que fuesen lo más variadas en

peso, tamaño y forma. Así, las muestras varían entre 262 g y 622 g, con promedio y desviación estándar de 421,88±78,04 g.

El chasis de la máquina fue diseñado en función de los elementos que debe soportar para el procesado del pescado según la propuesta realizada en este trabajo. Este chasis se fabricó con tubos cuadrados de acero de 40×40 mm (grosor de 2 mm), y acero inoxidable para los elementos más cercanos a la actuación sobre el pescado y en contacto más directo con el agua. Se diseñó un chasis de 2.8 m de longitud, 0.85 m de altura y 0.7 m de anchura. En la parte inferior del chasis se ubican las poleas de transporte para el canal de circulación de las piezas de pescado, incluyendo estabilizadores y elementos de ajuste fino para que el canal de transporte esté ajustado y con un funcionamiento suave longitudinal y transversal, permitiendo asimismo ligeras correcciones en caso de desajuste.

Una vez establecidos los parámetros de diseño y ya construidas algunas partes de la máquina (previamente diseñadas en el software CATIA), se emplearon 100 piezas de pescado para verificar el adecuado funcionamiento del canal de transporte. Las piezas de pescado se colocaron en el canal en forma de V con el pecho hacia arriba para verificar el sistema de arrastre. Tras la verificación, algunos elementos fueron rediseñados y ajustados (cadena de transporte, tamaño de piñones, poleas). Es necesario considerar que la pieza de pescado debe circular a través de las diferentes etapas de proceso, correctamente sujeta y sin interferir la acción de estos elementos móviles de procesado (corte y limpieza de determinadas zonas en la pieza de pescado). Por ello, se decidió realizar el agarre de la pieza de pescado por la cola. El sistema de transporte consta principalmente de las siguientes partes:

1. Pinza de agarre de pescado.
2. Canal de transporte de pescado que incluye las pinzas de agarre distribuidas a lo largo de la misma.

La longitud del canal o cinta de transporte se diseñó teniendo en cuenta el tamaño de los elementos de actuación (subsistemas de proceso) y la cantidad de piezas por minuto que es posible procesar, de modo que cada uno de los procesos pueda actuar simultáneamente sobre diferentes piezas de pescado. La distancia entre dos pinzas se diseñó de modo que fuese mayor que el tamaño máximo de pieza (en su longitud); en

concreto, cinco pinzas se distribuyen a lo largo del canal de transporte. El canal de transporte es rotativo, arrastrando una pieza cuando circula por la parte superior (avance) y vacío en su circulación por la parte inferior para agarrar una nueva pieza cuando comienza de nuevo su circulación por la parte superior. En este momento, las pinzas de agarre se cierran para sujetar una pieza de pescado por su cola y desplazarla para aplicar los diferentes pasos de proceso: adquisición de imágenes para obtención de puntos de actuación, corte de estómago, corte de cabeza, extracción de vísceras, etc.

1.3. Diseño mecánico

1.3.1. Subsistema de corte en vientre

La principal función de este subsistema es la realización de una incisión longitudinal en el vientre del pescado, comenzando en la aleta anal y terminando en la aleta pectoral.

1.3.2. Subsistema de corte de cabeza

Dado que la pieza de pescado está continuamente en movimiento, el sistema de corte de cabeza se diseña de modo que el corte sea preciso, rápido, y sincronizado con el movimiento del pescado sobre la cinta de transporte. Para ello, se ha diseñado un sistema neumático que permite una rápida actuación (subida/bajada) del cortador, variable en función de la velocidad de la cinta de transporte de piezas. El diseño analiza la velocidad de funcionamiento.

Se proponen y analizan dos diseños de corte de cabeza:

1. Cuchilla en forma de V para poder aplicar suficiente fuerza que produzca el corte de cabeza por presión, sin necesidad de giro de las mismas.
2. Dos cuchillas rotativas girando en dirección opuesta y en forma de V también, de modo que no es necesaria una gran fuerza de actuación pues el giro facilita el corte.

Para el diseño de las cuchillas, se considera un grosor suficiente de las mismas para soportar las fuerzas ejercidas durante el corte, pero también deben ser afiladas para un corte limpio y preciso. Para el sistema rotativo, se analizan diferentes velocidades de giro.

1.3.3. Subsistema de extracción de estómago, intestinos y vísceras

El objetivo de esta etapa de procesado es la extracción de las partes no comestibles del pescado: estómago, vísceras, tripas, etc. Dado que en una etapa anterior ya se realizó una incisión en esta parte, la extracción se realiza mediante unos tubos de succión que contactan con el pescado en esta zona. En concreto, este sistema se ha diseñado con varios tubos de succión que actúan sobre el pescado mediante un motor paso a paso en función del tamaño de éste (previamente determinado a través del sistema de visión). Con el giro del motor en sentido horario, se acciona un tubo estrecho, y un tubo más grande para piezas de mayor tamaño, con el accionamiento del sistema en sentido antihorario. Ello es posible con un diseño de piñón y engranajes que se describe en detalle. En el momento en el que un sensor detecta el tubo de succión cerca de la pieza, se activan las válvulas de aire de modo que se produzca la succión de los elementos extraídos del pescado.

Este diseño permite evitar posibles daños de los tubos de succión sobre las zonas útiles del pescado que idealmente deben permanecer sin dañarse. Además, para evitar colisión con el pescado, el tubo que no actúa se posiciona de modo que no colisione con el pescado. Este diseño permite emplear un único motor para ambos tubos, reduciendo costes y complejidad del sistema.

1.3.4. Subsistema de limpieza de la cavidad visceral

Este sistema tiene como objetivo la eliminación de restos viscerales y el material que pueda haber quedado adherido a la espina del pescado. En función de la longitud del pescado y más concretamente, del tamaño entre la aleta anal y pectoral, el tiempo de actuación de esta herramienta sobre el pescado es variable.

1.4. Simulación, análisis cinético y estimación de fuerzas realizadas por los motores y dispositivos mecánicos

Una vez realizado el diseño mecánico es necesaria la elección de los motores y elementos neumáticos. Para ello, se calculan las fuerzas que deben soportar los elementos de la máquina, y más concretamente, las fuerza que debe realizar cada motor para así poder seleccionar su potencia. También se realiza un estudio sobre la velocidad de giro necesaria

para cada motor.

Dado que existen numerosas piezas cuyas fuerzas interaccionan entre ellas, el proceso puede resultar complejo. Inicialmente se define el peso de cada pieza y se estiman las velocidades relativas entre ellas para calcular numéricamente las fuerzas de acción y reacción. Este cálculo se hace más complejo cuantas más piezas están relacionadas entre sí, con lo que se analizan unos casos con un número reducido de elementos relacionados entre sí. Para mejorar la estimación de fuerzas se hace uso del software Adams 2017 que permite el diseño dinámico de sistemas multipieza y proporciona estimaciones para el sistema en su conjunto. Para llevar a cabo la simulación es necesario importar el diseño desde CATIA y definir cuidadosamente cada una de las piezas así como los rangos de movimiento, peso, y en general, las condiciones de trabajo de la máquina, tanto rotacionales como traslacionales.

Para cada subsistema se consideran cuatro etapas en su ciclo de movimientos, definiendo todos los parámetros para cada una de ellas. Además, es necesario considerar la sincronización de los elementos, de modo que cada subsistema debe operar a una velocidad específica en función de la velocidad del canal de transporte de pescado. Con ello, se determinaron los valores de par (torque), velocidad rotacional, aceleración y consumo de energía para cada motor presente en la máquina. Como límite máximo de operación de la máquina, se fijó el valor de 10 piezas por minuto.

1.5. Visión artificial para determinación de puntos de operación de herramientas

1.5.1. Análisis previo

Para determinar los algoritmos necesarios a implementar en la máquina, inicialmente se realizó un análisis sin movimiento sobre un primer conjunto de piezas indicado anteriormente. Se simularon las condiciones de iluminación y distancia focal que se darían en el sistema final. Se utiliza un fondo blanco para que la imagen del pescado se pueda extraer más fácilmente.

En primer lugar, es necesario extraer la imagen del pescado de forma correcta pues de

ello depende la detección de los puntos de actuación. Especialmente importante es la zona del pecho y vientre del pescado dado que contiene colores más claros y puede generar confusión con el fondo. Una vez analizadas las características de la imagen obtenida y la diferencia entre los píxeles correspondientes al pescado y al fondo, se toma en canal 'B' del espacio de color 'RGB' como el más adecuado ya que muestra un mayor contraste entre el fondo y la pieza de pescado. La discriminación se realiza mediante un umbral de intensidad de este canal.

Para mejorar la velocidad del algoritmo, la imagen se reduce a un tamaño de 736×351 pixeles mediante un proceso de recortado y redimensionado. Esta reducción de tamaño no muestra pérdida de precisión en la detección de los puntos de actuación que se deben detectar.

El siguiente paso consiste la binarización de la imagen basada en el umbral del canal 'B' indicado anteriormente, obteniendo una imagen en blanco y negro. El resultado de este preprocesado es el de un rectángulo $L \times H$ (longitud y altura) ajustado a las dimensiones de la pieza analizada. De este modo, el algoritmo de computación sólo debe actuar sobre el conjunto de pixeles de este rectángulo, reduciendo así la carga computacional para obtener un resultado en el menor tiempo posible.

Dado que los puntos a obtener se encuentran en la parte delantera de la pieza (cabeza, aletas anal y pectoral), la mitad de la imagen correspondiente a la parte trasera o es necesario analizarla. Por tanto, el primer paso consiste en la detección de la parte delantera y trasera. Aunque todas las piezas deben ir colocadas con la misma orientación, se analiza la imagen para comprobar en qué parte de la imagen se sitúa la mitad delantera de la pieza. El principal criterio para obtener este paso se basa en la intensidad en escala de grises puesto que la parte trasera contiene mayores zonas oscuras. Así, la mitad que contiene un valor medio con mayor intensidad de gris (más oscuro) se considera que es la parte trasera del pescado.

El siguiente paso es la detección de la posición de las aletas dado que nos indicará los puntos de actuación de las herramientas. Para ello, se realiza un proceso de segmentación de la imagen para acotar las áreas donde se encuentra cada una de ellas. Finalmente, utilizando de nuevo el canal 'B' del espacio 'RGB' se obtiene la posición de las mismas.

Este proceso requiere de diferentes pasos de procesado de la imagen para corrección de la orientación, corrección de píxeles aislados y otras operaciones para optimizar la detección.

Para validar el método propuesto, se realiza un análisis de la ‘t de student’ y de varianza (ANOVA). El análisis de ‘t de student’ se emplea para comparar las diferencias significativas entre las áreas detectadas como ‘aleta’ y aquellas que no lo son, mostrando que existe una diferencia significativa entre ambas. El análisis ANOVA se realiza sobre la intensidad media de las zonas de la imagen detectadas como ‘aleta’.

En un total de 97 piezas de pescado (338 aletas), la posición de cada una de las aletas fue manualmente asignada y posteriormente comparada con la posición indicada por el algoritmo. Se obtienen los parámetros habituales para determinar la bondad del algoritmo como sensibilidad, especificidad y precisión.

1.5.2. Análisis de imagen en máquina

Una vez establecidos los principales parámetros y etapas de procesado necesarias para la correcta detección de los puntos de actuación de las herramientas, basados en la detección de las aletas, se realiza un análisis más detallado para las condiciones reales de funcionamiento en la máquina, con adquisición y procesado simultáneo para obtener un resultado que sea posible trasladar al sistema de control con un tiempo de antelación suficiente como para que los sistemas de actuación sobre el pescado puedan actuar en función de los valores obtenidos.

En este caso, se empleó una cámara Basler, modelo ‘daA1280-54uc, USB3, 1280×960, 1.2 MP’, con una lente Evetar ‘M118B029520W F2.0, f 2.95mm, 1/1.8", S-Mount’ que asegura una distancia focal adecuada para capturar la pieza de pescado al completo (independientemente del tamaño de la misma). Dado que esta lente es de campo extendido, se producen distorsiones en los extremos, por lo que se debe realizar una calibración y posterior compensación que ajuste la imagen. Un parámetro importante para la cámara es la capacidad de capturar un alto número de imágenes por segundo.

Durante las pruebas iniciales, se utilizó un umbral constante para la segmentación y establecimiento de criterios de clasificación de zonas de la imagen. En este caso, dadas las múltiples características en el color de la piel de la trucha, se detectó la incapacidad de

detectar correctamente las aletas para determinadas piezas de pescado y el color blanco de fondo. El color de fondo debe ser adecuado para todos los algoritmos involucrados en el procesado de imágenes dado que determinados algoritmos funcionan bien en función del color, por lo que resultó necesario encontrar el color más adecuado para todos ellos. Se realizó un estudio del color de fondo teniendo en cuenta los materiales usados habitualmente en el sector de la alimentación debido a las restricciones sanitarias, y se encontró que el color azul permite obtener los mejores resultados de clasificación para diferentes tipos de coloración en la piel de la trucha.

La elección de este color de fondo impuso la adecuación de la iluminación y la modificación de los algoritmos inicialmente propuestos. Se incluyó una plancha de plexiglás azul para realizar una iluminación trasera (backlight). Se analizó exhaustivamente las zonas de las aletas que se desean detectar teniendo en cuenta múltiples piezas con variaciones de color de la aleta. Con estas condiciones, se obtiene que el canal de color ‘R’ del espacio ‘RGB’ proporciona los mejores resultados.

Para reducir el número de imágenes a analizar por el sistema de cálculo, se incluye un sensor para detectar la posición del pescado que circula por el canal de transporte que dispara la adquisición de una imagen. Ubicando el sensor en la posición donde la cola del pescado alcanza el final de la cápsula de iluminación, se asegura que todo el pescado está en su interior y la imagen capturada contiene el pescado en su totalidad, listo para ser analizado.

Respecto de las etapas de procesado, primeramente se obtiene el rectángulo donde se inscribe el pescado, descartando el resto de imagen para su posterior análisis, y se extrae el canal ‘R’ de la imagen ‘RGB’. Seguidamente, se binariza la imagen y se compara con la imagen ‘RGB’ para obtener un fondo negro. La posición de la cabeza del pescado se obtiene a través de la detección de la aleta pectoral situada junta a ésta. Así, la posición exacta de corte será establecida en la zona de contacto entre la aleta pectoral y las agallas (branquias). Se analiza también la obtención del punto de corte a través de la obtención del arco que forman las agallas, pero se obtiene menor precisión dadas las variantes de piezas de pescado analizadas.

Para la obtención del punto de corte y actuación sobre la zona de vientre y vísceras es

necesario realizar modificaciones sobre los algoritmos iniciales debido a la posición del pescado sobre el canal de transporte y el modo en que la imagen del pescado es obtenida. Dado que el canal de transporte tiene forma de V, el pescado queda orientado de modo vertical en lugar de lateral, quedando en la imagen las zonas de color más claro (zona del vientre, es decir, zona inferior del pescado).

En este caso, los canales de color 'R' y 'B' se utilizaron para obtener la posición de las aletas anal y pectoral, respectivamente. El empleo de dos canales de color diferentes en cada aleta es debido al color de fondo y la iluminación, dado que la luz impacta de modo diferente en cada aleta, lo que hace que sea un canal de color diferente el que proporcione mejor detección.

1.6. Sistema automático de control

Los componentes electromecánicos de la máquina se han diseñado teniendo en cuenta las consideraciones de diseño mecánico y actuación de cada subsistema sobre las piezas de pescado. Además, se diseña un sistema de control que incluye un interfaz de usuario y todos los sensores necesarios para la correcta detección de posición y actuación para el corte y limpieza del pescado. Se emplean botones de inicio/paro, interruptores de seguridad para evitar posibles daños personales en caso de invasión de las zona de peligro, sensores inductivos y magnéticos para detectar el paso de los mecanismos por determinadas zona que permitan secuenciar la actuación por parte del programa de control, y el sistema de automatización basado en autómata programable (PLC). El sistema de control incluye además todos los elementos de alimentación eléctrica y sus protecciones para el correcto funcionamiento de cada uno de los equipos eléctricos de la máquina.

La programación del PLC se estructura en tres partes principales: inicialización de la máquina para asegurar la correcta posición de todas las partes de la máquina tras un paro de emergencia o arranque de la máquina, modo manual para poder mover los equipos de la máquina de forma individual, y funcionamiento automático donde los equipos de la máquina son controlados en función del análisis de imagen realizado. El PLC empleado es de la familia S7-1200 de Siemens programado mediante el software TIA Portal.

El proceso automático de automatización comienza en el momento en que una de las

pinzas del canal de transporte agarra una pieza de pescado, arrastrándolo por la misma. Cuando la pinza alcanza la posición de un sensor inductivo situado al final de la cúpula de imagen, se dispara el sistema de visión para adquirir una imagen de la pieza de pescado. Se ejecuta el algoritmo de procesado de imagen y se obtienen los puntos de actuación de las herramientas. Se coloca un sensor inductivo en la posición en que debe actuar cada una de las herramientas para detectar la pinza que agarra el pescado, lo que da inicio a la actuación de la herramienta correspondiente sobre pieza, en función de las posiciones obtenidas por el sistema de visión. En caso de no haber pieza de pescado agarrada por las pinzas, el sistema de visión lo detecta y no se ordena ninguna activación de las herramientas.

Dado el tamaño de la máquina, un máximo de tres piezas de pescado pueden ser procesadas simultáneamente. Para ello, se definen tres bloques de datos donde se almacena la información sobre los datos de actuación de cada herramienta para cada pieza. Estos datos se organizan en forma de pila FIFO, eliminando los datos de la pieza procesada para dar paso a los de una nueva pieza entrante.

1.6.1. Automatización del sistema de incisión en el vientre

Una vez que el detector inductivo se activa por la cercanía de las pinzas de agarre de la pieza de pescado, se inicia la actuación de la herramienta de corte sobre el vientre. Un motor paso a paso gira para hacer descender un brazo mecánico con una cuchilla en su extremo que se introduce en la zona del vientre durante el tiempo estimado por el PLC en función del tamaño de la pieza reportado por el sistema de visión, haciendo girar el motor en sentido contrario para levantar el brazo nuevamente. Este brazo dispone de un sensor de límite de recorrido para evitar que el avance del brazo exceda el límite mecánico en caso de una medida incorrecta. También dispone de otro sensor de posición inicial (de reposo) para asegurar la posición desde la que comienza el recorrido. Al tratarse de un motor paso a paso es posible controlar la posición del brazo de forma precisa.

1.6.2. Automatización del sistema de corte de cabeza

Dado el tamaño y peso del sistema de corte de la cabeza, éste se controla mediante un sistema neumático que mueve el sistema de cuchillas hacia la pieza de pescado tras la

activación de aire a presión (SC-50 × 250-S). En este caso no es necesario controlar el avance de la herramienta ya que ésta debe insertarse completamente para todas las piezas de pescado hasta un límite establecido por un sensor magnético (AIRTAC CS1-F) adecuadamente ubicado en el sistema de corte. En cambio, sí es necesario establecer el momento exacto en el que debe actuar este sistema, en función del tamaño de la pieza de pescado. Esta información es proporcionada por el PLC en función de los datos obtenido por el algoritmo de visión.

Por tanto, una vez que las cuchillas han cortado la cabeza, ésta se separa del resto de la pieza de forma inmediata debido al avance continuo de la cinta de transporte. El sistema neumático se contrae nuevamente hasta su posición de reposo y se cierra el flujo de aire comprimido para reducir el consumo, quedando preparado para la siguiente pieza.

1.6.3. Automatización del sistema de extracción de estómago y vísceras

Para el control preciso de este proceso se emplea un motor paso a paso. Tal y como se obtuvo a través del software de simulación dinámica Adams, la potencia requerida es de 7,5 Nm. Se emplea un sistema de engranajes de reducción que aumenta al par del motor reduciendo la velocidad de giro. Dado que en este caso la velocidad de giro es reducida, se incluye una caja reductora de 1:18 y se emplea un motor de 0,8 Nm. El motor gira en un sentido u otro según sea necesario hacer actuar el sistema de succión grande o pequeño. Tal y como se describió en la etapa de diseño, existen dos sistemas de succión en función del tamaño de la pieza, por ello, según la longitud establecida por el sistema de visión, si la pieza es menor de 275 mm, el sistema de succión de menores dimensiones es el que actúa, y viceversa. Por otro lado, la profundidad de penetración del sistema de succión depende de la pieza y los valores obtenidos por el algoritmo de visión.

Al igual que en el resto de herramientas y etapas, existen detectores de final de carrera para evitar desplazamientos anómalos o excesos en la actuación de los tubos de succión que puedan dañar la pieza de pescado hacerla inservible.

1.6.4. Automatización del sistema de limpieza de la cavidad ventral

En este punto, la herramienta consiste en un cepillo rotativo controlado por un equipo

neumático y sus correspondientes sensores. Esta herramienta actúa en función de la longitud de la pieza.

1.6.5. Comunicación entre el sistema de visión artificial y sistema de automatización

El software Matlab y las librerías correspondientes se emplean para el cálculo del algoritmo de visión artificial y la comunicación con la cámara de visión y el sistema de automatización. En ambos casos, se emplea Ethernet (TCP/IP) para la comunicación entre dispositivos. En el caso de la cámara, ésta es el servidor y el PC es el cliente. Para el caso del PLC, el PC es el servidor y el PLC el cliente. Tras la ejecución del algoritmo de análisis de la imagen de la pieza de pescado, cuatro datos principales son transferido al PLC para el control de las herramientas:

1. Longitud del pescado desde las pinzas (cola) hasta la cabeza.
2. Distancia entre las pinzas (cola) hasta la aleta anal que marca el inicio de la actuación de la herramienta de corte del vientre.
3. Distancia entre las pinzas (cola) y la aleta pectoral que marca el punto de corte de la cabeza.
4. Profundidad de penetración para las herramientas de corte de vientre y de succión de vísceras. Este valor es función del grosor de la pieza.

Como se indicó anteriormente, estos datos se almacenan en el PLC de forma individualizada para cada pieza, manteniendo los datos para cada una de las tres piezas que la máquina puede procesar en paralelo. El sistema de control debe asegurar que para cada herramienta de proceso se lee el valor correspondiente a la pieza de pescado que sobre la que se actúa.

1.7. Resultados

Para un correcto diseño de la máquina, cada etapa de desarrollo e investigación ha requerido del análisis de los resultados obtenidos por las herramientas de simulación, tanto a nivel estático y dinámico como a nivel mecánico y electrónico/informático.

Los resultados de simulación han permitido el adecuado diseño y dimensionamiento de

cada uno de los componentes de la máquina. Posteriormente, los resultados se han validado de forma experimental con la máquina de prototipo construida.

Los resultados experimentales muestran que las herramientas funcionan de forma adecuada para realizar las funciones requeridas y las potencias de los motores y los sistemas de detección de pieza funcionan correctamente. Se han realizado pruebas de velocidad para comprobar que la máquina es capaz de procesar el máximo de piezas de pescado para las que ha sido diseñada (diez piezas por minuto), verificando que la máquina es capaz de realizar las operaciones de corte, extracción y limpieza en los puntos determinados mediante el sistema de visión artificial. Se analizan diferentes piezas de pescado con variadas dimensiones para evaluar el funcionamiento.

1.8. Conclusiones

La inclusión de procesos automatizados en las actividades humanas es una realidad. Este trabajo ha desarrollado su investigación en los sistemas automatizados para la limpieza de pescado, tarea que habitualmente se realiza de forma manual, excepto para grandes industrias con maquinaria muy costosa. La investigación realizada, a través de la combinación de sistemas mecánicos y electrónicos (mecatrónicos) ha permitido el diseño de una máquina de pequeñas dimensiones con alta capacidad de procesado de pescado y calidad en los resultados obtenidos.

Se han diseñado, modelado, simulado y finalmente construido todos los elementos de la máquina, desde el agarre del pescado empleando unas pinzas de agarre especialmente diseñadas para evitar deslizamientos en superficies de baja fricción como la piel del pescado, hasta la obtención del pescado limpio de vísceras y cabeza, pasando por etapas intermedias de corte y extracción de las partes del pescado a eliminar.

El sistema realizado permite el ajuste automático de las herramientas de limpieza y corte en función del tamaño del pescado gracias a la inclusión de un sistema de visión artificial que analiza individualmente cada pescado, obtiene sus características a través de algoritmos de visión e inteligencia artificial, y proporciona los datos dimensionales para que las herramientas de actuación, controladas electrónicamente, se posicionen de forma adecuada según las dimensiones del pescado a procesar.

El sistema procesa en paralelo diferentes pescados a través de un diseño basados en estaciones de procesado: análisis de imagen, corte de vientre, corte de cabeza, extracción de vísceras y limpieza de cavidad visceral.

Cada una de las estaciones de procesado ha sido simulada a nivel mecánico y electrónico para obtener las fuerzas que se ejercerán y así poder adecuar el diseño de las partes mecánicas con la adecuada resistencia, así como el diseño de las partes electrónicas con la potencia de los motores que controlan el movimiento. El sistema de visión artificial se ha diseñado para obtener el mejor contraste de la pieza de pescado y poder realizar una detección adecuada de los puntos singulares de la pieza de pescado (posición de aletas, dimensiones, etc.), se han investigado diferentes métodos en posición del pescado respecto de la cámara de imagen, iluminación, óptica, etc.), algoritmos de imagen y clasificadores de imagen. Para ello, se han generado bases de datos de pescado para su análisis.

Además de las investigaciones realizadas, se prevé seguir investigando en nuevas áreas que permitan seguir optimizando el sistema, en concreto, se plantean las siguientes actividades:

1. Utilizar sistemas de identificación de pescado en lugar de análisis de imagen.
2. Diseña y modelar una estación adicional para el fileteado del pescado y extracción de espina.
3. Aumentar la capacidad de procesado de pescado (mayor número de piezas por minuto).
4. Investigar nuevas técnicas de corte para el fileteado y cabeza, así como el agarre de la pieza por la cabeza en lugar de la cola.
5. Eliminación de la estación final de limpieza si el sistema de fileteado se incorpora.

Summary

Fish sorting with the sorter systems will reduce costs as well as increase production rate and efficiency. After sorting the fish, it is time to supply them in markets. In small and large fish centers, highly demanded fish species are usually available in different sizes. The fish are generally opting based on the size, and it is cleaned on the customer's request. Usually, in fish supply stores as well as aquaculture processing plants, cleaning the fish involves some cleaning steps, or all the cleaning steps are done In the case of non-processed fresh fish, some prefer gutted fish; others opt for gutted and beheaded, or just in fillets. It should be noted that trout scales are finer compared to other species, and it can be processed without scaling.

Due to the broad automation in industry, the need to design and manufacture automated devices with high capabilities in the fish and aquatic processing industries is of great importance. Because of the importance of fish consumption in the food basket and the need to use automatic industrial devices to increase efficiency and improve the quality of fish processing, the need to design and develop systems with higher capabilities compared to the current models are essential. In fish processing factories and fish supply stores, it is necessary to stabilize the fish for any cleaning operations properly.

Due to the slippery skin of the fish and the low coefficient of friction, it is usually challenging to control. If we want to clean the fish with a high capacity, the fish must pass in front of the cleaning tools, and the desired operation can be performed on the fish at any stage. Since the fish processing operation is done step by step, the gripper must meet proper stabilization and convenience of processing arms. Regarding the high price of fish cleaning systems and also the limited capabilities of the available systems, a device with the ability to perform the steps of belly cutting, beheading, gutting, and cleaning the fish was designed and fabricated. Besides, since the customers choose their desired weight, the system with the accurate visual unit can facilitate the cleaning of trout fish with different dimensions.

The image processing system was applied to measure the size of the fish. In this system, as the fish is passing in front of the video camera, a frame is saved, and the related cutting points are extracted for further processes. To prevent any contact between cleaning

parts with the conveyer grippers, we developed an automatic controlling algorithm to control the system operators to satisfy the safety of the system operation in different cleaning stages.

2.1. Objectives

The main purpose of this dissertation is to design, fabricate, and evaluate a trout head and belly cutting and cleaning system, which is expected to achieve the following sub-objectives:

1. Designing and fabricating the mechanical part of the system, including the main body, grippers, beheading, and gutting subsystems.

2. Implementation of electrical and controlling parts of the system

3. Providing an algorithm in order to properly identifying and detecting the trout together with defining fish length and width, cutting points, and cutting lengths.

4. Evaluating the accuracy of the developed algorithm to determine the appropriate head and belly cutting points to compare with the actual points.

5. Implementing the online of the controlling and image processing algorithm evaluating the system process.

6. Qualitative evaluation of the processed fish and visual and quantitative assessment of the cleaned fish in terms of proper cutting of the head to prevent fillet loss.

In general, this device consists of the following parts and subsets:

1- Image processing case and a digital camera.

2- The main chassis of the device, which is the combination of stainless steel (in wet parts) and painted steel.

3- Fish carrier subset (grippers)

4- Belly cutting subsets: a 0.25 hp AC electromotor, stainless steel arm carrying rotary

shafts, belt and pulley, motor shaft and blade shaft, rotary cutting blade with a diameter of 100 mm and a thickness of 1.5 mm, stepper motor, power screw connected to the stepper motor and the nut connected the cutting arm.

5- Head cutting subset: a pneumatic jack, two ribbed rotary blades installed in the angle of 90 degrees with opposite revolution, two air motors for rotary blades, a small frame carrying the moving components, and a set of wagons and guide rails used to guide the entire assembly in the vertical direction.

6- Gutting subsystem: one stepper motor with a mounted gear, two rack gears, two suction tubes with different diameters for small and large fish, and a set of wagons and guide rails to move the rack gears in the vertical direction.

7- Belly cleaner subset consisting of a 0.25 hp AC electromotor, stainless steel arm carrying rotary shafts, belt and pulley, motor shaft and blade shaft, rotary cleaner brush with a diameter of 125 mm, and pneumatic jack.

8- Pneumatic system..

9- Controlling and transferring system the send the command to the motors and driving arms of the device

In the following sections, the designed system, all calculations, and system fabrication are explained. The initial evaluation was required to design the device to obtain basic information on trout. Therefore, a number of fish units were applied to get the primary data.

2.2. Initial samples (before starting the fabricating of the device).

In this study, in the first stage and before fabricating the device, 97 samples of salmon from 262 g to 622 g with an average weight of 421.88 ±78.04 kg with the total weight of 36.5 kg were considered. In the second stage, 100 trout samples were selected in the fish marketing center. Unlike the initial stage, the fish were placed inside a V-shaped canal; so that the back of the fish was placed inside the canal with its chest upwards. In the first step, the initial model was designed in CATIA software and the structure of the machine was

fabricated. Then some necessary parts such as conveyor chains and gears were provided. By entering the exact dimensions of these parts in the software, other parts of the device were designed and the other steps were done in the same way. To fabricate the main chassis of the system, we applied 40 × 40 mm steel with a thickness of 2 mm was used. In the construction of the internal parts of the chassis, especially the parts that are in contact with water, the stainless steel part and profiles were applied.

To enable different fish processing steps in this system, we considered the dimensions of the chassis 2.8 m in length, 0.85 m in height, and a width of 0.7 m. Under the main chassis of the device, carrier wheels with stabilizing bases were considered, so in addition to easy movement of the device, the longitudinal and transverse alignment of the system is possible. One of the most critical points in designing a system with the ability to perform different trout processing stages is to consider a place in the fish body. It does not interfere with cutting and cleaning tools during the various stages of cleaning. Therefore, the tail of the fish was selected as the appropriate area.

The fish carrier subsystem consists of four main parts:

1- Fish grippers

2- Gripper guides and fish guiding canal

Using the grippers suggested in this dissertation, it is possible to perform different steps of fish processing in an integrated system. To increase the capacity of the system (number of fish per minute), we considered a balance between the length of the system and the number of grippers so that with the maximum number of the grippers in the conveyor length, a sufficient space provided for the system operators. Therefore, in this design, five sets of grippers were considered.

2.3. Mechanical design

2.3.1. Belly cutting subsystem

The function of this subsystem is to make a longitudinal incision in the trout belly from the beginning of the anal fin to the pectoral fin.

2.3.2. Head cutting subsets

Like other designed parts of the system, including the main chassis, the fish head cutting subsystem was also designed in CATIA software. Since the fish is moving along the system, it is necessary to provide the best head cutting condition. In order to have a proper cut, a precise, fast cut can provide the cutting condition. Therefore, a pneumatic jack was applied to carry the cutter subset. As mentioned before, when the grippers reach the beginning of the guide rails, the fingers contact the rails and the fishtail stocks between the gripper clamps. In this condition, any clamped trout is pulled along the system. Therefore, to define the system processing capacity (fish per minute), it is necessary to determine the optimal working speed. By knowing the linear velocity of the conveyor, the penetration velocity of the cutting blade will be investigated. In fact, the speed at which the cutting blade approaches the fish is directly related to the fish transferring speed. Two different types of blades have been studied for trout head cutting:

1- ‘V’ shaped cutting blade by applying sufficient force to cut the head

2- Two rotary cutting blades without extra force on the fish (two reciprocating), rotary

In order to have a fast and accurate cut, it is desired to select the blade as thick as possible, but since but these blades are subjected to vertical forces, it is necessary to the trade-off between blade thicknesses and quality of the head cut. In order to select the air motors, we tested head cutting with a typical air motor with 1800 rpm. The results showed that although the head can be cut without any stock in the motor, a higher speed is required to have the desired cut. By testing different motors, an air motor with a rotating speed of 2500 rpm resulted in a proper cut.

2.3.3. Gutting subsystem

In this subset, as the fish reaches the gutting position, the stepper motor is activated by receiving the start command from the control unit and rotates in clockwise and counterclockwise directions depending on fish size. In case the size of the fish is determined as small by the machine vision section, the narrower tube enters the fish belly. In fact, the stepper motor is rotated counterclockwise, and due to the engagement of the pinion with the rack gear, the set of sliders together with the suction tube move toward the fish. As the suction pipe gets closer to the fish belly in a vertical direction, the valve in the

entrance of the suction pipe hits the barrier, causing the suction valve to open. It should be noted that due to the suction in the suction pipes, it is necessary to close all the valves in a neutral position (non-functioning position), so the suction process can be done through the relevant pipe.

Since different sizes of trout will be processed in this machine, using a big tube to clean small fish will collide the fillet and bones and affect the final product quality or stack in the middle of the process line. Therefore, to avoid this problem, two different suction pipes have been applied. The function of the gutting subsystem is such that, once of the suction pipes get closer to the fish, the other pipe raises so that preventing from any contact with the grippers. In fact, using this design instead of using two separate stepper motors for each of the suction pipes reduced the cost and complexity of design and manufacturing.

2.3.4. Belly cleaner subsystem

This subset is designed and built to clean the inside of the fish belly and remove any material attached to the fish spine. When the fish reaches the cleaning position, the command is transferred to the pneumatic jack from the control unit and performs the cleaning operation by lowering the jack. The time duration in which the pneumatic jack is extended mode is directly related to the fish length. As the fish passes in front of the cleaning station, the jack retracts to the initial position.

2.4. Device simulation, kinetic analysis and extraction of forces and torques of motors and jacks

After designing the system in CATIA, it was necessary to choose the motors and pneumatic jacks. Therefore, it is required to calculate the required torque and rotational speed of stepper motors and the force and speed of pneumatic jacks. The simplest method is to design all the parts and define their weights to calculate the forces using the conventional method and numerical calculations. This method is applicable when the dynamic parameters are calculated for a single part or, in some cases, the limited number of parts within the relation. Using this method to determine accurate inertia reaction forces in a multibody system faces a significant challenge unless the problem is simplified. Therefore, to have closer results to the real operating conditions and reduce the numerical

calculations and increase output accuracy, the designed system in Catia software was imported to Adams 2017 software and simulated for dynamic analyses. After importing the designed model into Adams software, the first step is to nominate the parts. The related constraints were assigned for all the parts, and any possible errors were solved. At the next step, the associated motions for the moving parts were considered For this purpose, a rotational motion was considered for the stepper motor's hinge in the belly cutting and gutting subsystems. Likewise, for the linear moving parts, pneumatic jacks, and suction tubes the linear constraints were considered.

Therefore, four-movement steps were considered for each of the four operators of the device based on the movement time and rotational and linear speeds. Each pair of steps was considered for each operator's round trip. For example, the belly cutting stepper motor start runs based on the written step function. Since the linear velocity of the fish varies in different feeding capacities, it is necessary to bring the cutting arm closer to the fish concerning linear transmission speed. It should be mentioned that the belly cutting time at which the arm is in cutting position is also concerning the fish transfer speed. In addition to determining motor torque, rotational speed, acceleration, and energy consumption were extracted. Finally, the maximum torque required for system functioning at a capacity of 10 fish per minute was selected to determine stepper motor characteristics in both belly cutting and gutting subsystems.

2.5. Machine vision

2.5.1. Offline processing

Image segmentation is one of the significant steps of image processing that directly influences other post-segmentation processes. This fact imposes a specific image processing procedure; otherwise, the fish will be inappropriately segmented from the white background. Since, in some cases, the area near the trout chest and belly had similar pixel intensity values to those of the white background, the trout region was not completely segmented using this method. Finally, the channel 'B' of the 'RGB' color space showed a high contrast between the pixel intensity values of the trout and the background providing the best results. Finally, a threshold intensity value of 150 was selected as the initial step in the segmentation process.

This image was converted to a 736×351 matrix after resizing and cropping, considering a trade-off between the image quality and processing time. As the dimension of the initial image matrix is large, we resized the images to an optimized size regarding the balance between acceptable reduced image quality (preserve any required small objects like pelvic fins and their color features) and the computation time gets more significant in fast real-time systems. In the next step, the resized images were converted into binary images: the pixels with intensity values lower than 150 were considered as '1' (white), and the rest were considered as '0' (black). Finally, the samples were completely segmented from the background and a bounding box with the final dimension was assigned.

The extracted dimensions (length and width) are applied in the image processing algorithm as stated in the following:

(1) The image was cropped in two different steps to reduce the computational load. In the first step, the initial image was resized, and a wide margin of the image was cropped to remove a significant part of the background. In the next step, the image was cropped based on the second bounding box area with the length of 'L' and the width of 'W'.

(2) Defining two lines from 10% of the length on both sides and further seven lines between these two lines.

(3) Defining two lines from 1/15 of the length of the fish from both sides along its length and further 45 lines between these lines.

(4) Defining structure element as equal to the 0.001% of trout bounding box area.

By determining the central line, the images were divided into two parts to discard the back side of the fish. These parts were analyzed to identify the belly and back sides by comparing the gray intensity values of both parts. Since the color near the trout belly is lighter than its back, the part with greater mean gray intensity value is considered the belly side. One of the parts including the trout fins were further divided into two parts. This was done by determining the horizontal lines and connecting their center points similar to the initial line determination process. Since the new shear is a narrower area containing the fins, more horizontal lines were considered in the second fin detection stage. At the next stage the channel 'B' of the RGB color space was chosen to segment the fins. In this stage

all fin segmentation errors were removed to have successful cutting point determination. Any corrections in fin segmentation including extra object removing, filling the holes and other morphological operation were applied.

Two further analyses were conducted to verify the channel ‘B’ performance in fin segmentation: t-test and analysis of variance (ANOVA). The t-test is applied to compare the most significant difference between two groups of data. In this case, it is desired that the difference between the mean intensity values of the fins and the corresponding non-fin area results in higher t-values. This shows that there is a significant difference between the fin and non-fin region which facilitates fin segmentation. The analysis of variance (ANOVA) is applied among the mean intensity values of the segmented fins in all the samples. In this method, the least ‘F’ value shows the least difference between the mean intensity values of the fins. In order to determine the capability of the image processing algorithm for fin determination, 97 fish images (a total of 388 fins) were selected. The position of each fin was manually annotated and compared with the region obtained by the algorithm. Three common statistical parameters including Sensitivity, Specificity, and Accuracy were used to describe the performance of the offline image processing algorithm.

2.5.2. Online processing

As described in the offline image processing section, the proper operation of the machine depends on the precise cutting point determination resulting in proper cut with the least fillet loss. At the next step, the images were examined online. In order to capture the images, an online video camera (Basler, daA1280-54uc, USB3, 1280 × 960, 1.2 MP) was applied. To cover the total fish length considering the distance between the camera and the fish, a wide view lens (Evetar Lens M118B029520W F2.0, f 2.95mm, 1/1.8", S-Mount) was applied. Since this camera will be applied in an online system, we need a higher frame rate to guarantee an explicit image. In order to get the fish images, three frames were saved from each snapshot based on the input number. Since, in this study, a fisheye lens is applied to cover the total length of the biggest tried fish sample, it is necessary to remove any distortion from the initial image. Thus a checkerboard page with a square dimension of 21 mm was applied. In order to calibrate the camera, 17 images were captured from the checkerboard in different positions.

In the offline stage, a constant value considered as a trout segmentation criterion. Considering the diversities in trout color, they justified that the Otsu method could not segment the fish from the white background (for sanitary restrictions) because of the little nuance between the background and trout belly. It should be noted that choosing lighter backgrounds facilitates the segmentation process in darker regions (the fins, head, and back part), but segmenting the whole target was performed using manually assigned intensity value. Since, in this study, different species of fish with different colors are processed, it is impossible to segment all the samples in the white background. Therefore, it is essential to select a background in which all species are easily segmented. By proposing a new method for fish transfer, the contact between the fish and any conveyer is resolved, so it is possible to select various colors in the background. After conducting different trial and error, the pure blue color was selected for fish segmentation.

Among all fish species, the skin color is so light that the light background is not a proper option. Therefore, choosing a darker background can solve the segmentation process in these species, but it causes the problem in the species with dark skin unless the darker background intensity is so close or equals to ‘0’. Therefore applying a black background seems to be a proper option It is clear that the pixel intensity values of the black background are distinct enough for lighter fish segmentation, but considering the intensity values of the background and the trout body, especially at the darker parts of its back and the fins, the segmentation process will face a great challenge in numerous fish samples. Since the mean intensity value of the fins in channel R is higher among the three color channels of RGB color space, by selecting this channel, the most significant difference between the background and the fins is accomplished. The easiest way to create a pure blue background is to use a blue color behind the fish. One of the challenges to reach a pure blue background is changing the background brightness in opposite illumination. The light generated by the opposite LED lights brightens the blue background, which results in an impure color. Therefore a blue Plexiglas with a backlight illumination was considered in online stage.

Since one frame will be saved for further process in the online system, a snapshot is captured as the tail reaches the end of the imaging case. In this condition, the total length of the fish is exposed in front of the camera vision, and it can ensure a complete image

with total body length in all samples. At the next step, the frames are processed for fish segmentation. Before segmenting the fish, it is necessary to crop the images based on the defined bounding box to cover the maximum length and width of the fish. Therefore, a 320×320 bounding box was applied to cut the initial image in which the processing task and time decreased. At the next step, channel R of the RGB color space is applied to segment the fish sample from the background. As mentioned above, in this color space, the difference between the fish and the background is distinct enough to segment almost all the fish species from the background properly.

To perform the second phase of segmentation (segmentation of fins from fish), the color image was masked on the binary image; so that by matching binary and the color images, the pixels of the color image with the corresponding indices in the binary image with the value of '0' is converted to '0' and the rest of the pixels remained constant. Therefore, the color image of trout will be obtained on a black background, which will be used to extract the characteristics of the fins. To find the head cutting point in trout fish, the most significant region is to segment the pectoral fin near the head. The joint point of the fin with the gill is the exact position to cut the head. Another option is finding the gill arc in trout fish, but since there is no significant intensity difference in this region, the pectoral fin was considered the head cutting point. Therefore, if the pectoral fin is properly segmented, the beginning of this fin will be considered the exact head cutting position. It must be noted that in some fish species, the gill arc has distinct contrast with the body so that it can be easily segmented to identify the head cutting point.

One of the main objectives of this study is to extract the belly cutting area, belly cutting length, and the head cutting position. All of these dimensions are extracted by image processing and will be the basis of the trout processing system operation. In the offline step, since the fish is placed on its side, a line was drawn from the center of the fish to omit the backside of the trout, but in the online stage, as the fish is transferred inside the V-shaped canal, the majority of the dark area in trout back is placed inside the canal and is easily discarded from machine vision process. It should be noted that in this condition, the area in trout back is removed and further unnecessary areas are omitted, so the accurate and simple fin segmentation will be achieved. Therefore separating the narrowest shear covering the fins can guarantee an accurate fin segmentation process and subsequently an

accurate machine performance.

The method of separating this shear is different from the offline stage. In the offline stage, a primary line is used to separate the fish into two parts, the belly, and the back sides, and in the second stage, the secondary line divides the belly part into two other parts so the final shear serves as a target for fin segmentation, but in the online stage after fish segmentation, the edge along the belly was applied to separate the belly shear. To segment the fins, the color image mask of channel R and B were used to identify the anal and pectoral fins, respectively. The reason for using two different color channels in the online stage is the effect of blue backlight on the anal fin. In this case the amount of blue color in the anal fin color will increase and result in high intensity values. Therefore, the channel R and B were considered to segmentation the anal and pectoral fins, respectively.

2.6. Controlling section

This section includes start/stop switches, emergency disconnect switch, alarm, and sensors, computer, and any required control components. Inductive and magnetic sensors were used to control operators and stepper motors movements. Because the movement of the device arms in each of the work steps requires unique control, the device control algorithm was written in three parts: initial setup, manual operation, and online automatic function. To develop the controlling algorithm, Tia Portal software was used. At the initial start-up stage, it is essential to consider the homing routine to return the operating arms to the home position. This algorithm is also applied while the main power supply of the device is cut off, or the operator presses the emergency bottom. With the initial setup of the device and returning the arms to their initial position, the machine will be ready to process the fish. In the next step, by pressing the start pushbutton of the motors, the electro motors of the rotary cutter, cleaner brush, and suction pump are turned on.

By reaching each gripper to the feeding position, the trout tail is caught by the clamps and transferred along the machine. When the gripper passes in front of the inductive sensor of the machine vision section, one frame is saved and processed in the primary (trout segmentation from background) and secondary (fin segmentation and cutting point extraction) image processing steps. Since inductive sensors are applied in each of the five subsets (machine Vision, belly cutting, head cutting, gutting, and cleaning subsets), in case

there is no fish in the gripper, the dimensions extracted by machine vision will be calculated as “0', and the system operators will perform no function. Since the maximum number three fish are simultaneously processed in the total machine length, a set of data receiving a block for three different fish were created. In fact, by reaching the second fish to the machine vision unit, the first fish is still in the middle of the processing stage, so any new data without considering a data logging block will erase the previous sample data. Upon the availability of the data, each fish sample will be cleaned based on the relevant data. Different types of controllers can be used for system controlling such as microcontrollers and programmable logic controllers (PLC). Therefore, while PLCs are applied in the systems it is necessary to adapt the PLC output voltage with the required voltage for the operators like stepper motors and their drives.

2.6.1. Belly cutting subsystem

After capturing the image and extracting the required dimensions in the machine vision section, the fish continues the path toward the inductive sensor in the belly cutting subsystem. As soon as the metallic shaft of the gripper reaches the sensor, the start command is sent to the stepper motor. As the stepper motor starts, the belly cutting arm descends towards the fish, and the blade enters the trout belly and penetrates the fish as it rotates counterclockwise (in front view). At the end of the cut, the stepper motor rotates in the reverse direction and returns to its initial position.

As soon as the fish arrives at the belly cutting position, the stepper motor starts its rotation. In case there is incorrect data for any fish sample which exceeds a defined range of the arm, the cutting arm reaches the down sensor and returns to the home position. In fact, the expected performance of this section is to create a longitudinal cut on the fish belly based on the specified length and depth, but if the arm exceeds the specified path, it is necessary to avoid any contact with the channel and grippers. Therefore, by activating the lower sensor, the return command is sent to the stepper motor and returns to the initial position. As the arm moves upward and reaches the upper induction sensor, the arm stops, and the homing process is updated. Figure 8-4 shows the details of the belly cutting subset.

2.6.2. Head cutting subsystem

As the head cutting subsystem contain multiple components moving together to cut the head in vertical direction, a pneumatic jack (SC-50 × 250-S) was used to move the head cutting subset. According to calculations based on the speed and displacement of rotary blade, a magnetic sensor was applied to limit the moving path. As soon as the inductive sensor is activated by reaching the fish to the head cutting position, the air motors start working and continue spinning until the trout head is completely removed. Meanwhile, after a delay (depending on the size of the fish and the position of the pectoral fin), the piston extract and the rotating blades separate the fish head as moving downwards. As soon as the blade terminates the cutting process, the magnetic sensor sends the termination signal to the control unit, and subsequently, the retracting command is sent to the pneumatic jack and rotary blades. The air motors stop working after 2 seconds to avoid high air consumption by the motors.

2.6.3. Gutting subsystem

In this section, based on the calculations performed by Adams software, the maximum amount of required torque for the stepper motor is calculated as 7.5 Nm. Since the motor is expected to provide the required torque at low spinning speeds, the stepper motor is equipped with a 1:18 gearbox (Vexta model PK243A1-SG18 Six wires with a torque of 0.8 Nm) was applied. After cutting the head, the fish reaches the position of the gutting subsystem. At this station, the belly content is evacuated based on the fish dimension. So, two suction pipes have been applied for the small (less than 275) and big fish samples. As the narrow suction tube descends, the bigger pipe rises upward, and the belly content is evacuated.

In this section, an inductive sensor is used to detect the presence of fish. In addition, a stepper motor with a gearbox and two sensors are used to control the displacement of the suction pipes. The suction tubes return to the home position by starting the system. This function is the same as the machine emergency stop functioning. Once functioning arms and moving parts are in their home position, the device is ready for use. By passing the fish through the head-cutting subset and reaching the gutting sensor, the suction operation is performed based on the data sent from the control unit. Depending on the calculated data in

the machine vision section, the penetration depth will be different. As soon as the sensor sends the signal to the control unit, the time delay and cutting time is assigned to the corresponding fish.

When the discharge tube enters the trout belly, all the contents are evacuated while the fish pass in front of the suction tubes. As soon as the fish gutting is performed, the stepper motor spins in the reverse direction and the tubes return to the home position. Although the algorithm is developed properly to have a successful operation, in some cases if the tube exceeds the defined path, the indicator installed in the suction tubes approaches the left sensor. So the stepper motor rotates in the opposite direction and returns to the home position. Besides the course controlling sensors in this subsystem, physical guards were considered to control the moving course.

2.6.4. Cleaning subsystem

By continuing the path in the V channel and reaching the end of the machine, the fish is cleaned using a rotary brush. At this station, as the fish is sensed by the sensor, the cleaner subset is activated and sends the necessary command to the control unit. The applied controlling components in this section are the pneumatic jack, solenoid control valve, and magnetic sensor. Depending on the trout size, the arm descends toward the fish and performs the cleaning operation. The cleaner brush stops as equal to the fish length cleaning time and returns to the home position. The controlling algorithm of the cleaning subsystem is presented in Figure 8-12.

2.6.5. Data transfer

In this thesis, MATLAB 2015 software was applied for image processing and data transmission. In order to increase the speed of image processing and data transmission, only the necessary toolboxes were installed in the software package. To capture the images in the online mode image acquisition package was installed. As the fish gripper reaches the end of the imaging case, the trout is in full vision of the camera at which all the length of the fish can be processed as soon as the frame is captured. In the next step, the trout is segmented, and related dimensions are extracted based on the fins positions.

To transfer the data from the machine vision unit to the control unit, the TCP / IP protocol was selected from the MATLAB software toolbox. In this protocol, MATLAB is considered as the server, and TiaPortal software is considered a slave. To transfer the data, a network cable is applied. When the fish reaches the end of the image processing chamber, the visual sensor is activated and sends the frame capturing command to the control unit. It should be noted that the camera is on and is ready to receive commands from the control unit during the entire operation.

As soon as this signal is received, a frame of the camera is saved, and all processing steps are performed on the images. By terminating the processing and dimension extraction steps, these data are sent to the controlling unit. Since, in this device, it is possible to clean three fish simultaneously along with the device, the data related to each fish are processed with the relevant indexes in MATLAB, and similar indexes are substituted in data reception functions of the TiaPortal software.

The data transferred for the fish sample are:

1- Length of the fish from the gripper to the end of the trout head

2- The distance from the gripper to the anal fin (belly cutting start point).

3- The distance from the gripper to the pectoral fin (head cutting point)

4- Penetration depth (to determine the rotary belly cutting and suction tube penetration

Although the data is sent to Tia Portal software, in order to use it in the next steps, it is necessary to store each of these data in the relevant receive functions. By storing the data and matching the index of each fish sample in the cutting stations with the initial number of fish, the desired fish size for the cutting operation is obtained. This will store the data for each instance in the corresponding function and be used in later steps to avoid data overlapping. In other words, after determining the fish number, new indexes with a sequence of 3 are created and assigned to each of the data receiving functions. As soon as the fish number is equal to any of these numbers, the receive functions are activated, and the number assigned to each sample is stored in the corresponding block.

As the new fish sample arrives, the data is updated older numbers so that data from each sample is available until the end of the fish cleaning path. In fact, one number is assigned to the fish sample as it enters the machine vision section, and another number is assigned by the sensors in each of the fish cleaning subsystems. In these functions, the equal operator is used so that while the number of the fish in the machine vision unit is equal to the number of fish in each of the cleaning stations, the relevant data is allocated to perform the cutting process. In order to control the system operation, especially in manual mode, besides the sensors and physical keys used in the device, the WinCC toolbox of Tia Portal software was used.

The trout processing machine was designed in CATIA software. In the next step, to extract the required force and torque in each of four subsystems (belly cutting, head cutting, gutting, and cleaning subsystems), Adams software was used. By extracting this result, machine fabrication was simultaneously conducted together with design optimization.

2.7. Results

In addition to the analytical results extracted by the software, some of the results were calculated in the initial step. This part of the results is related to the working capacity and processing quality of the operators during machine functioning. The results are related to the amount of fish movement in each of the capacities of the device.

By increasing the feeding rate, the fish transfer speed increases. Since it is desirable to increase the capacity of the system, the appropriate solution is to increase the penetration rate of the blades in the fish. In addition to the analytical results extracted by the software, some of the results were calculated in the initial step. This part of the results is related to the working capacity and processing quality of the operators during machine functioning.

As three different feeding rates were tested in Adams software, the functioning of the system and stepper motors and any other actuators such as the pneumatic jacks were selected based on the maximum value among the values of the feeding rated. As it is definite, to ensure the proper function of the system, the largest value must be selected to choose the driver motors. Therefore, the extracted value of the system in a feeding rate of

10 fish/min was selected in all four operating subsystems. In the image processing section, the fish length and any necessary data were extracted for system functioning. To have the required functioning data, the calibrated fin position is sent to the control unit. The controlling unit sends signals and pulses to the processing actuators of trout fish.

2.8. Conclusion

Today, due to the increase of industrial automation in various industries, the need to design and manufacture automated devices with high capabilities in the fish and aquaculture industries is required. Considering the importance of trout consumption in the food basket of people, and the increasing efficiency in production, the quality requires designing and developing systems with higher capabilities compared to previous systems is essential. Due to the slippery skin of the fish and the low friction coefficient, it is so difficult to control the fish. Since the fish processing operation is done step by step, in addition to providing fish stability, the gripper must enable different processing operations along with the system. Therefore, an automatic system with trout belly cutting, beheading, gutting, and cleaning stages on different sizes was designed and manufactured based on the extracted dimension of the image processing section.

Due to the high price of fish cleaners and the limited capabilities of the available systems, a system capable of performing belly cutting steps, beheading, gutting, and cleaning steps were designed and fabricated. Besides, because the choice of fish size is completely in line with customer order, the image processing system was used to measure trout size and extract the precise cutting points. In order to prevent any contact between the grippers and the system operators, and the automated controlling system was designed to control the system operators to process different cleaning operations on fish of different sizes together with providing the system security.

One of the most important points in designing a system that can support different operation is to choose a place at which no interfere occur with cutting and cleaning tools during the various processing steps. Therefore, the fish tail was selected as the roper region, and five grippers were fabricated and installed on the conveyor. By using these clamps, it was possible to perform different cleaning operations in an integrated system. This system is designed in a way that the fish are placed and transferred inside a V-shaped

canal. In this system, as the clamp rises, the tail is caught by the gripper fingers and pulled along the machine.

As trout image is capture and processed by machine vision, the necessary dimensions are sent to the controlling unit. In this device, five grippers are considered, in which each fish is placed independently and pulled on their back along with the machine. As soon as the gripper passes in front of the cutting blades and suction tubes, each of these tools performs the corresponding operation on the fish. After extracting the fish dimensions, the cutting arm descends to create a longitudinal cut along the fish length and returns to its initial position. In the next step, by activating the head cutting jack, the rotary cutters remove the head. As soon as the head is cut, the belly content is evacuated using suction tubes, and the fish is completely cleaned by a rotary brush.

Using this integrated system, it is possible to perform several fish processing steps. In this regard, the use of machine vision as a non-destructive and fast method in fin identification and cutting point determination will increase the system capabilities to process the fish of different types. By designing the system and simulating and analyzing the motion, a system with the highest efficiency was fabricated.

In order to improve the device, the following items are suggested:

1- Using fish identification systems rather than image processing

2- Completing fillet cutting section

3- Increasing the number of fish grippers to increase the processing capacity.

4- Using fish grippers with the possibility of catching fish from the head side and investigating cutting possibilities.

5- Omitting the final cleaning section if the filleting subsystem is added to the machine if the bone separator is designed and built.

Introduction and motivation

Introduction and motivation

Due to the slippery skin of the fish and the low coefficient of friction, it is usually challenging to control. If we want to clean the fish with a high capacity, the fish must pass in front of the cleaning tools, and the desired operation can be performed on the fish at any stage. Since the fish processing operation is done step by step, the gripper must meet proper stabilization and convenience of processing arms.

Regarding the high price of fish cleaning systems and also the limited capabilities of the available systems, a device with the ability to perform the steps of belly cutting, beheading, gutting, and cleaning the fish was designed and fabricated. Besides, since the customers choose their desired weight, the system with the accurate visual unit can facilitate the cleaning of trout fish with different dimensions.

The image processing system was applied to measure the size of the fish. In this system, as the fish is passing in front of the video camera, a frame is saved, and the related cutting points are extracted for further processes. To prevent any contact between cleaning parts with the conveyer grippers, we developed an automatic controlling algorithm to control the system operators to satisfy the safety of the system operation in different cleaning stages.

3.1. Studies conducted on designing and fabricating fish processing systems

Buckingham et al. (2001) developed a head-cutting fish cleaner in their design. In their prototype, the fish was held using two metal plates to separate the fish head in the appropriate place. In order to cut the head, they proposed another mechanism to keep the head in the right position while gripping the body. The designed clamp only allowed the system to cut the head. In this system, the fish was held steady and the head cutting tool cuts the head by moving toward the fish.

In another system, De Silva and Wickramarachchi (1997) designed a machine to cut the fish head into different sizes. In this machine, the fish were moved using a conveyor chain system. On the conveyor, stainless steel semicircular seats were provided for each

fish. In this model, as the fish passes over the conveyor, the holding arm from the top of the line approaches the moving fish in the proper position for head cutting, together with stabilizing. Like the previous model, this machine was only able to cut the fish head. The difference between these samples with the model designed by Buckingham et al. (2001) is the processing condition of the fish (stable or moving fish). Due to the high inertia of the cutting tools, it is preferred to process the fish while moving with minimum movement of cutting tools. On the other hand, the capacity of the system is high if the fish moves in front of the cutting arms. Therefore, the system used by Da Silva and Wikramarachi (2006) is in the design priority in terms of meeting the proper dynamic conditions compared to the system designed by Buckingham et al.

In another system, Lang et, al (2008) designed a device for cutting salmon heads. In this machine, the fish were placed manually in their seat and then transported to the cutting position by a hydraulic jack. In order to provide linear motion of the system, a rotary motor was used to convert rotational motion to linear motion. This device was also developed to catch fish for beheading.

Grosseholz and Neumann (2008) designed a device for cutting and cleaning trout belly in which the tail was caught by two rotating fingers. After placing the fish in the appropriate place, the fingers are closed to catch the tail, and the fish is moved along the conveyor. Since the system was designed only to cut and clean the contents of the fish belly, the fish carrier also moved with the fish, like a conveyor chain. Compared to the previous models, this system showed high capabilities in the functional capacity and sufficient accuracy in performing automatic operations of cutting and belly cleaning. A similar project was carried out by Paulsohn et al. (2010).

In another study, ketels et al. (2008) proposed a system for placing fish correctly in the processing line during head cutting. In this design, they used metal seats mounted on the chains. Since the sorted fish were fed to this system, the fish conveyer seats were designed in fixed sizes. Therefore, if the fish are of different sizes, this mechanism cannot be used unless specific conveyor chains are considered for each of the different sizes of the fish. In this design, as the fish arrives at the cutting position, a fixing mechanism fixes the fish in its position. They were fixed in place by a lowering mechanism. This mechanism is

mechanically activated by raising the tail of the fish during the head cutting process, which activated the fixing arm to stabilize the fish by pressing the body.

In the design proposed by Kragh (2007), conveyor belts consisting of metal seats were used, as the design of ketels et al. (2008). In addition to the clamp designed for beheading, another clamp was used to separate the fishbone. It should be noted that although the designed device was able to perform two different operations, two different types of clamps were used for each step of beheading and deboning. In the proposed system in the present study, in addition to the ability to perform various steps of belly cutting, gutting, and beheading, all these steps will be possible to be performed in one integrated system.

In another study, Urushibara et al. (2007) designed a device for beheading and gutting without cutting the belly. In this design, the fish were transported while lying on their sides for cutting the head and evacuating the belly content. First, by placing the fish on the fish seats, a clamp and a jack fixate the fish from the tail and body. In the next step, the same method was used to catch the fish, and the belly content was pushed out from the beheaded fish by a rotary elastomer arm while turning along the fish length. In this system, although two simultaneous operations of fish cleaning are performed in one system, it should be noted that applying pressure with a rotary rubber arm to remove the belly contents from beheaded fish will not satisfy the complete gutting and cleaning processes.

In another system, Ryan et al. (2013) designed a device to grip the fish and clean the belly content. In this system, contrary to the model proposed by Costa et al. (2010), the fish were transported downward between two support straps along with the device. One of the advantages of belt grippers compared to the finger clamps is easy supporting and transporting, but it is impossible to perform different operations simultaneously (beheading, belly cutting, and gutting). If the fish is transported between the parallel straps or conveyers, it is impossible to cut the head because of the collision of the cutting blades with the conveyor belt. This case (simultaneous beheading and belly cutting and gutting) has not been fulfilled even in devices with finger clamps suggested by previous researchers.

Kowalski et al. (2015) designed a device to catch the fish for removing blood clots near the spinal cord. This tool is only for catching fish to suck the blood and blood clots of

fish and is a single-use clamp in the fish processing industry. This clamp was applied in the fish filleting machine.

In another study, Kristensen et al. (2016) used special conveyors to carry the fish samples. In this design, unlike the previously suggested clamps, the fish are perpendicular to the moving direction and are secured by hooks from the head area. This device is recommended for the gutting process.

In another project, Ryan et al. (2017) proposed a small chain as a carrying clamp for the salmon process. In this design, the fish are mounted on a conveyor chain as soon as the head is removed. Then the belly content is evacuated so that the sharp excrescence on one side of the chain penetrates the fish's spinal cord from the inside of the abdomen. By engaging the carrier chain and moving machine direction, the deboning process is performed by cutting tools. This clamp seems to be suitable for carrying fish along with the machine for processing operations, but since it is necessary to gut and behead the trout in the current study, this gripper type cannot be applied as a suitable clamp.

Braeger et al. (2018) proposed a tool for extracting belly content. They have offered this tool for cutting fish fillets, but they have also suggested this tool for evacuating the belly content. In this system, as the fish moves towards the cutting tool, the blade contacts the belly content and removes it from the belly cavity. It was necessary to separate the fish head from the body in the previous step.

In another project, Finke (2018) proposed a device in which the material attached to the spinal cord was cleaned by two sets of rotating disks at the top and bottom of the fish. The first set of the discs guides and presses the fish, and the other set under the fish performs the cleaning operation from beneath the fish. The second set of the disks were placed opposite with angles. In this design, the fish is pulled from the tail, and the belly is downward. In order to use this tool, it is necessary to clean the belly and remove the head in the previous step.

Any of the described designs are special tools for fish gutting and beheading. In order to control the mentioned tools manually or automatically, different methods are available. Since in most of the mentioned schemes, fish processing is carried out in constant

dimensions of the fish, so the control unit sends signals from the mechanical and electronic sensors as the fish reaches to the processing position. Since in the current study, a larger range of fish dimensions will be processed, so it is necessary each of the cutting, cleaning, and suction tools can function based on exclusive data received from the image processing and control units. One of the methods to determine fish size is to use mechanical measurement sensors that operate by passaging the total fish length in front of the sensor to extract the length and other necessary dimensions, based on the fish shape.

Among the above systems, only in the two designs proposed by Paulsohn et al. (2010) and Ryan et al. (2017) a combination of mechanical and electronic sensors has been applied to detect the dimensions of the fish, which can be applied to extract the fish size and cutting points. Since in each of these systems, only a single operation of cutting or gutting is done, using these sensors is sufficient for dimension determination.

In the design proposed by Paulsohn et al. (2010), the head of the fish remains on the fish head, and only the gutting process with the details of belly cutting, suction, and belly cleaning steps are done in a single system. Also, in the system designed by Ryan et al. (2017), the head of the fish is removed in the previous stage, and subsequently, by passing through the conveyor belt, the gutting process is performed. These sensors are used while cutting and cleaning operations are performed on the belly because the exact head cutting position requires special methods like machine vision. It should be noted that even in the belly cutting process, a high rate of error appears in fish of different sizes. Therefore, using image-based methods, besides determining the size of the fish in two dimensions, the exact head cutting point can be determined based on the position of the pectoral fin. Therefore machine vision was applied to extract both trout dimension and cutting points.

A conventional machine vision system (MVS) includes an image capturing unit (camera), image processing, and statistical analysis (Hong et al., 2014). Machine vision has been used in the field of aquaculture has been used mostly for classification, sex determination, and quality assessment. Machine vision is also applied in fish post-processing steps like removing unwanted parts and cutting the fillet edges. Still, this method is rarely used for the early stages of fish processing (up to filleting). The scarcity of machine vision applications in the early stages of fish processing is the lack of an

integrated system with the ability to perform several steps. The following are examples of research conducted in this area. In order to adapt the fish cleaning system to the individual characteristics of each fish, it is necessary to provide special tools for cutting, gutting, cleaning, and gripping fish of different sizes.

3.2. Studies in the field of machine vision

In research conducted by Strachan (1993), fish dimensions were measured using machine vision. He applied a 512 x 512 camera with 8 bits per pixel. This camera was mounted on the top of the conveyor belt inside an imaging case. Fish transfer speed variations were done by changing the speed of the conveyor belt motor. In order to measure the fish length, a specific location in the image was first considered, and length changes were measured by moving along the belt per frame. Finally, the error values for parallel fish along the conveyor belt and for non-parallel fish were 1% and 3%, respectively. Also, to measure the dimensions of the fish, a transparent conveyor belt was used with underneath lighting. The processing time for each image took 0.8 seconds. Fish head and tail lengths were extracted, considering to10% of the fish length at the end and beginning of Hadook fish. In order to measure the dimensions of the fish, various methods can be used to define fish length regarding time, cost, measurement accuracy, and proper performance and purpose of the design.

White et al. (2006) also extracted the lengths of different species of fish using machine vision. In this study, they used a conveyer belt with a linear velocity of 1.5 m/s, in which the fish was placed on the belt parallel to the moving direction. They applied a camera with a resolution of 1024 × 640, where each pixel represented one square millimeter. They also performed the following steps to identify fish species:

1- Calibration of the background color once an hour.

2- Color thresholding, which was done for 20 seconds per hour to correct the threshold.

3- Detecting the fish in the images using perpendicular lines to the fish movement direction to scan the target area. If the intensity of 40% of the pixels inside the square was

different from the background, the square was shifted 2 cm to the right, and if the squares contained the desired pixels, the target (Fish) was identified.

4- Detecting the fish edges

The next five steps to detect the fish are in the following:

5- Fish orientation detection: the fish orientation was determined as soon as the major axis of the fish was defined. The angle between the major axis with the horizontal line describes the sample deviation with the moving direction.

6- Identifying fish head and tail sides: to detect head and tail sides, vertical lines along the fish length were considered from 15% of the fish length, and the larger length was considered as a fish head side.

7- For the back and belly sides of the fish: for this purpose, the average of gray intensity pixels in the upper and lower half of the fish was compared.

8- Extracting the color and shape of the fish: To achieve this goal, they used the average color and shape of the fish.

9- Fish length: to measure the size of the fish, they considered eight points along the length. These points are considered as the first point of the nose or one of the two points of the upper and lower lips. The second point was selected at 10% of the head, and the third one was considered at approximately 60%. The other point was considered at 70% of the distance from the fish head. The other four points were considered near the fishtail, including three points felt on the center axis and the final point at the end of the fish. They reported a fish length variance ratio of 1.2 mm. They applied canonical analysis to measure the length of the head, tail, and total fish length.

Misimi et al. (2008) used machine vision to sort Atlantic salmon (Salmo Salar). They used dimensional features to grade and determine the quality of the fish. These properties were extracted from binary images.

Lang et al. (2008) designed an industrial automatic fish cutting machine with automatic controlling, error detection, and remote management capabilities. Their research

included four parts related to the hardware construction, controlling and error detection design, and remote control. After fabricating the hardware of the systems, including conveyor belt, hydraulic and pneumonic system, the fuzzy position and PID control systems applied for in horizontal cutting control were simulated in Matlab software to compare with real fuzzy control / PID mode. The results of software simulation showed that if the specified conditions and the relationships between inputs and outputs are linear, the PID controller performs better than the fuzzy logic controller mode. In the unknown and nonlinear conditions, a fuzzy logic controller would be an appropriate option. In this study, they used a CCD camera to determine the proper cutting position. In addition to the first camera, another camera was used to assess the quality of the cut near the output of the machine. To monitor the performance of the system, in addition to cameras, four types of sensors were used, including four accelerometer sensors, two-position sensors, four pressure sensors, and two microphones. An amplifier was used between the data storage board and accelerometer sensors to increase the range of the sensors.

Next, they trained the artificial neural network in offline mode with the following data to identify errors:

1- Jamming fish between the blades

2- Hydraulic cylinder failure

3- Hydraulic pump failure

4- Hydraulic servo valves Failure

5- Pneumatic cutting blade failure

6- Conveyor belt failure

7- Normal operation of the device

Since the system failure could be related to each part of the system mentioned above, so detecting these failures is impossible with a single sensor. In other words, using a vibration-sensitive sensor is possible to detect the malfunction of the system, but it is not possible to determine which part of the system faces with an error. Therefore they used

multiple sensor combination technology for failure detection.

In another study, Steen Bondo et al. (2011) designed an automated line for slaughtering and cutting fish heads using machine vision. They used three-dimensional vision and applied pneumatic actuators in the cutting. They applied electric shock for numbing the fish before injuring. The machine was programmed to divide the fish entering the system into three different channels to have equal feeding rates to each of the cutting blades. Their designed system was capable of slaughtering 85-95% of the incoming fish at a rate of 30-80 salmon per minute. In the samples that had not been slaughtered successfully, the injury was done manually near the gills.

To slaughter the fish, the pneumatic jacks were equipped to narrow blades. The general structure of the device used in this study is similar to those of Storbeck and Daan (2001) and Mathiassen et al. (2006) with the difference that in addition to all devices applied as mechanical tools, the stunning technology enabled the feeding of alive fish so that they can be processed simultaneously. It was also necessary to identify the fishtail and head sides in order to make an injury on the right side. On the other hand, in order to create an incision in the head, it was necessary to send a cutting order to the control unit. Based on the written algorithm, the incision must be done at a distance of 10 mm from the gill arch of the fish. Since various factors are involved in determining the proper location of fish gills, multivariate regression was used to determine the appropriate place in which the accuracy of the system was calculated by the software based on the minimum square error.

After segmenting the image, some geometric features such as area, volume, maximum height, width, and deviation of the fish and in total, 11 geometric features were extracted from the image. These indicators were considered as input for the fish head and tail detection using Linear Discriminant Analysis (LDA). In order to train the artificial neural network, the captured images during the incision step were applied. In the next step, a V-shaped blade was used to cut the head. The time and previous cutting positions were calculated, taking into account the arrival time of the new blade, and the head was separated by the cutting blade. For optimal beheading, different blades were tested. Despite the high shear force compared to the V shape blade, they selected a W-shaped blade because of the proper cut. Their results showed that among 1531 salmon and 681 trout fish,

1327 salmon and 640 trout fish were cut correctly, respectively. Out of the total number of fish, 201 and 36 fish were not cut, and four and five fish were cut from the wrong place, respectively.

In another study, Hu et al. (2012) used color and texture characteristics to classify different species of fish. In this machine vision system, the images taken from the mobile phone were sent to the processing system to analyze the color and texture of the images. They provided the best classification based on the extracted feature from the HSV color space.

Costa et al. (2013) measured the size, direction, and heterogeneity of fish based on edge analysis. In this study, the edges were extracted by the image processing algorithm. Their research aimed to develop tools for online grading of bass species to detect the size, sex, and heterogeneity. Using this method, the size estimation based on weight was obtained with a correlation coefficient of 0.9772 compared to the conventional method of measuring length with a regression coefficient of 0.9443. To identify fish species and also to identify fish with inappropriate shape, they used partial least squares detection analysis, which detected 82.50% and 88.21%, respectively.

Dowlati et al. (2013) used machine vision to predict the freshness of the golden head fish. For this purpose, changing the color of the eyes and gills of fish was considered as a criterion for predicting fish freshness and quality. They used RGB and L * a * b * color spaces to segment the eye and extract the features. Poonnoy et al. (2014) also classified boiled shrimp using shape features as relative internal distance (RID). They used red, green, and blue channels to extract these features.

Teimouri et al. (2018) classified different parts of the chicken using intelligent modeling based on machine vision. They used both linear and nonlinear methods for classification. To analyze the effect of speed on classification accuracy, they set two different velocities of the conveyor belt, including 0.11 m/s- and 0.22 m/s were considered. They reported the total accuracy of 94% and 93% for classification in two speeds, respectively. Taheri-Garavand et al. (2019) also examined the freshness of Ramvard fish by real-time monitoring. In this study, they used color image processing of R, G, B, H, S, I,

L *, a *, and b * channels. After reducing the input data dimension, fish freshness was predicted by a neural network, support vector machine, and K-nearest neighbor methods.

In the current study, an automated system is designed for trout beheading, gutting, and cleaning. As this system consists of mechanical, controlling, and machine vision sections, the whole system needs an accurate design and synchronization. The mechanical system was designed in Catia software and simulated in Adams simulation. All the constraints and real conditions were applied in simulation to extract the required forces and torques. At the next step, the controlling algorithm was developed in TiaPortal v15 software and tested to solve any errors. Then, to send the extracted data from the machine vision unit to the control unit, we applied the TCP/IP protocol. Finally, by installing all the magnetic and inductive sensors, pneumatic cylinders and actuators, and controlling panel on the mechanical system, machine functioning was synchronized and calibrated.

Research objectives

Research objectives

The main goals of this thesis is to design, fabricate, and evaluate a trout head and belly cutting and cleaning system which is expected to achieve the following sub-objectives:

1. Designing and fabricating the mechanical part of the system, including the main body, grippers, beheading, and gutting subsystems.

2. Implementation of electrical and controlling parts of the system

3. Providing an algorithm in order to properly identifying and detecting the trout together with defining fish length and width, cutting points, and cutting lengths.

4. Evaluating the accuracy of the developed algorithm to determine the appropriate head and belly cutting points to compare with the actual points.

5. Implementing the online of the controlling and image processing algorithm evaluating the system process.

6. Qualitative evaluation of the processed fish and visual and quantitative assessment of the cleaned fish in terms of proper cutting of the head to prevent fillet loss.

Physiology of trout fish

Physiology of trout fish

Trout, with the scientific name "*Oncorhynchus mykiss*" is from the salmon genus. It has 19 bones in the caudal region with 60-66 bone nuts in its back. The color of salmon changes from blue to olive green and converges to pink and light silver at the bottom. There are also small black spots on the sides, including the head and fins. The color of this fish changes depending on its size, habitat, growth, and fertility conditions. The color of fish that are grown in the rivers are darker, while those are grown in ponds are lighter and more inclined to silver (FAO 2013). This species of fish can tolerate a wide range of different temperatures from zero to 27 degrees Celsius. The appropriate temperature range for aquaculture should be less than 21 degrees. Trout fish are bred in most countries, but the production rate is insignificant compared to European countries, North America, Chile, Japan, Australia, which are comprehensively planned to breed and produce (FAO 2013). The distribution of trout production in the world is shown in

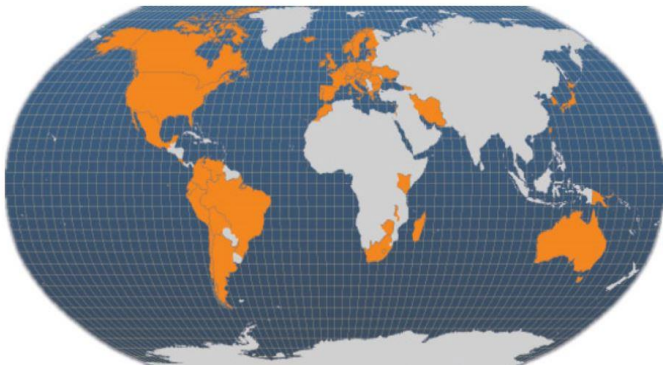

Figure 5-1. Torut Fish production distribution

Compared to other species, tout has a high spawning rate, high growth rate, and high resistance to the environmental and breeding methods. Depending on the ecological conditions, trout fish hatch from 100 days at a temperature of 3.4 degrees Celsius and up to 21 days at a temperature of 14.4 degrees. After a short period, these fish should reach ten percent of the desired weight in 2-3 weeks. The fish are then transported into special containers with 2 x 2 m and a height of 50-60 cm to obtain sufficient oxygen and access to massive water flow. Trout can be supplied after about nine months when it reaches 30-40 cm. Some of these fish are also bred for more extended periods and are available in larger sizes (FAO 2013). To comply with economic principles and prevent food loss, fish

producers stop feeding three days before fishing, so that their stomach is as empty as possible. This fish is supplied both in fresh and frozen conditions. It should be noted that the shelf life of this fish is 10-14 days in the frozen state without cleaning and gutting.

5.1. Trout fish processing steps

Fish sorting with the sorter systems will reduce costs as well as increase production rate and efficiency. This process increases the final quality of the product, but requires an initial investment and carries with structural complexities (Booman et al. 1997). After sorting the fish, it is time to supply them in markets. In small and large fish centers, highly demanded fish species are usually available in different sizes. The fish are generally opting based on the size, and it is cleaned on the customer's request. Usually, in fish supply stores as well as aquaculture processing plants, cleaning the fish involves some cleaning steps, or all the cleaning steps are done In the case of non-processed fresh fish, some prefer gutted fish; others opt for gutted and beheaded, or just in fillets. It should be noted that trout scales are finer compared to other species, and it can be processed without scaling. Trout cleaning steps are shown in Figure 5-2.

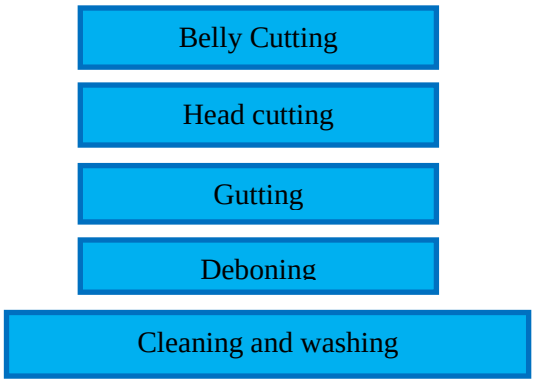

Figure 5-2. Trout fish processing steps.

Due to the broad automation in industry, the need to design and manufacture automated devices with high capabilities in the fish and aquatic processing industries is of great importance. Because of the importance of fish consumption in the food basket and the need to use automatic industrial devices to increase efficiency and improve the quality of fish processing, the need to design and develop systems with higher capabilities

compared to the current models are essential. In fish processing factories and fish supply stores, it is necessary to stabilize the fish for any cleaning operations properly.

The initial evaluation was required to design the device to obtain basic information on trout. Therefore, a number of fish were applied to get the primary data. So the number of the

5.1.1. Initial samples (before starting system fabrication)

In this study, in the first stage and before fabricating the device, 97 samples of salmon from 262 g to 622 g with an average weight of 421.88 ±78/04 kg with the total weight of 36.5 kg were considered. These samples were randomly selected from fresh fish in the self-service restaurant of the college of agricultural and natural resources of the University of Tehran. These samples are shown in Figure 5-3.

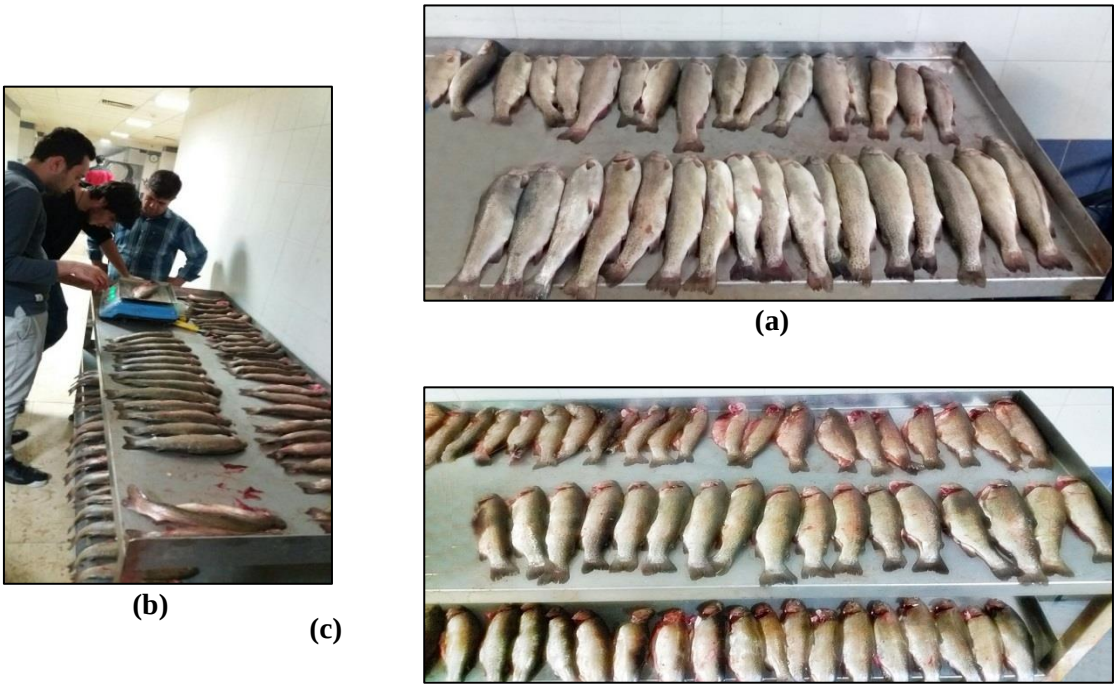

Figure 5-3. The applied fish sample in the initial stage of the study to weight, measure, and capture the images: a) unprocessed samples, b) weight measurement and c) samples after processing (gutting).

The dimensions and weight of the fish samples in the initial stage are presented in Table 5-1. A digital balance with a measurement accuracy of 0.1 g was applied to measure

the weight of the samples. A standard ruler was used to measure the length of the fish, and a digital caliper with an accuracy of 0.02 mm was applied to measure the smaller dimensions.

Table 5-1. Weight and Dimension of the trout in the offline stage

	Dimension (mm)					Weight (g)		
	(L)	(W)	(T)	(D1)	(D2)	(W1)	(W2)	(W3)
Minimum	365	60	30	41.5	54.5	222	182	138
Maximum	395	90	50	59	73.5	622	510	474
Average	334.1±24.3	77.9±5.8	40±3.8	48±3.4	62.2±3.9	421.9±78	344.9±64.9	310.5±61

In this table, (L), (W), and (T) are the length, width, and thickness of the fish, respectively. D1 and D2 are the distance from the fish lips to the center of the eye pupil and the end of the fish gill, respectively. It should be noted that these samples were also used to develop the image processing algorithm.

5.1.2. Second set of the samples

In this stage, 100 trout samples were selected in the fish marketing center at Tabriz-Iran. An image was captured from all the samples, and the weight and dimensions of the samples were measured for 50 randomly selected samples. Unlike the initial stage, the fish were placed inside a V-shaped canal; so that the back of the fish was placed inside the canal. The images were also captured from all 100 fish samples. Table 3 shows the changes in length, width, and weight of the measured samples.

Table 5-2. Dimension and weight of trout in second stage

	Dimension (mm)					Weight (g)
	(L1)	(L2)	(L3)	(L4)	(W)	(W1)
Minimum	350	300	225	60.5	33	475
Maximum	510	460	350	100	83	1750
Average	443.9±33.9	386.4±37.4	300.3±30	76.9±9	65.7±12.7	1124.3±314.9

In Figure 5-4 the measured dimensions are presented. These dimensions are used to transfere the vision based data to the control unit.

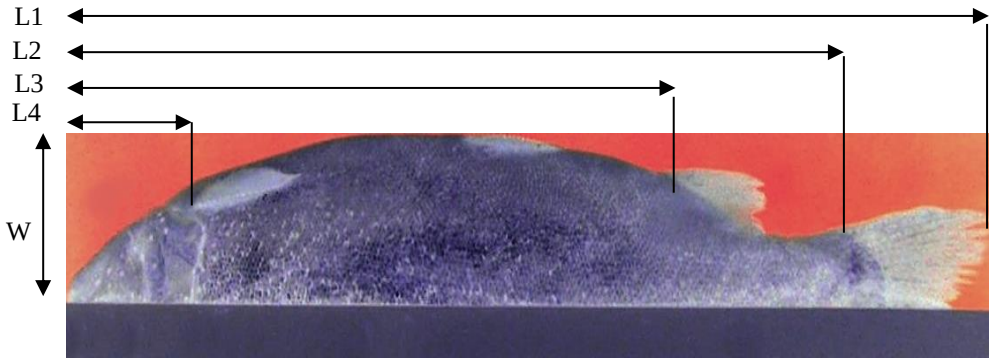

Figure 5-4. The measured dimensions for camera calibration in the online stage.

Mechanical design, simulation, and fabrication

Mechanical design, simulation, and fabrication

In general, the system consists of the following units and subsets:

1- Image processing case and a digital camera.

2- The main chassis of the device which is the combination of stainless steel (in wet parts) and painted steel.

3- Fish carrier subset (grippers)

4- Belly cutting subsets: a 0.25 hp AC electromotor, stainless steel arm carrying rotary shafts, belt and pulley, motor shaft and blade shaft, rotary cutting blade with a diameter of 100 mm and a thickness of 1.5 mm, stepper motor, power screw connected to the stepper motor and the nut connected the cutting arm.

5- Head cutting subset: a pneumatic jack, two ribbed rotary blades installed in the angle of 90 degrees with opposite revolution, two air motors for rotary blades, a small frame carrying the moving components, and a set of wagons and guide rails used to guide the entire assembly in the vertical direction.

6- Gutting subsystem: one stepper motor with a mounted gear, two rack gears, two suction tubes with different diameters for small and large fish, and a set of wagons and guide rails to move the rack gears in the vertical direction.

7- Belly cleaner subset consisting of a 0.25 hp AC electromotor, stainless steel arm carrying rotary shafts, belt and pulley, motor shaft and blade shaft, rotary cleaner brush with a diameter of 125 mm, and pneumatic jack.

8 -Pneumatic system.

9- Controlling and transferring system the send the command to the motors and driving arms of the device

6.1. System Design

In the first step, the initial model was designed by CATIA software and the Structure

of the machine was fabricated. Then some necessary parts such as conveyor chains and gears were provided. By entering the exact dimensions of these parts in the software, other parts of the device were designed and the other steps were done in the same way.

To fabricate the main chassis of the system, we applied 40 × 40 mm steel with a thickness of 2 mm was used. In the construction of the internal parts of the chassis, especially the parts that are in contact with water, the stainless steel part and profiles were applied. These majorities of these parts are located near the fish passing channel and fish gripper section.

To enable different fish processing steps in this system, we considered the dimensions of the chassis 2.8 m in length, 0.85 m in height, and a width of 0.7 m. Under the main chassis of the device, carrier wheels with stabilizing bases were considered, so in addition to easy movement of the device, the longitudinal and transverse alignment of the system is possible.

6.1.1. Fish carrying subsystem

One of the most critical points in designing a system with the ability to perform different trout processing stages is to consider a place in the fish body which avoid interfering with cutting and cleaning tools during the various stages of cleaning. Therefore, the tail of the fish was selected as the appropriate area.

The fish carrier subsystem consists of four main parts:

1- Fish grippers

2- Gripper guides and fish canal

3- Driver AC motor

4- Gripper conveyer

6.1.1.1. Fish grippers

Using the grippers suggested in this dissertation, it is possible to perform different steps of fish processing in an integrated system. To increase the capacity of the system (number of fish per minute), we considered a balance between the length of the system and the number of grippers so that with the maximum number of the grippers in the conveyor

length, a sufficient space provided for the system operators. Therefore, in this design, five sets of grippers were considered. Each set of grippers includes the following parts: a) Driver and driven gears, b) steel shafts, c) shaft bearings, d) return springs, e) polyethylene blocks, and f) gripper finger and stainless steel screws to connect the upper and lower blocks.

In Figure 6-1 the grippers with the detailed components are presented. As shown in this figure, the fish is caught using the fingers (5) on the shaft (4). These fingers are connected to the shafts using screws (6). By rotating the shafts, the fingers rotate and press the ribbed surface (8) onto the fishtail, gripping the fish. These fingers are connected to the shaft (4) by screws (6). In order to convert linear movement to rotational motion, four gears were used in this system. in this design, the gears (10) were considered as the driver gears, and the gears (17) were considered as the driven gears. The stainless steel appendixes (11) were connected to the gears (10) by the welding process. The gears and internal parts of the clamp are shown in Figure 6-1. The driver gears (10) shown in this figure are located on steel shafts (9) with a diameter of 12 mm and a length of 185 mm. Similarly, the driven (17) are mounted on steel shafts (4).

The inner diameter of the driver and driven gears are 12 mm, the outer diameter is 35 mm, and their thickness is 12 mm with a modulus of 1.5. To achieve the rotation of the shafts as well as the proper gear stabilization, we used two bearings (12) with 6000-2NSE standard with an outer diameter of 26 mm, a thickness of 8 mm, and an inner diameter of 10 mm was applied in the top and bottom of the gears. The bearings are shown in Figure 6-1-b. These types of bearings have covers on both sides to prevent the possible permeation of moisture and water into the interior.

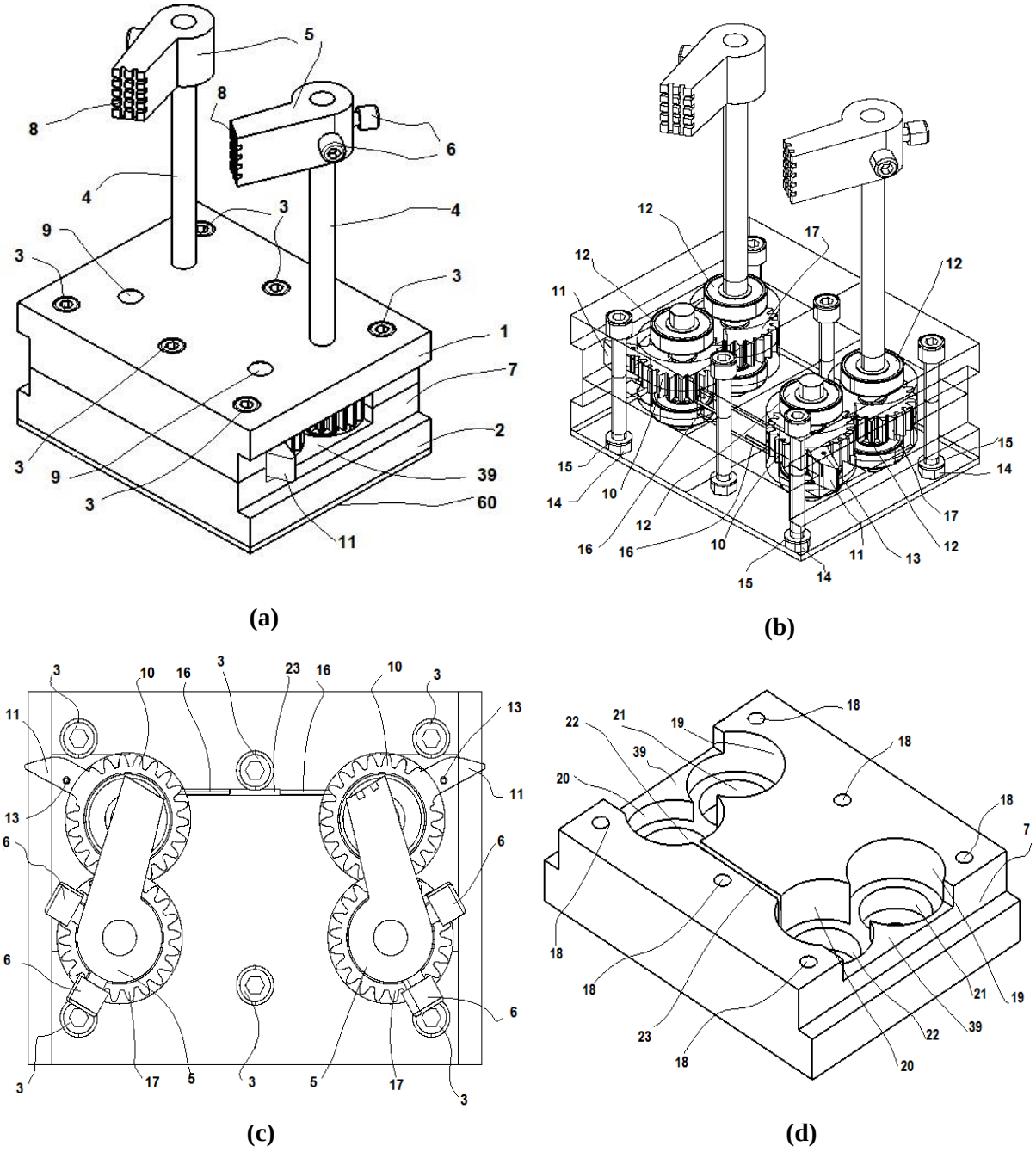

Figure 6-1. Fish gripper design: a) 3D view of the gripper set with the fingers in the open position, b) internal components of the gripper, c) lower block, d) 2D image of the gripper with the driver and driven gears.

In order to assemble the internal parts inside the body, the clamp consists of two separate blocks, upper (1) and lower (2) blocks. The dimensions of these blocks are 140 × 110 × 30 mm, and they are made of polyethylene. In each of these blocks, four holes were

created. In order to ensure the free rotation of the gears inside the clamping system, the depth of each of these holes was considered as 15 mm. Then another hole with a diameter of 26 mm with a depth of 8 mm was made on the holes of the gears to place the bearings.

Figure 6-1.d shows the location of the driver gears (10), driven gears (17), and bearings (12) on the lower block (2). In this figure, the holes (18) correspond to the screws (3). Similar holes are made in the upper block of the clamp. Holes (19) and (20) with a diameter of 36 mm were made to accommodate the driver (10) and drive (17) gears, respectively. This figure also shows the location of bearings for shafts (4) and (9) with the numbers (21) and (22), respectively. The grooves for the returning springs (16), the rail groove (25), and the movable gear tab groove (11) are represented by the numbers (23), (7), and (39), respectively.

In order to connect the clamp assembly to the chain, a 304-grade steel plate (60) with a thickness of 2 mm and with dimensions equal to the upper and lower block of the clamp was used. This steel plate was connected to the chain (34) by welding operations. In order to provide linear motion of the gripper assembly inside the rails (25), a longitudinal groove (7) with a depth of 6 mm and a width of 15 mm was created along the side edges of the upper and lower blocks. In the next step, to provide free rotation of the driver gears and the welded tongue (11, a groove (39) with a length of 50 mm, and a width of 9 mm was created on each of the blocks inside the groove (7).

Figure 6-2.a shows the return springs and other components a three-dimensional exploded view. By placing the fishtail between the fingers of the clamp, the fish is gripped and pulled along the device. Figure 6-2.b shows the fabricated components of the gripper.

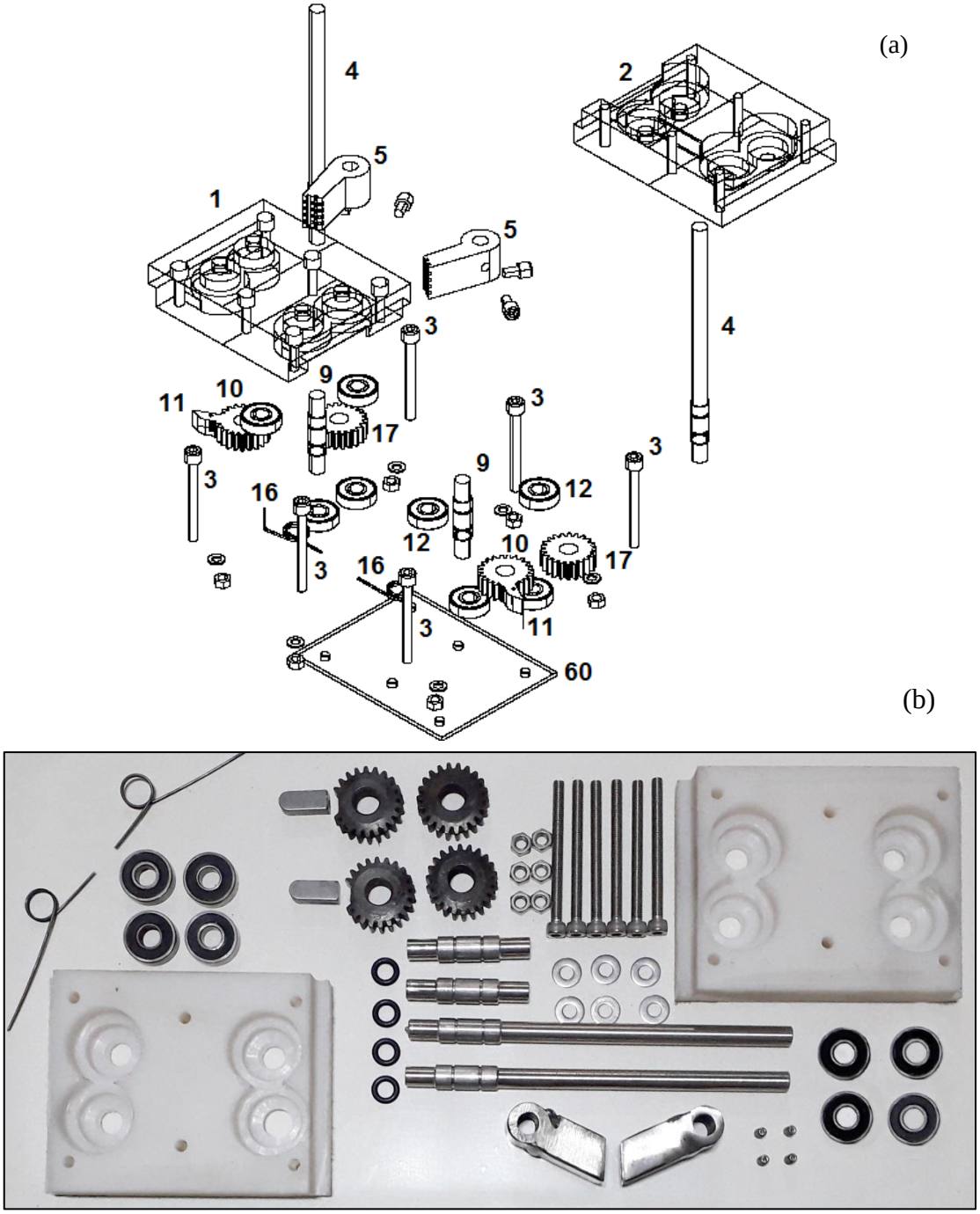

Figure 6-2. The internal components of the gripper: a) the exploded view and b) fabricated components.

6.1.1.2. Gripper guide, fish canal and conveyer chain

In order to avoid the contact between the gripper finger with the fish carrying canal, the entrance and exit of the canal were cut of (37) from the proper position.

Figure 6-3 shows the machine driver subsystem, gripper sets, and gripper guides. By moving the grippers towards the guides (25), the gear's fingers contact the guide, therefore the fish is clamped and the gripper assembly is supported in line while the groove (7) is set with the guides.

As shown in this figure, by contacting the gripper tabs on the steel rails (25), according to Figure 6-1.b, the driver gears (10) on the left and right sides of the gripper set, Rotate counterclockwise and clockwise, causing the left and right driven gears to rotate clockwise and counterclockwise, respectively. This brings the left and right fingers closer and grabs the fish's tail between the clamps. As the actuated grip (26) reaches the end of the rail (25), the fish is detached from the gripper, and the fingers return to their initial position. To guarantee the proper returning of the driver gear to the initial position, we applied springs (16) on the shafts (9).

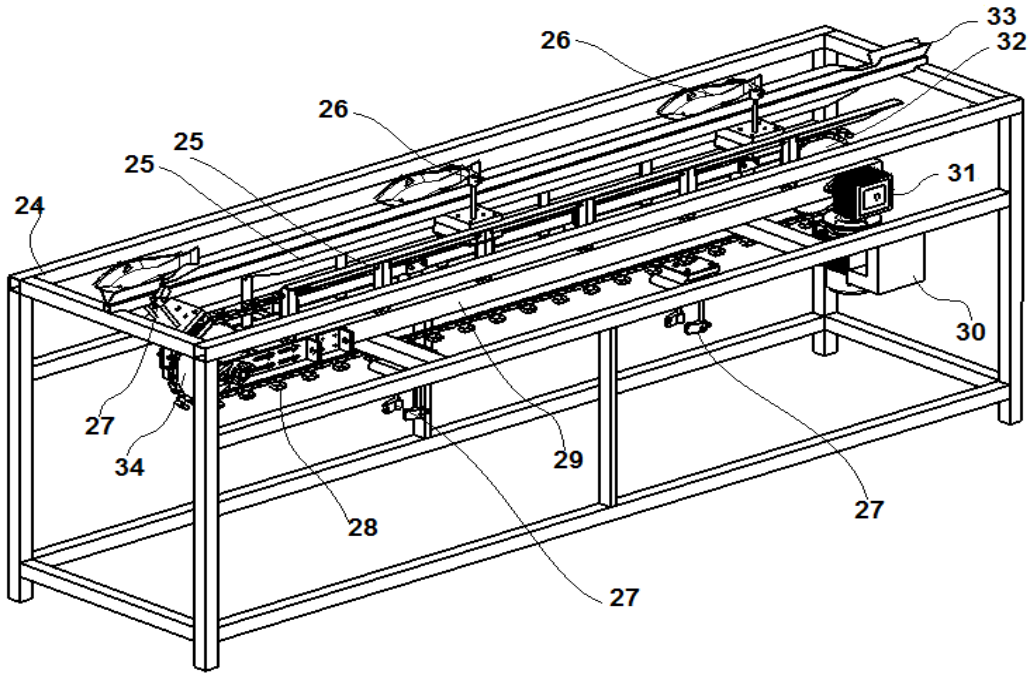

Figure 6-3. Main chassis of the system, the moving parts, gripper guide, and fish canal

As shown in Figure 6-3, the chain (34) is driven by the drive gear (32) attached to the motor-gearbox set (31). To supply the conveyor chain power, a 0.5 hp AC electromotor with 1: 40 reduction gearbox (TS Transmission, NMVR 040, i40) was applied. In order to

adjust the rotational speed and avoid changing the engine torque, an inverter a TECO, 220V, 4kw was applied.

Two adjustable sliders (35) were also used to install and adjust the chain stiffness. In order to stain and increase the wear resistance of steel gears, hard chrome electroplating operation was used. To transmit the power from the motor to the grippers, we selected a stainless steel chain with the length of the 4800 mm. By dividing this length into five equal parts, the distance Dg resulted in 960 mm. Since five clamps are designed to catch the fish, it can be considered that 5+1 fish will be processed in one complete turn. Figure 6-4 shows schematic view of the chain and grippers.

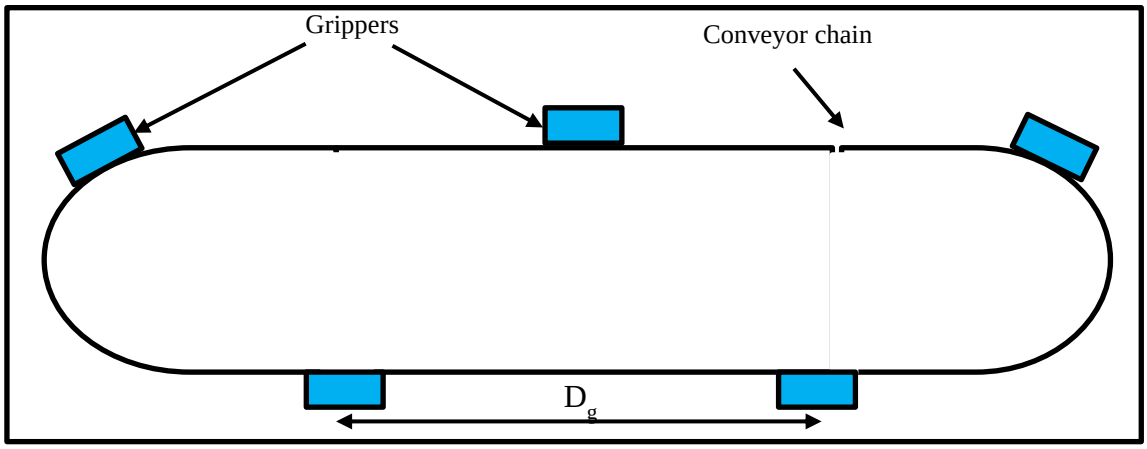

Figure 6-4. Conveyor chain and the grippers with the gripper distance of Dg

This figure shows the gripper position and the conveyor chain with the gripper distance (Dg). Now, if the complete cycle of the conveyor chain is performed for one minute, the number of six fish per minute will be processed by the machine. Under these conditions, the linear velocity of the carrier chain will be calculated using the equation 3.1:

$$\boldsymbol{v = \frac{x}{t}} \qquad 3.1$$

In this equation, “v” is the linear velocity (mm/s), “x” is the length of the carrier chain (mm), and “t” is one complete path of the chain (60 seconds). Based on equation 3.1, we considered six fish to be processed in one minute; the linear velocity will be calculated 80

mm/s. Other linear velocity values in different processing capacities are presented in Table 6-1.

Table 6-1. The linear velocities in different system capacities

System capacity	M_F_4	M_F_5	M_F_6	M_F_7	M_F_8	M_F_9	M_F_10
Linear velocity of the conveyer chain (mm/s)	53.33	66.66	80	93.33	106.66	120	133.33

As shown in this table, by increasing the system capacity from four to ten fish per minute, the linear velocity increased from 53.33 mm/s to 133.33 mm/s. These values are the base inputs for designing and simulating the system in Adams software.

6.1.2. Belly cutting subsystem

The function of this subsystem is to make a longitudinal incision in the trout belly from the beginning of the anal fin to the pectoral fin. The belly incision subset consists of the following components:

1- Power screw bearings
2- Stepper motor moving arm
3- Power screw
4- stepper motor frame
5- belt and pulley
6- Rotary cutting blade
7- Blade shaft
8- Rotary blade
9- AC electromotor
10- Electrometer’s shaft and bearings

Figure 6-5 shows the position of the belly cutting subsystem in the machine together with its components.

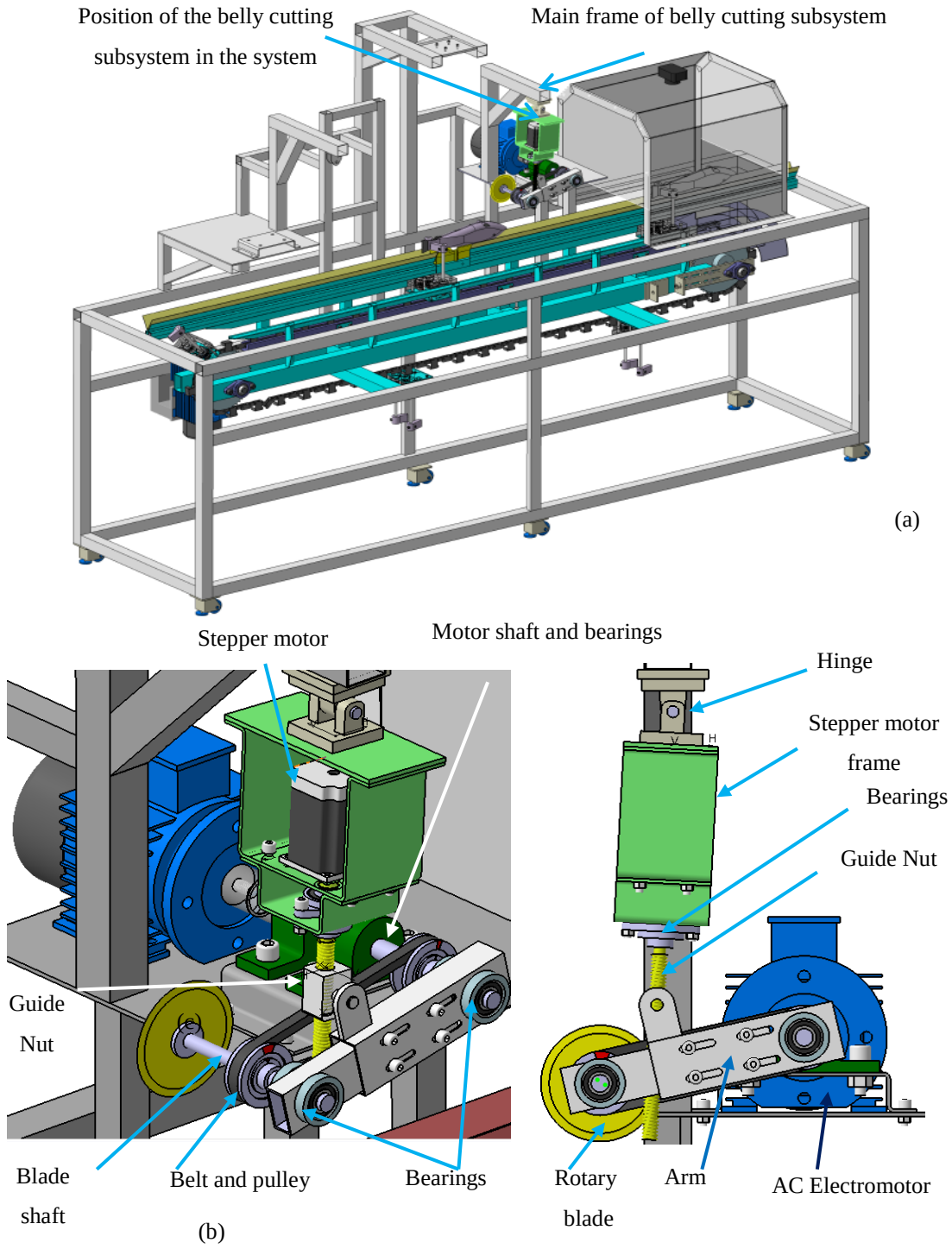

Figure 6-5. Belly cutting subsystem: a) position of the belly cutting subsystem in the system, b) belly cutting component in isometric view, and c) the belly cutting components in front view.

After extracting the required dimensions, the first step in device operation is to make a longitudinal incision in the abdomen of the fish from the anal fin to the pectoral fin based

on fish size. By sending the commands from the control unit to the stepper motor, the carrier arm moves downward, so the rotating blade cuts the belly. After cutting the abdomen, in order to avoid any contact between the blade and the subsequent fish gripper, the arm is raised again and placed in its home position. An AC 0.25 hp electromotor with a rotating speed of 1400 rpm was used to provide blade rotation. To transfer power from the electromotor to the blade, we applied a belt and pulley system.

A power screw is a device for changing the angular motion to linear motion. (Budynas et al., 2011). As mentioned above, the cutting arm converges the fish belly while the fish is passing in front of the rotary cuter. The position of the arm in a vertical direction and the stop time I cutting position is based on the dish dimension. Therefore, a power screw with a standard pitch of 3 and the outer diameter of 13.8 mm was selected according to the position of the electromotor and the minimum and maximum displacement length. In the next step, in order to determine the proper stepper motor and also to determine the lifting arm speeds in dynamic mode, the selected screw was modeled in Catia software. To model this screw in the software, power screw relations were applied in both screw and nut designing steps. Figure 6-6 shows the dimensions of the trapezoidal power screws.

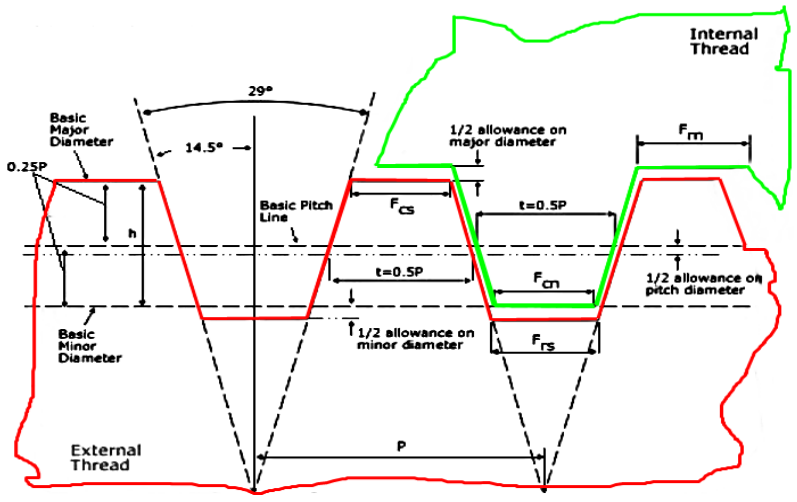

Figure 6-6. The cutting view of the power screw with the related signs and tooth angle.

The following equations have been used to model the power screw and its nut: The tooth angle between the power screws is 29 degrees. The allowable limit value (ac) in the inner diameter of the screws and the inner diameter of the nut equals 0.25 mm in the

screws with ten teeth in less than 25.4 mm. For the other modes with more teeth, the "ac" value is 0.125 mm. The allowable step limit (ap) for screws with a diameter of 11.11 to 14.29 mm is 0.0057. Other related values were calculated according to the following equations:

$$p = 0.5p \tag{3.2}$$

$$h = 0.5p \tag{3.3}$$

$$t = 0.5p \tag{3.4}$$

$$F_{cn} = 0.3707p \tag{3.5}$$

$$F_{cs} = 0.3707p - 0.259 \times a_c \tag{3.6}$$

$$F_{rn} = 0.3707p - 0.259 \times a_c \tag{3.7}$$

$$F_{rs} = 0.3707p - 0.259 \times (a_c - a_p) \tag{3.8}$$

In these equations, p, h, and t are the pitch, gear height, and gear thickness, respectively. Also, Fcn and Fcs are the size of the gear crown in the nut and screw, respectively. Frn and Frs also indicate the size of the root in the nut and screw, respectively.

Since it is not possible to access the exact dimensions of the power screw, especially its nut, with these relationships, the sample power screw, and its nut were modeled in CATIA software. The proper modeling of the nut and power screw was modeled to achieve accurate results by Adams software. As the stepper motor raises the cutting arm, it is essential besides the free connection of the screw nut relative to the main arm, the frame of the stepper motor also rotates around the Y-axis. By rotating the stepper motor and subsequently rotating the power screw, the nut moves upward or downward. As the nut

rises, the cutting arm comes upward, which shortens the distance between the motor and the nut, and consequently increases the angle of the motor seat relative to the vertical line. Therefore, a hinge was applied between the stepper motor frame and the main body.

6.1.3. Head cutting subsets

Like other designed parts of the system, including the main chassis, the fish head cutting subsystem was also designed in CATIA software. Since the fish is moving along the system, it is necessary to provide the best head cutting condition. In order to have a proper cut, a precise, fast cut can provide the cutting condition. Therefore a pneumatic jack was applied to carry the cutter subset. As mentioned before, when the grippers reach the beginning of the guide rails, the fingers contact the rails and the fishtail stocks between the gripper clamps. In this condition, any clamped trout is pulled along the system. Therefore, to define the system processing capacity (fish per minute), it is necessary to determine the optimal working speed. By knowing the linear velocity of the conveyor, the penetration velocity of the cutting blade will be investigated. In fact, the speed at which the cutting blade approaches the fish is directly related to the fish transferring speed. Two different types of blades have been studied for trout head cutting:

1- ‘V’ shaped cutting blade by applying sufficient force to cut the head

2- Two rotary cutting blades without extra force on the fish (two reciprocating, rotary blades with a 90-degree angle). The images of the ‘V’ shaped blades are shown in Figure 6-7.

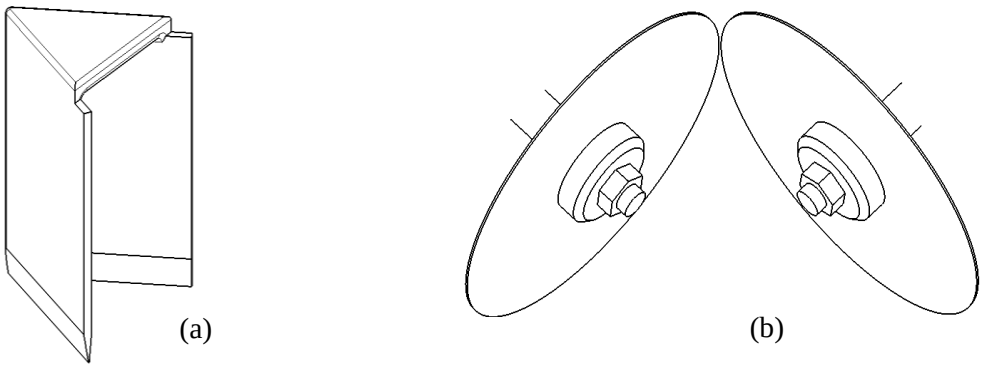

Figure 6-7. Two possibles options of the head cutter blades: a) ‘V’ shaped blade and b) rotary blade.

Figure 6-8 shows the cutting path in trout head. As the fish moves backward, CF cutting path is created to cut the head as equal as WF. During this cut, the fish head will also move backward as equal to MF. It should be noted that the mentioned dimensions will be different according to the vertical speed of the cutting blade and the linear velocity of the fish along with the machine.

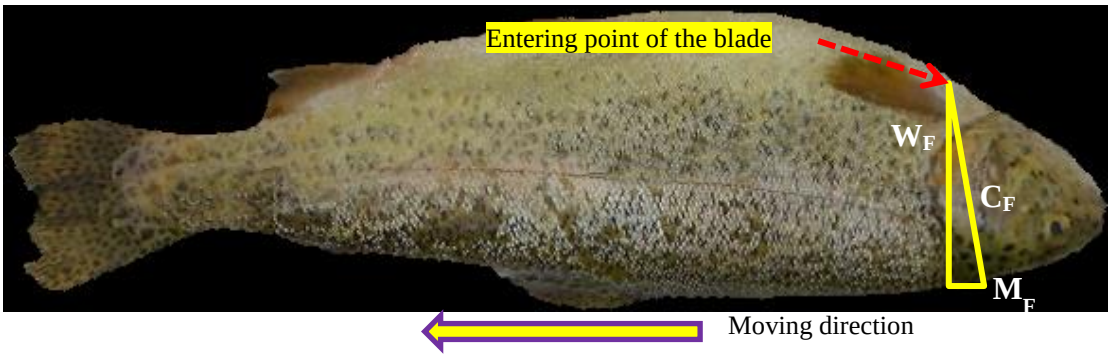

Figure 6-8. Penetration of the blade into the fish head: By moving the fish backward, the cutting blade will follow the CF path. WF and MF are the width of the fish near the head and the movement length of the fish during the head cutting process, respectively.

6.1.3.1. Investigating head cut using a typical 'V' shape cutting blade

If we want to use ordinary 'V' shape blades, it is necessary to choose higher speeds for the blade to penetrate. Another solution is to reduce the linear velocity of the fish; So that there is enough opportunity for the blade to penetrate without causing any damage on the fish or detaching the tail. In other words, if the transferee speed is higher than the vertical velocity of the blade penetration speed, the tension created along the fish will cause detaching the tail. In this type of the blade, it is necessary to install 'V' shape anti-blades beneath the main blade. Besides, to provide a proper cut, it is necessary to apply a high-velocity force on the fish head. So to control speed and absorb the force created by the blade, it is essential to install a fender, which in practice installing such parts is not possible due to the movement of the gripper sets.

Besides, using this type of blade will cause high vibration in the device. In addition, due to the movement of the fish will result in an improper cut in which the fish skin is peeled instead of precise cutting and will cause crushing of fish fillets, which affects the final

quality of the product. One possible way to avoid releasing the fish in mid-operation is to stop the chain while cutting the head, but in this case, due to changes in moving speed in different system capacities or any retard in the actuator's function, the exact timing of the system will face a real challenge. Therefore, to avoid the mentioned problems related to the 'V' shaped blade, the rotary blades were applied.

6.1.3.2. Investigating head cut using the rotary cutting blades

The condition for using the 'V' shape blade was investigated in the previous section. As mentioned above using this type of blade faces a different challenge that is not suitable for the system. Therefore, in this dissertation, the rotary blades were applied in the head cutting subsystem. Using this type of blade, there is no need to have more force on the fish which results in fillet damage or releasing the fishtail from the gripper. Besides, using theses blades provides optimal cutting at low penetration speeds. It should be noted that using this type of blades faces more design complexity together with higher manufacturing costs. The head cutting subset consists of the following components:

1- Pneumatic jack
2- Main frame
3- Two rotary cutting blade
4- Two air motors
5- Air motor fasteners
6- Timing pulleys and double tooth belt to change the rotation direction
7- Guide shafts
8- Linear sliders
9- Bearings
10- Shafts of the pulleys and blades

The details of the head cutting subsystem with the designed components are presented in Figure 6-9.

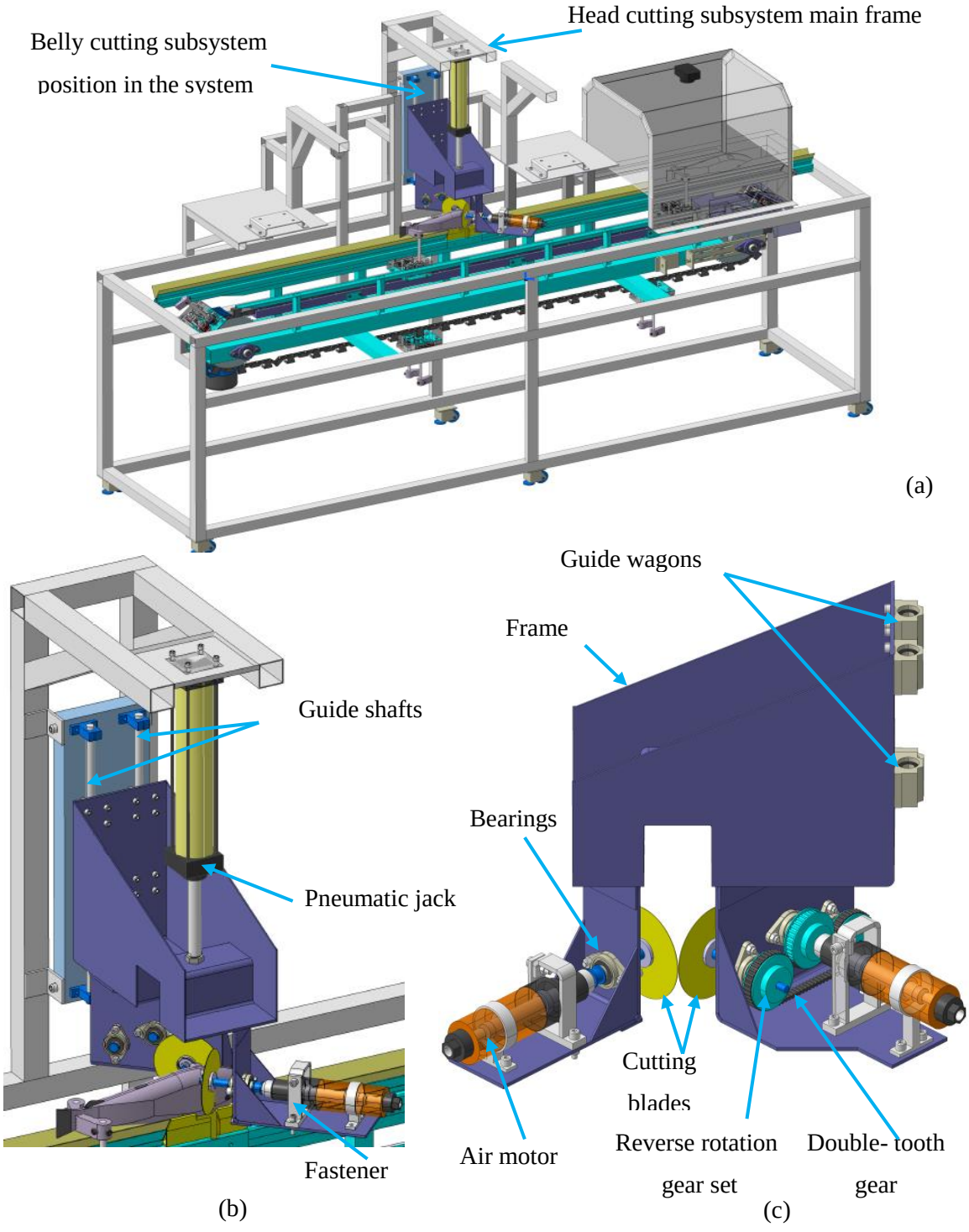

Figure 6-9. Head cutting subsystem: a) the position of the head cutting subsystem in the machine, b) isometric view of the subsystem, and c) right view of the subsystem.

As shown in this figure, two rotary blades are applied to cut the head. Since a complete cut of the fish, including bone, fillet, and the skin, is performed in the system, it is necessary to use serrated rotary blades. To achieve a proper cut, the important parameters in blade selection are diameter, number of teeth, and blade thickness. In order to have a proper cut in the head width, a High-Speed Steel (HSS) rotary blade with a diameter of 100 mm was selected.

In order to have a fast and accurate cut, it is desired to select the blade as thick as possible, but since but these blades are subjected to vertical forces, it is necessary to the trade-off between blade thicknesses and quality of the head cut. Finally, a blade with a thickness of 0.6 mm was selected. As the fish passes in front of the head cutting subsystem, the cutting subset comes down toward the fish and cuts the head while the trout are moving inside the channel. Due to this water splash in this subsystem and to avoid any damage to the driver motor, two air motors were selected.

In order to select the air motors, we tested head cutting with a typical air motor with 1800 rpm. The results showed that although the head can be cut without any stock in the motor, a higher speed is required to have the desired cut. By testing different motors, an air motor with the 2500 rpm resulted in a proper cut. Therefore, two direct air motors (VGL air pro-9198-2500rpm) were selected. In selecting these drills, the optimal rotational speed and sufficient shear force were determined based on the force required for the largest size.

As shown in Figure 6-9-c, it is necessary to provide an opposite rotation in which the fish is pressed toward the channel. Therefore, the motors on the left and right sides must rotate clockwise and counterclockwise, respectively. Since the selected motors rotate only clockwise (in back view), a counterclockwise rotation mechanism was applied. Among different possible mechanisms to change the rotation direction, the gear and pulley-belt mechanisms were investigated. Although a gear set can change a direction with just two gears, using this type of transmission system needs lubrication, especially at higher speeds, to avoid wear and reduce the friction and temperature of the gears.

Therefore, considering the challenges facing the gear mechanism and the higher cost, the belt and pulley set was used. For this purpose, three-timing pulleys were applied along with a double-toothed timing belt. As shown in the figure, by rotating the air motor in a

clockwise direction as well as engagement of the gear (1) from the outer teeth of the belt, gear (2) will rotate counterclockwise.

To transmit the power and change the direction a double tooth belt with a perimeter of 430 mm, a width of 10 mm, and a thickness of 3 mm was applied. Besides, in this set, three-timing pulleys with a diameter of 40 mm, a thickness of 10 mm, and a modulus of 5 were used. To fabricate the mainframe of the head cutting subsystem steel sheets were applied and covered with industrial paint. Finally, these sheets were joined using electric arc welding. To install the bearings and install pass the rotary shafts, the necessary holes were made according to the system design plan.

In order to install and stabilize the cutting motors, two steel clamps were designed and the groove on the air motor was placed inside the clamps. The motors finally were fastened by screw and nut. Since the speed of any actuating parts in each of the subsystems is related to machine capacity, the dynamic analysis was done to determine any necessary parameters such as velocity, acceleration, and torque. All designed parts in Catia software was imported to ADAMS software and simulated and extract the results for each part.

6.1.4. Gutting subsystem

The gutting subsystem presented in Figure 6-10. This section consists of the following components:

1- Main body
2- Sliders
3- Gide shafts fasteners
4- Pinion
5- Rack
6- Large suction pipe consisting of: stainless steel drain pipe, pipe valve, valve conductor, spring, drain pipe
7- Small suction pipe
8- Stepper motor
9- Connection shaft between the stepper motor and pinion
10- stepper motor seat frame

11- Rotary bearings

In this subset, as the fish reaches the gutting position, the stepper motor is activated by receiving the start command from the control unit and rotates in clockwise and counterclockwise directions depending on fish size. In case the size of the fish is determined as small by the machine vision section, the narrower tube enters the fish belly. In fact, the stepper motor is rotated counterclockwise, and due to the engagement of the pinion with the rack gear, the set of sliders together with the suction tube move toward the fish.

As the suction pipe gets closer to the fish belly in a vertical direction, the valve in the entrance of the suction pipe hits the barrier, causing the suction valve to open. It should be noted that due to the suction in the suction pipes, it is necessary to close all the valves in a neutral position (non-functioning position), so the suction process can be done through the relevant pipe. Since different sizes of trout will be processed in this machine, using a big tube to clean small fish will collide the fillet and bones and affect the final product quality or stack in the middle of the process line. Therefore, to avoid this problem, two different suction pipes have been applied.

The function of the gutting subsystem is such that, once of the suction pipes get closer to the fish, the other pipe raises so that preventing from any contact with the grippers. In fact, using this design instead of using two separate stepper motors for each of the suction pipes reduced the cost and complexity of design and manufacturing. In this design, as there are two suction sets in each side of the stepper motor, the pipes are in balance with each other, and the applied torque and power for the stepper motor is less than the expected condition in which one motor is applied for each of the suction sets.

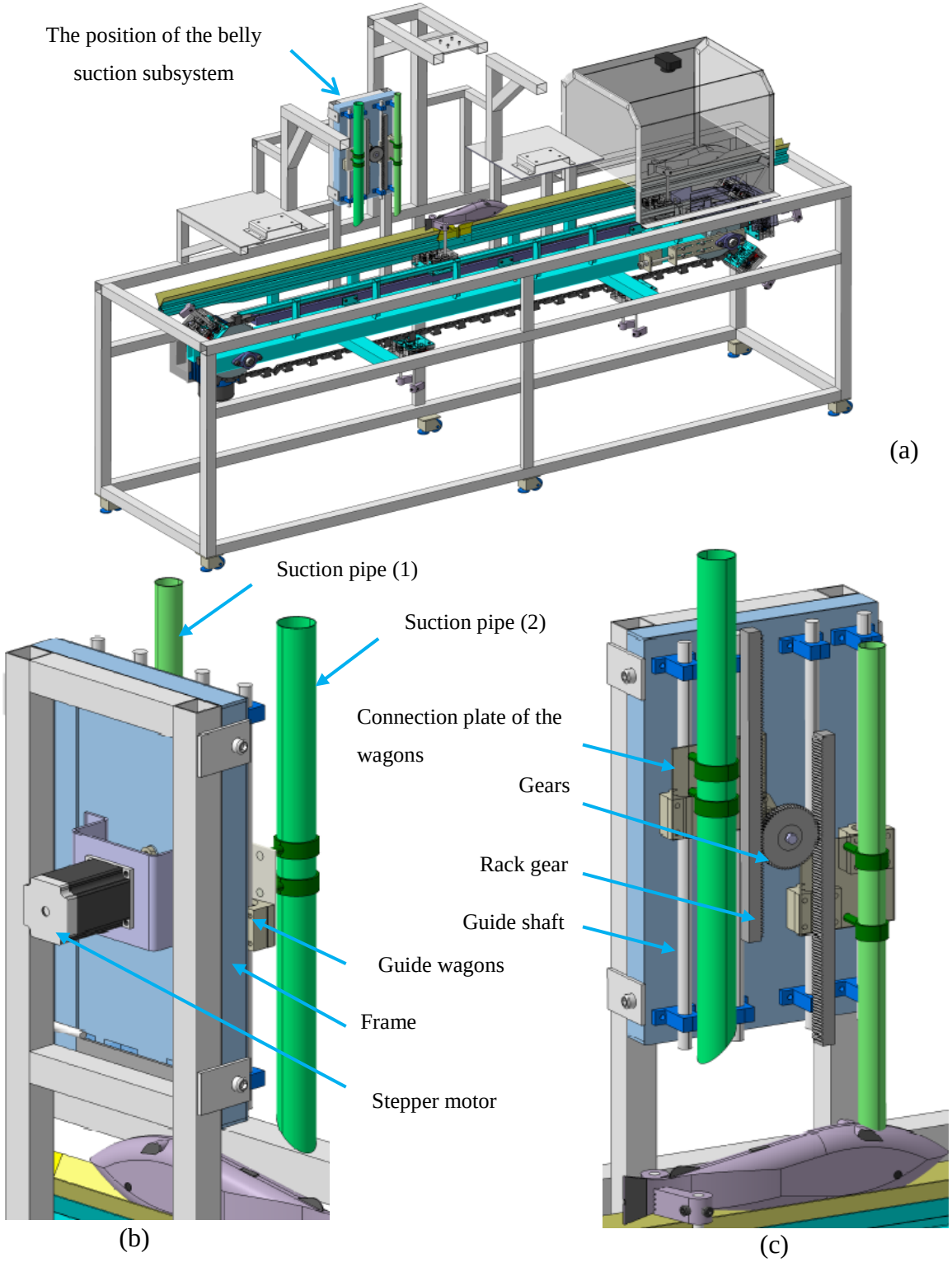

Figure 6-10. Gutting subsystem: a) position of the gutting subsystem in the machine, b) 3D view from behind, and c) Isometric view.

6.1.5. Belly cleaner subsystem

The belly cleaner subsystem is presented in Figure 6-11. This section consists of the following components:

1- Rotary brush
2- Pneumatic jack
3- Belts and pulleys
4- Main arm
5- Cutting shaft
6- Shaft bearings
7- AC Electromotive
8- Engine shaft and bearings

This subset is designed and built to clean the inside of the fish belly and remove any material attached to the fish spine. In order to rotate the brush, an AC electromotor with the power of 0.25 hp and a rotational speed of 1400 rpm was applied. To reduce the rotation speed of the brush, small and large pulleys with a diameter ratio of 1: 2 were used.

When the fish reaches the cleaning position, the command is transferred to the pneumatic jack from the control unit and performs the cleaning operation by lowering the jack. The time duration in which the pneumatic jack is extended mode is directly related to the fish length. As the fish passes in front of the cleaning station, the jack retracts to the initial position.

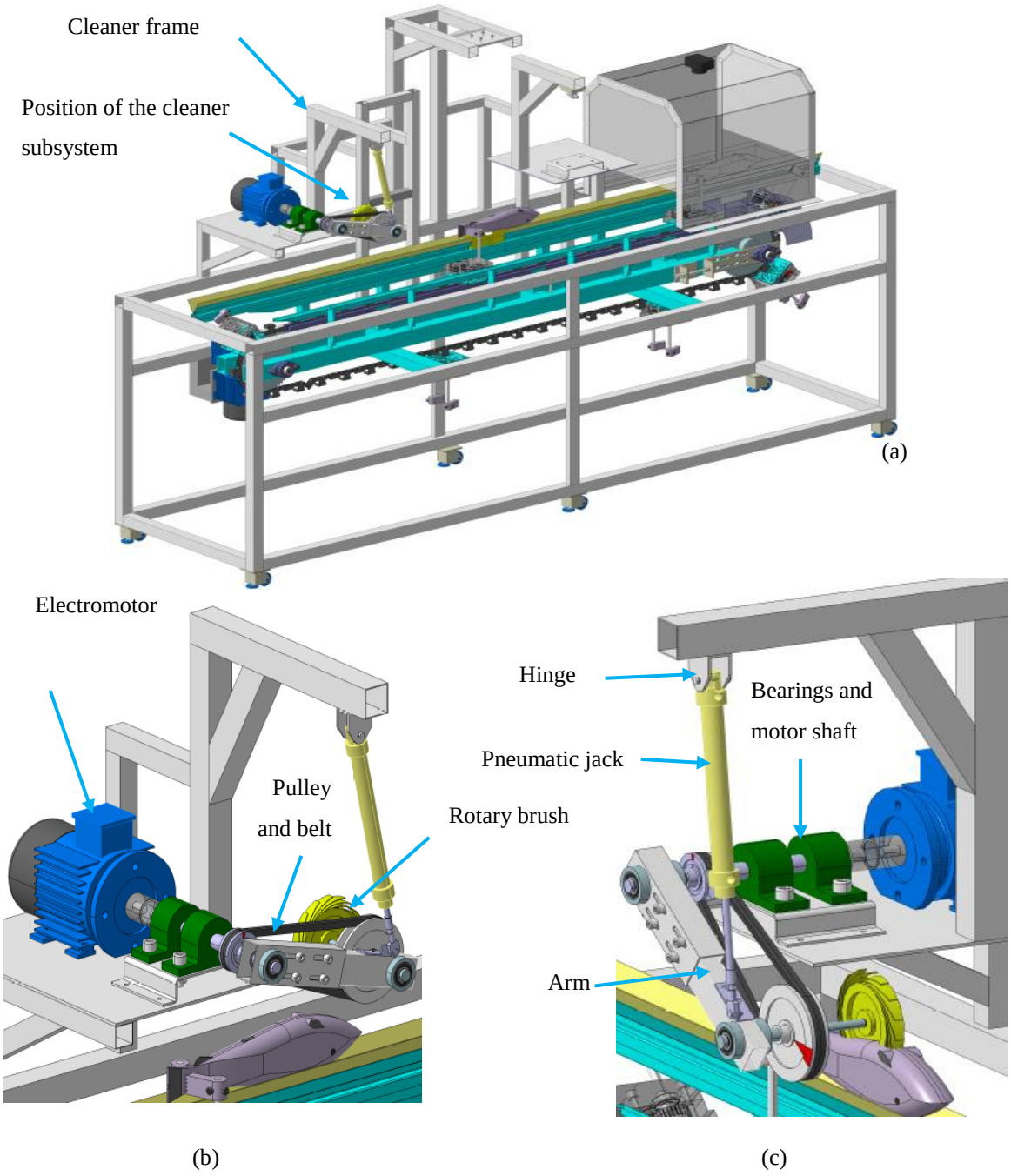

Figure 6-11. Fish cleaner subset: a) the position of the subsystem in the machine, b)isometric view, and c) 3D view of the subsystem.

The complete design of the trout processing system is presented in Figure 6-12.

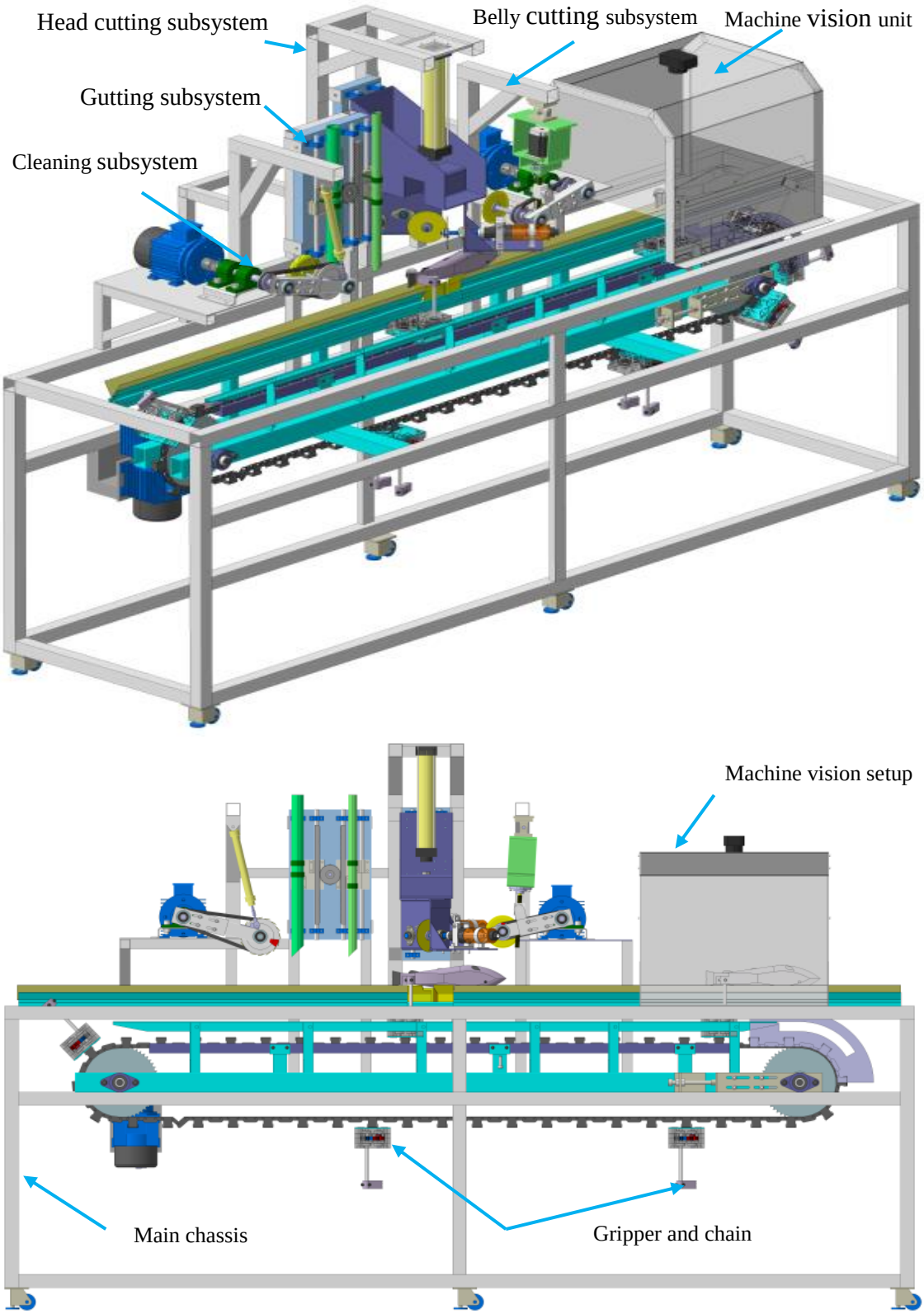

Figure 6-12. The complete design of the trout processing machine: a) isometric view, and b) front view.

6.2. Device simulation (kinetic and dynamic analysis, and extracting forces of the jacks and torques of the motors)

After designing the system in Caria, it was necessary to choose the motors and pneumatic jacks. Therefore, it is required to calculate the required torque and rotational speed of stepper motors and the force and speed of pneumatic jacks.

The simplest method is to design all the parts and define their weights to calculate the forces using the conventional method and numerical calculations. This method is applicable when the dynamic parameters are calculated for a single part or, in some cases, the limited number of parts within the relation. Using this method to determine accurate inertia reaction forces in a multibody system faces a significant challenge unless the problem is simplified. It should be noted that in the simplification method, in addition to the time-consuming computational steps, the reaction forces and the dynamic and static friction conditions will not be the same as the real condition. Therefore, to have closer results to the real operating conditions and reduce the numerical calculations and increase output accuracy, the designed system in Catia software was imported to Adams 2017 software and simulated for dynamic analyses. The steps simulation steps in ADAMS software are presented in Figure 6-13.

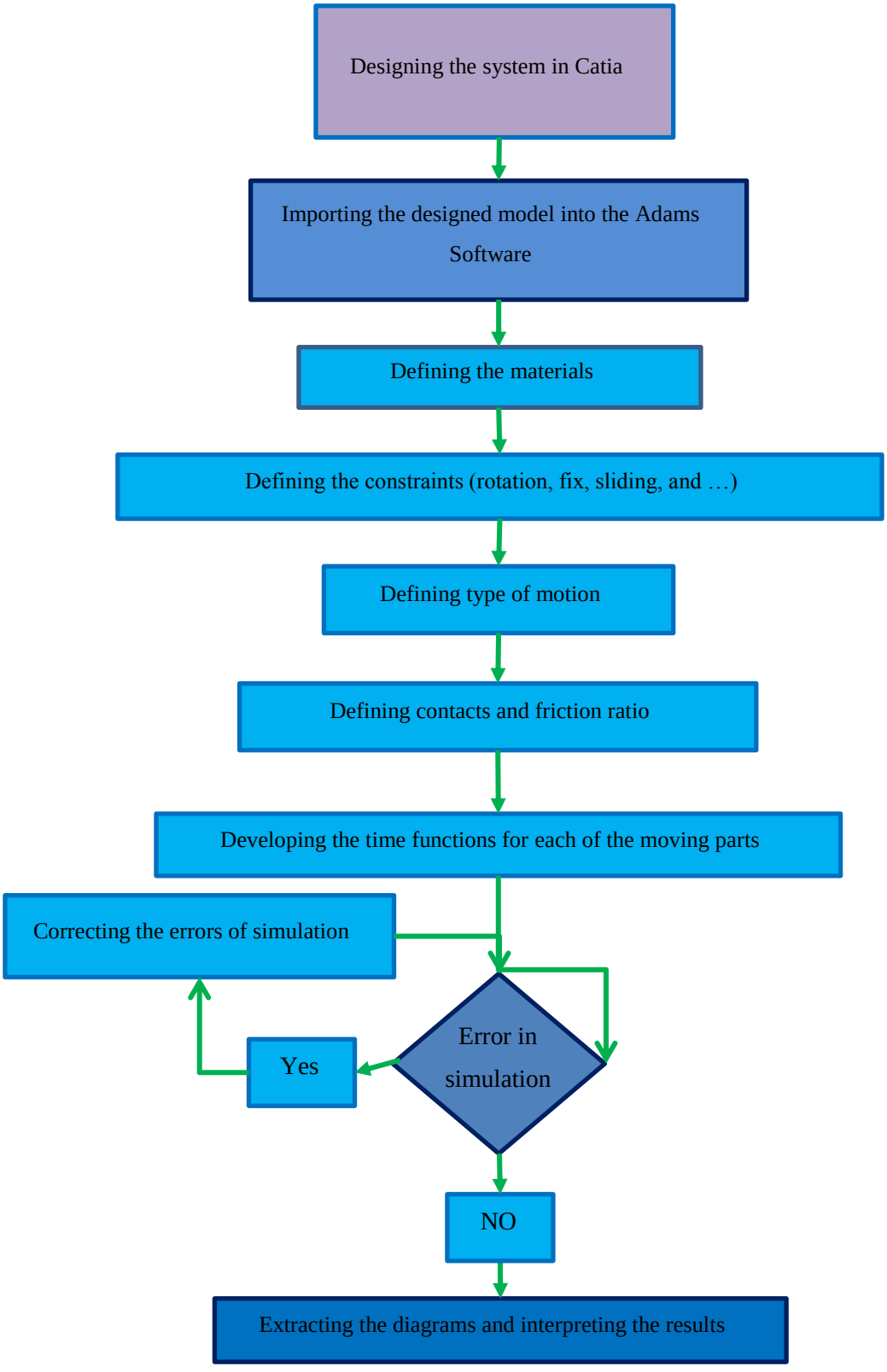

Figure 6-13. Simulation steps in Adams software for dynamic analyses of the trout processing system

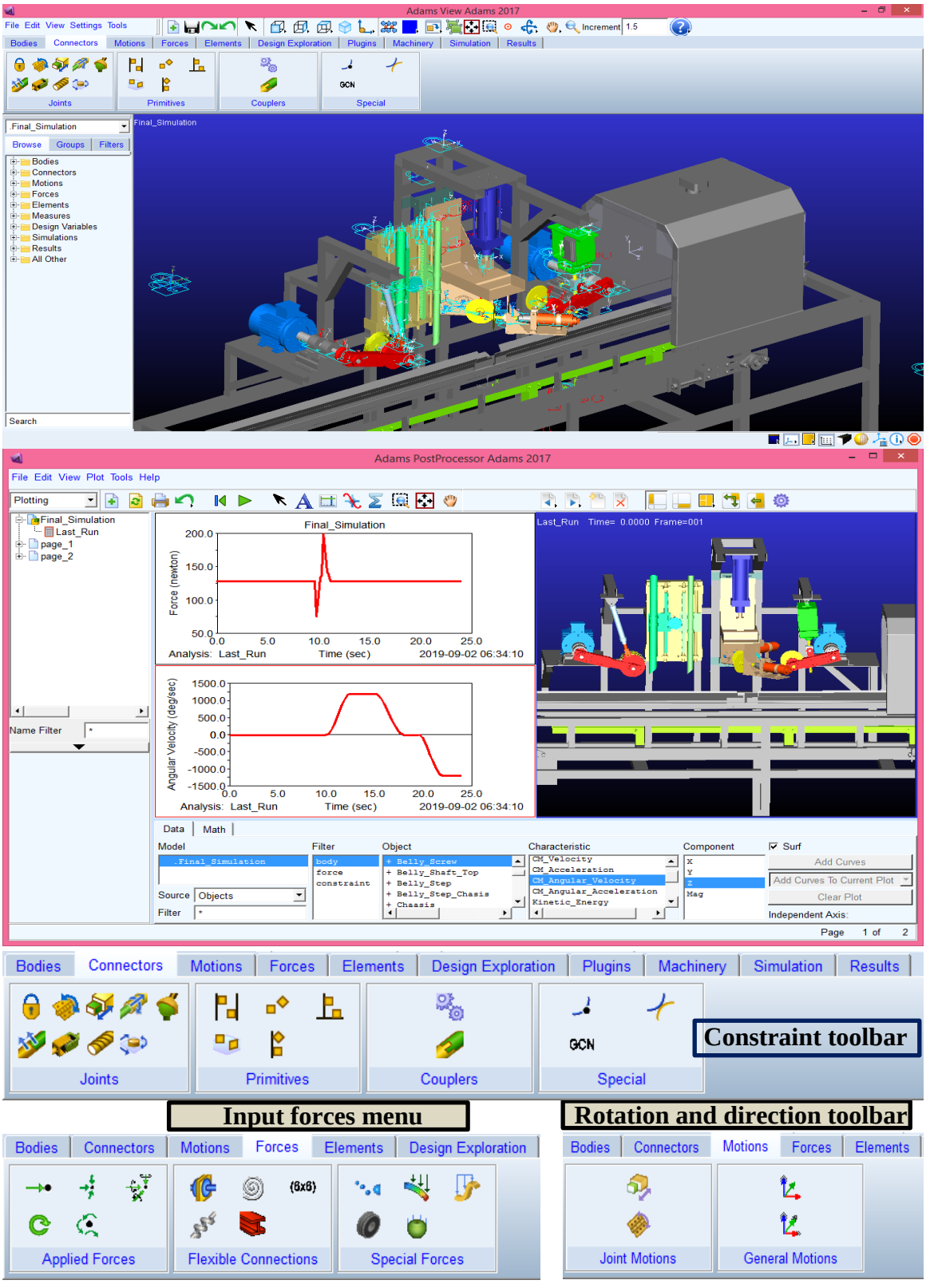

Figure 6-14. Simulation process, extracting the dynamic diagrams, and constraint toolbars.

After importing the designed model into Adams software, the first step is to nominate the parts. The related constraints were assigned for all the parts, and any possible errors were solved. At the next step, the associated motions for the moving parts were considered For this purpose, a rotational motion was considered for the stepper motor's hinge in the belly cutting and gutting subsystems. Likewise, for the linear moving parts, pneumatic jacks, and suction tubes the linear constraints were considered.

In some parts of the device and determining the constraints and types of movement, it is necessary to consider the collision between the components involved. This collision was considered between the pinion and the rack gear in the gutting subsystem. Columbus friction model was used to determine static and dynamic friction between the parts. As the power screw and nut in the belly cutting subsystem are both made of steel, grease lubrication will be used as between these parts. The static friction coefficient was considered 0.16 for steel-steel contact (Godfrey 1964) Also, the dynamic friction coefficient was set to 0.08 (Gray, 1964). For other dry parts of the device, the values of static and dynamic coefficients of friction were considered 0.1 and 0.2, respectively.

In order to determine the motion for the moving parts, the “Step” function was applied. The machine's movement sequence is such that as the fish enters the machine, and the size is extracted, fish length and cutting points are defined using machine vision. The rotary cutter creates the longitudinal cut in the belly cutting subsystem in the first stage. In the next step, the trout is beheaded and gutted. In this regard, it was necessary to consider the sequences of each operator in the simulation.

Therefore, four-movement steps were considered for each of the four operators of the device based on the movement time and rotational and linear speeds. Each pair of steps was considered for each operator’s round trip. For example, the belly cutting stepper motor start runs based on the written step function. As soon as the arm reaches the end of the path, the second step is applied to control the speed and acceleration. The same steps were also considered for the returning path. As the operator reaches the end of the path in the first run, the arm stops as equal to the time required for cutting the trout length. This time is considered between the second and third steps. By finishing the cutting process, the arm returns to the initial position based on the defined speed to complete the fourth step. In this

step, when the cutting blade arm reaches the end of the path, a stop command is issued to the stepper motor. It should be noted that in the simulation process, for all of the arms and moving parts, a motion function is considered so that all the contacts, collisions, and moving paths are visible. In such a condition, the timing of arms and actuators is set in an optimized condition. Therefore, by trial and error, the motions in the real system face the least errors and collisions. The method of the assigning the step functions in Adams software is presented in Figure 6-15.

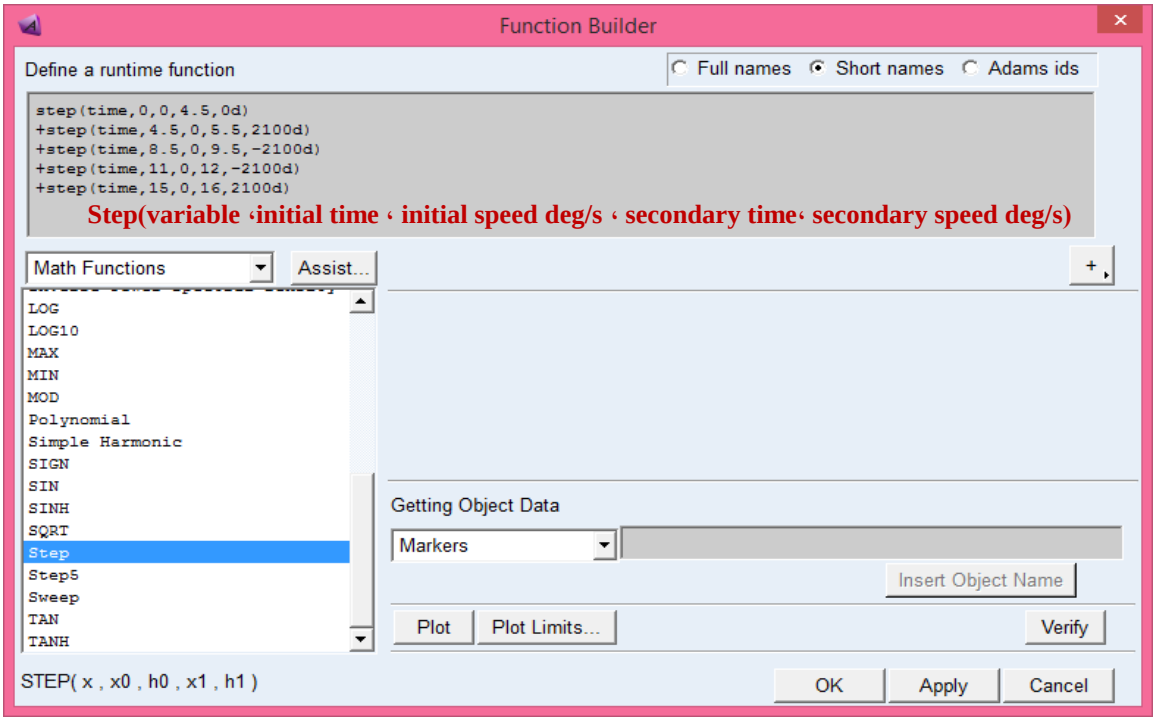

Figure 6-15. Writing the step functions in Adams Software

Since the minimum and the maximum number of fish is considered 4-10 fish per minute, the simulation of the device is performed for the minimum and maximum number and the average number of the fish (4, 7, and 10 fish per minute). To perform the simulation in these conditions, some preliminary considerations and calculations were required. For example, it was necessary to determine fish transfer speed in the canal in terms of fish per minute, because the operator's speed, performing all calculations, and writing step-functions will be done based on fish transfer speed. The function of each operator is shown in Figure 6-16.

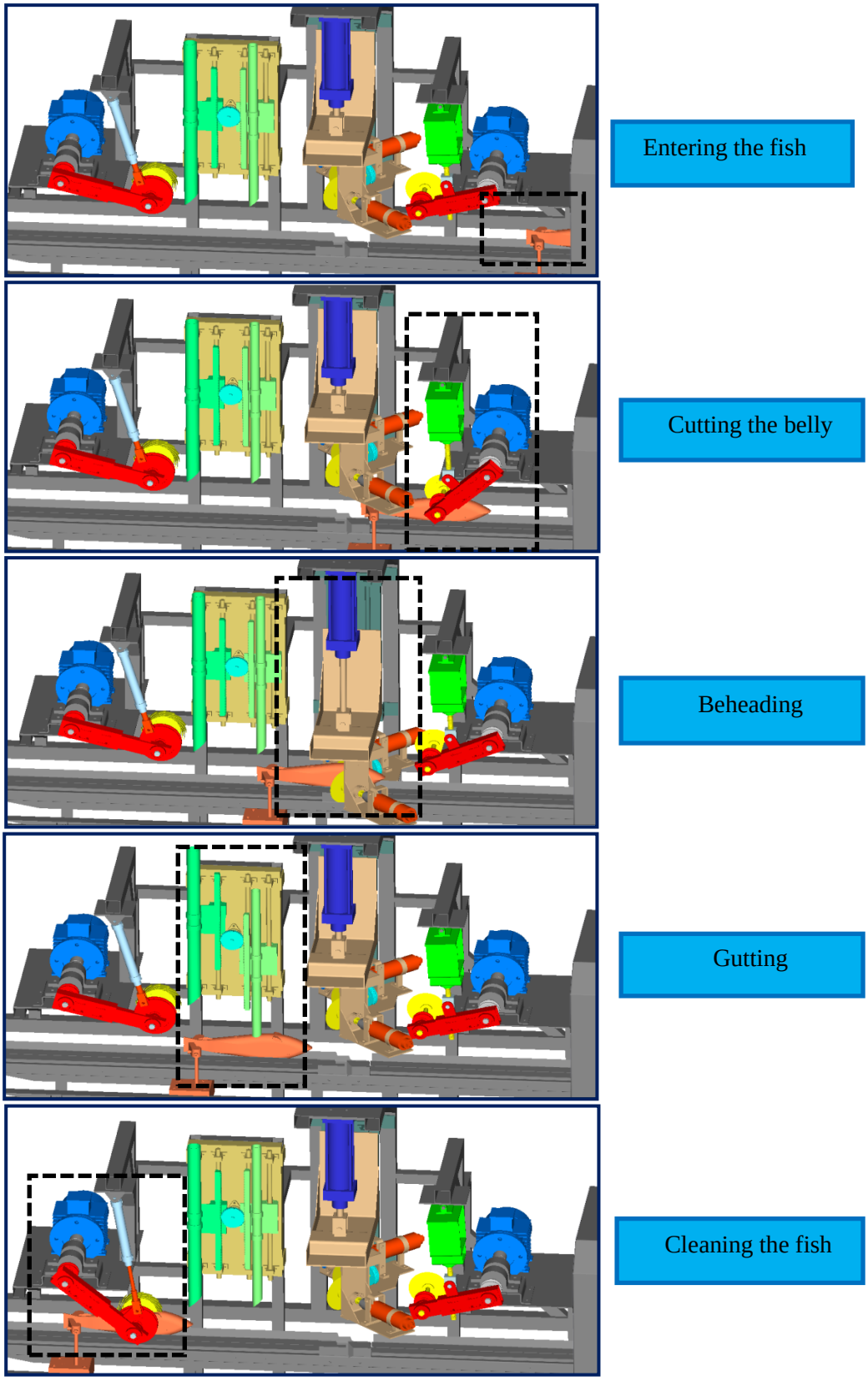

Figure 6-16. System simulation and fish processing in each subsystem.

6.2.1. Calculations related to stepper motors of the belly cutting and gutting subsystems

To determine the required torque to actuate the cutting arm and gutting tubes, the system simulated in Adams software. Considering the working conditions in the system, all the necessary parameter and considerations such as static and dynamic friction coefficients, any collisions, all the constraints, and motion simulation was performed.

Since the linear velocity of the fish varies in different feeding capacities, it is necessary to bring the cutting arm closer to the fish concerning linear transmission speed. It should be mentioned that the belly cutting time at which the arm is in cutting position is also concerning the fish transfer speed. In addition to determining motor torque, rotational speed, acceleration, and energy consumption were extracted. Finally, the maximum torque required for system functioning at a capacity of 10 fish per minute was selected to determine stepper motor characteristics in both belly cutting and gutting subsystems.

A power screw was used to move the cutting arm. Due to the self-locking property of the power screw in non-working condition, no force will be applied on the stepper motor in idle condition. Since the gutting subset has a different structure, it was necessary to use a stepper motor with a gearbox system due to the inertia of the moving parts so that the suction tubes would stop as soon as the motor stops.

6.2.2. Calculations related to pneumatic the jacks of head cutting and cleaner subsystems

Two pneumatic jacks were applied in a trout processing system in head cutting and cleaning subsystems. As the piston moves downward during the extraction step, the jack is expected to prevent the subset from free falling. To know whether the pneumatic jack will empower or prevent free fall, we investigated the piston velocity in free-fall conditions from a height of 180 mm. The falling situation is depicted in Figure 6-17.

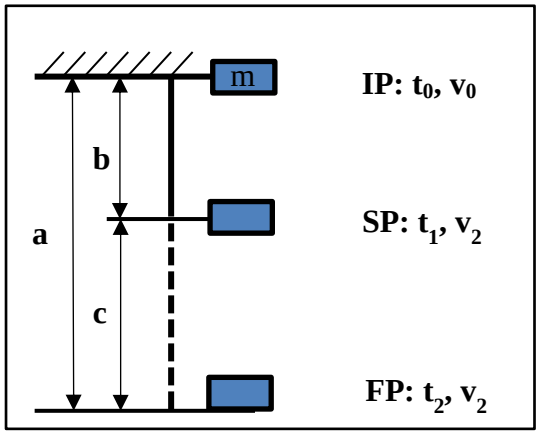

Figure 6-17. Free falling condition of the head cutting subset: a) distance from the home position of the head cutting subset to the end of the cutting path, b) the length from the home position to the initial contact of the blade and trout (80 mm), and c) cutting width.

The following are the equations for calculating the final velocity of the head cutting subset in a free-fall condition. According to these relationships, considering the weight of all stimulus parts was regarded as a single mass, and by simplifying the fall conditions, the penetration speed in initial contact and termination step was calculated.

$$U_0 + K_0 = U_2 + K_2 \tag{3.9}$$

$$m.g.h_0 + \frac{1}{2}.m.{v_0}^2 = m.g.h_2 + \frac{1}{2}.m.{v_2}^2 \tag{3.10}$$

$$g.h_0 = \frac{1}{2}.{v_2}^2 \tag{3.11}$$

$$9.81 \times 0.18 \times 2 = {v_2}^2 \tag{3.12}$$

$$v_2 = 1.88 \tag{3.13}$$

In these relations, U and K are potential and kinetic energies in terms of (J), m is body mass (kg), v represents body velocity (m / s), h is the falling height (m), and g represents gravitational acceleration (m /s2). According to the energy conservation law, the sum of

kinetic and potential energy at two points at the beginning and end of the motion path must be equal (Equation 3.9 and 3.10). After simplifying the relationship, the velocity value at the end of the path resulted in 1.88 m/s. Assuming that the cutting head subset has a free fall, the time required for the piston to reach the end of the path will be obtained using Equation 3.14.

$$v_1 = g.t_1 + v_0 \quad (3.14)$$

$$v_1 = g.t_2 + v_0 \quad (3.15)$$

By setting the values of 1.25 m/s and 1.89 m/s for v1 and v2, t1 and t2 were calculated as 0.13s and 0.19s, respectively. The blades will travel the distance from IP to FP (180 mm) in 0.19 seconds in the vertical direction. Also, the head cutting blades will travel distance b in 0.13 seconds. At this distance, the cutting blades will descend freely to reach the fish in the SP position. Considering the fish's average width as 100 mm, the cutting time from SP to FP resulted in 0.06 seconds. It should be noted that the penetration velocities in the SP and FP region are high values; this value is also higher than the maximum speed provided by the pneumatic jack.

By comparing the velocity values in different states, it is not allowed to consider different speed ranges for the piston. Obviously, the least amount of longitudinal displacement of the fish during the cutting process will be achieved at the highest blade penetration speed and the lowest processing capacity. Therefore, a penetration velocity of 500 mm/s was considered as the final velocity for cutting blade. Under these conditions, as this speed is considered maximum, the other feeding rates will be processed even better than the maximum feeding rate of 10 fish per minute. By comparing the velocity and time of the free fall with the maximum speed piston speed, it is expected that the piston must exert the opposite force against the free fall. This can also be seen in the output of Adams software. By defining the required force by Adams software, the pneumatic jack was selected for both the head cutting and cleaning subsystems. Since the total displacement range of the head cutting subset is 180 mm, a 250 mm course jack was selected. It should be noted that the amount of applied force is different in jack extraction and retraction

courses. The amount of supplied force in extraction and retraction steps is calculated by equations 3.16 and 3.17, respectively.

$$F_e = \frac{\pi \times D^2}{4} \times P \times 9.81 \quad 3.16$$

$$F_r = \frac{\pi \times (D^2 - d^2)}{4} \times P \times 9.81 \quad 3.17$$

In these equations, '*D*' and '*d*' are the outside and inside diameter of the piston rod in millimeters, '*F*' is the force of the jack in Newton (N), and P is the air pressure in terms of (bar), respectively. Since the one-way pneumatic jack exerts more force in the extraction course, it is preferred to use the cylinder in extraction retract until the next fish arrives, the jack can return to its original position slower than the extraction course.

Assuming the fish moves at a constant speed in the guided canal, the faster the blade penetrates the fish body; the more precise the head cut will result. Knowing that the force exerted by the jack resists the free fall of the cutting sub-section, especially at the end of the course, the designed model is entered into Adams software, and all the necessary constraints, their movements, and friction coefficients were entered into the model. Among the tested speeds for the jack, the maximum required force was obtained for the speed of 500 mm/s. After determining the amount of force, the next step is to select the pneumatic jack. The following items will be considered in selecting the jack:

1- Design factor
2- Jack Force
3- Load coefficient in vertical operation mode
4- Air pressure
5- Speed coefficient

Considering the design factor, the maximum force was considered 1.5 times greater than Adams software. Therefore, the force is considered equal to 332.45 N in further calculations. If the pneumatic jack is considered to work in a horizontal position with a pressure of 0.8 MPa, a jack with a bore diameter of 32 mm will be a proper option. It should be noted that if the jack is used in the vertical position, the bearing load by the jack will be reduced to 50 %. This value can be reduced by up to 20 % at high operating speeds. In fact, in addition to considering the design factor, the vertical load factor must also be considered. Also, in order to have an optimal performance at low air pressures, the air pressure of 0.4 MPa was considered in calculations.

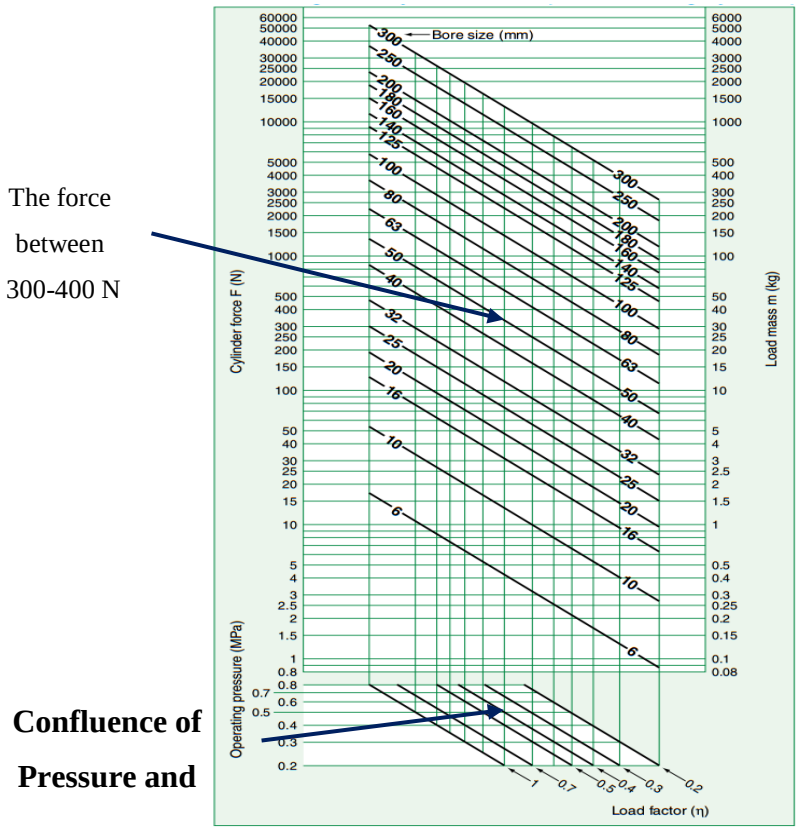

Figure 6-18. Bore size selection diagram based on the applied force, vertical operating coeficent and operating pressure

As shown in lower part of Figure 6-18, by considering the air pressure and vertical operation coefficient, a vertical line was defined. By tracing this line and contacting bore size of 32 mm, the supplied force between 100-150 N was anticipated which was less than the desired force of 332.45 N. Considering the vertical load factor as 0.5 at a working pressure of 0.4 MPa and the impact of the vertical force, an air jack with a 32 mm diameter

can supply force values between 100 and 150 N, which is less than the required value (332.45 N).

As another option, a jack with a bore size of 50 mm can supply the desired force values between 300-400 N. A similar process was performed to determine the jack force of the cleaning subsystem. Hence, at a load factor of 0.5 and air pressure of 0.4 MPa, a jack with a 20 mm diameter to supply active force between 30-40 N was selected in maximum fish processing rate (10 fish per minute). The trout processing machine was designed in CATIA software. In the next step, to extract the required force and torque in each of four subsystems (belly cutting, head cutting, gutting, and cleaning subsystems), Adams software was applied. By extracting this result, machine fabrication was simultaneously conducted together with design optimization.

In addition to the analytical results extracted by the software, some of the results were calculated in the initial step. This part of the results is related to the working capacity and processing quality of the operators during machine functioning. The results are related to the amount of fish movement in each of the capacities of the device. In Table 6-2 trout transfer length along the machine is presented in each feeding rate.

Table 6-2. Fish movement along the machine based on the feeding rate (fish per minute).

Pneumatic cylinder		Fish movement along the machine based in each feeding rate (mm)						
SPEED (MM/S)	TIME (S)	MF-4	MF-5	MF-6	MF-7	MF-8	MF-9	MF-10
100	1	53.33	66.67	80.00	93.33	106.67	120.00	133.33
200	0.50	26.67	33.33	40.00	46.67	53.33	60.00	66.67
300	0.32	17.78	22.22	26.67	31.11	35.56	40.00	44.44
400	0.25	13.33	16.76	20.00	23.33	26.67	30.00	33.33
500	0.20	10.67	13.33	16.20	18.67	21.33	24.80	26.67
600	0.17	8.89	11.11	13.33	15.56	17.78	20.00	22.22
700	0.14	7.62	9.52	11.43	13.33	15.24	17.14	19.05
800	0.13	6.67	8.33	10.00	11.67	11.85	15.00	16.67
900	0.11	5.93	7.41	8.89	10.37	14.22	13.33	14.81
FREE FALL	0.06	3.20	4.00	4.80	5.60	6.40	7.20	8.00

As shown in this table, by increasing the feeding rate, the fish transfer speed increases. Since it is desirable to increase the capacity of the system, the appropriate solution is to increase the penetration rate of the blades in the fish. The longitudinal displacement of fish at MF_4 and MF_10 capacity with the piston velocity with 100 mm/s was calculated as 53.33 mm and 133.33 mm, respectively. It should be noted that moving the trout as 133.33 mm while moving in front of the head cutter blades causes separation from the gripper or creating an undesirable cut in the head.

By increasing the blade penetration rate as 900 mm/s, the displacement values in both MF-4 and MF-10 capacities were calculated as 5.93 mm and 14.81 mm, respectively. These values are suitable for cutting the head, but it should be noted that increasing the speed of the pneumatic jack increases the inertia in the actuator sections, so the rod speed such as 400 mm/s and 500 mm/s is suitable for head cutting. The amount of fish movement in the minimum and the maximum capacity of the device at the speed of 500 mm/s are 10.67 mm and 26.67 mm, respectively. The head of the fish will be cut with a slight deviation from the vertical line, in which the fillet near the neck of the fish will be separated along with the body.

Figure 6-19 shows fish movement at different jack speeds. As shown in this figure, the displacement values at a particular capacity, such as the F-4, decrease nonlinearly by increasing jack speed, so that at piston speeds in the range between 100-200 mm/ s, fish displacement decreases with a high slope while the slope decreases at speeds of 600-1000.

This figure also shows that, at low transfer speeds, there is a large difference between the fish movement values, whereas as jack speed increases, the difference between these values decreases. In other words, considering the balance between the jack speed and the amount of fish displacement, it is appropriate to consider higher velocities of the carrier jack, but it should be noted that at higher jack velocities, the difference between the displacement values decreases. Due to the higher inertia of the moving parts and the high vibrations in the system, electing jack speeds such as 400-500 mm/s is a suitable speed for the head cutting blade set.

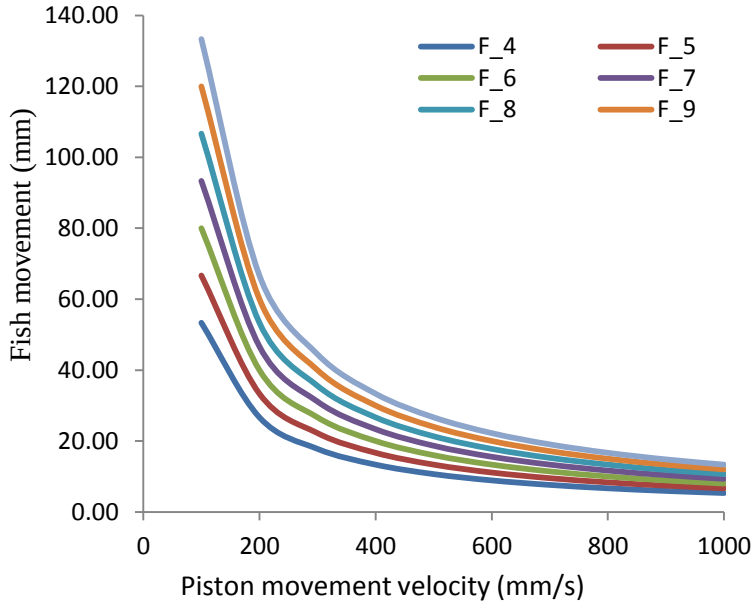

Figure 6-19. Fish Movement at different jack speeds.

6.3. Results of simulation

The results of system simulation in Adams software is presented in the following. In order to reach an optimized design and observe the force, torque, and speed trends, the system tested in three feeding rates. These capacities are the minimum, maximum, and average number of fish per minute (4, 7, and 10 Fish/min), respectively.

6.3.1. Selecting the stepper motor of belly cutting subsystem

The belly cutting subsystem is a subset of the machine in which a longitudinal incision is made from the anal fin to the fish head using a rotating blade mounted on the main arm. In Figure 6-20 to Figure 6-22 the motion simulation results are presented for the belly cutting subset. In these figures, the characteristics of the required stepper motor are determined. These characteristics are the required torque for cutting operations, angular velocity, angular acceleration, and energy consumption in three feeding rates.

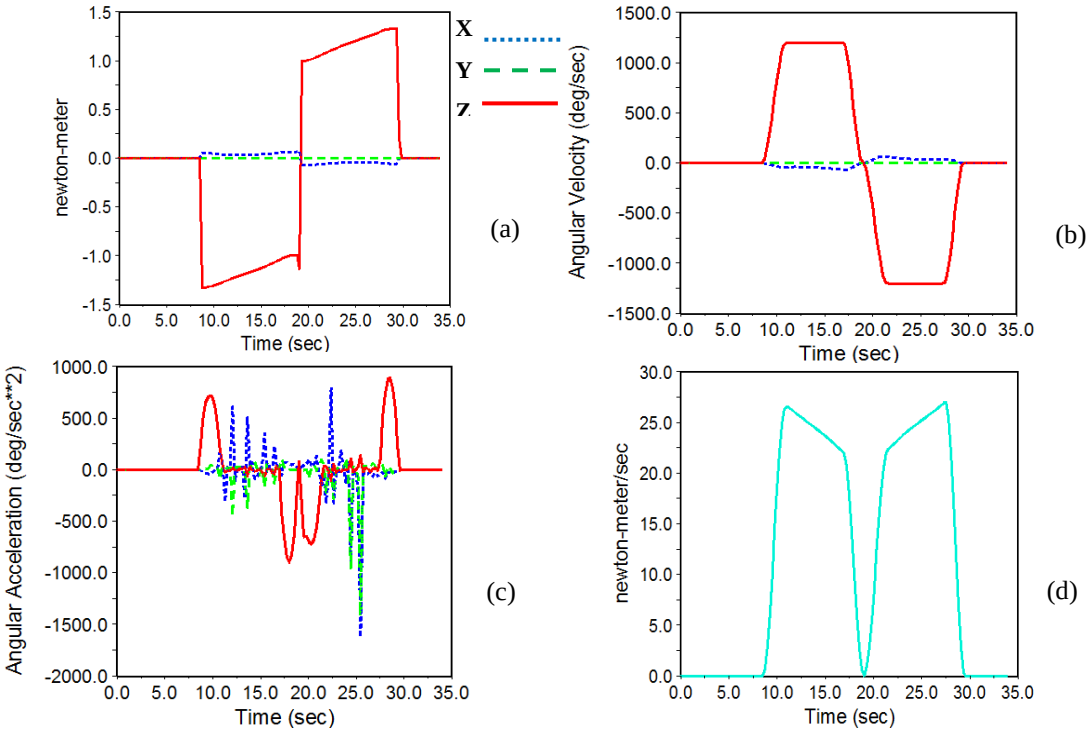

Figure 6-20. Results of Adams software simulation to determine the motor characteristics of the belly cutting subset (4 fish per minute).

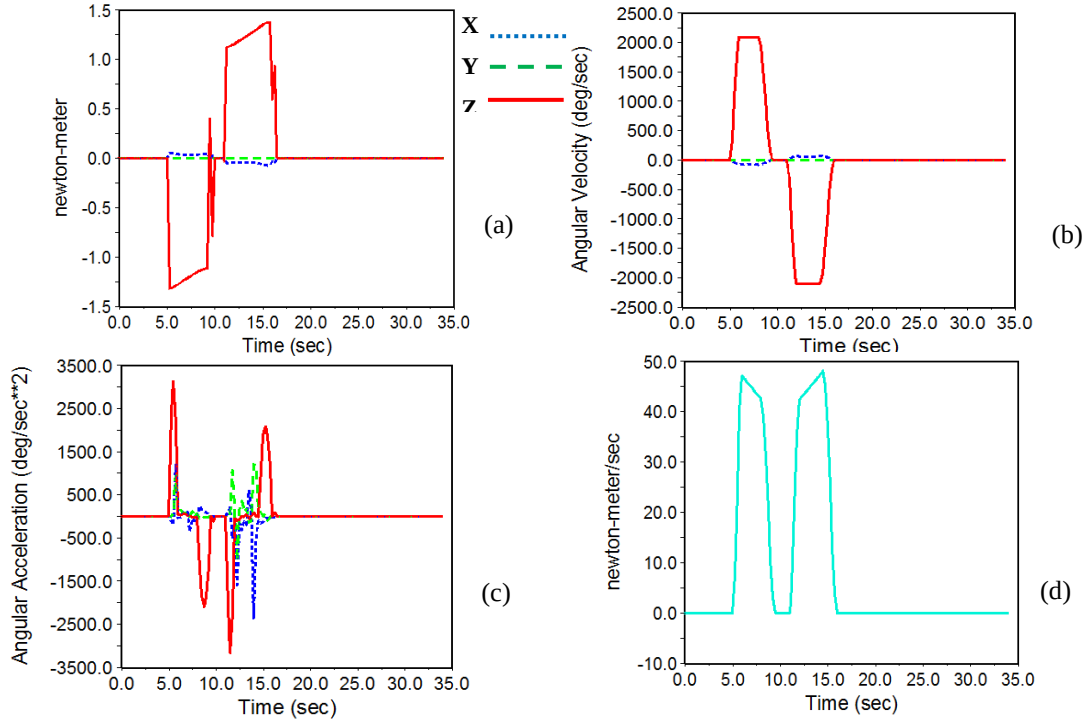

Figure 6-21. Results of simulation for the motor characteristics of the belly cutting subset (7 fish per minute).

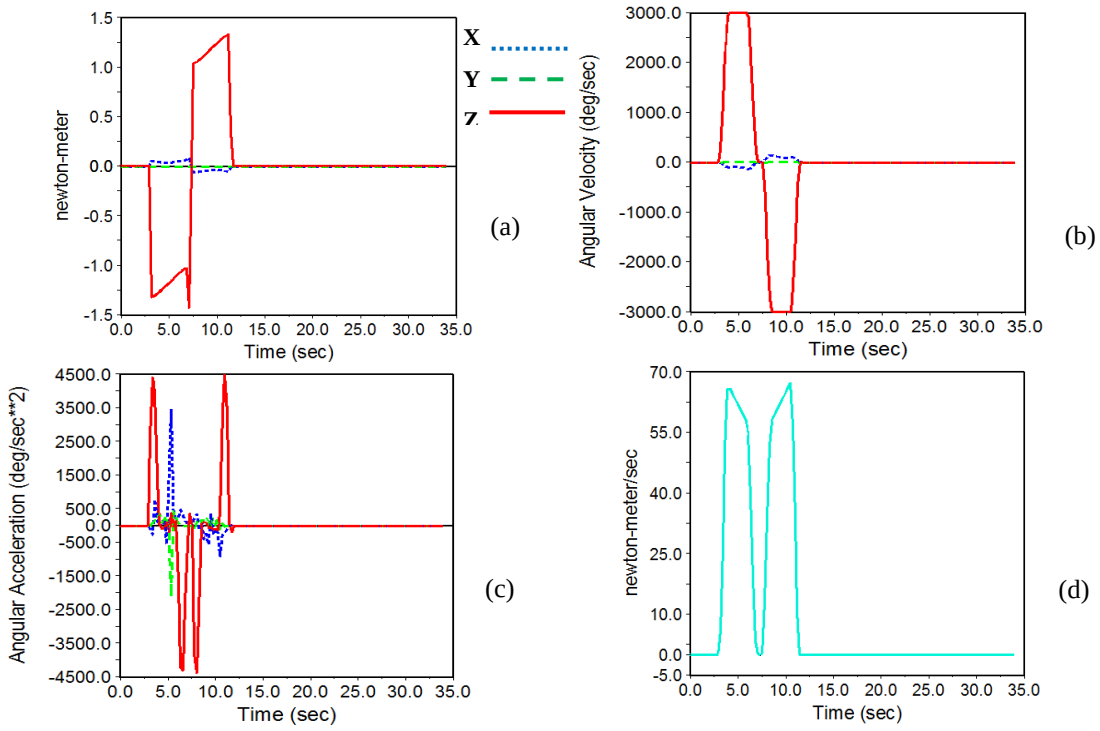

Figure 6-22. Results of Adams software simulation to determine the motor characteristics of the belly cutting subset (10 fish per minute).

As shown in these figures, the angular velocity and acceleration around the Z-axis are maximum. Also, the required energy increases by increasing angular velocity. The maximum torque values in three capacities of 4, 7, and 10 fish per minute were 1.334, 1.378, and 1.431, respectively. So, to select the required stepper motor maximum amount of torque (10 Fish/min) was selected. By considering the design coefficient of 1.25-1.5, the required torque for the stepper motor is in the range of 1.79-2.145 N.m. Therefore, a Nema 23 stepper motor (57PH20-20 kg.cm) stepper motor with a torque 1.96 Nm was selected. Considering this stepper motor, a design factor of 1.37 is obtained, which is acceptable for the device operation.

In Figure 6-20b, Figure 6-20c, and Figure 6-20d the angular velocity, acceleration, and energy consumption are presented, respectively. As shown in these figures, by increasing the fish feeding rate, the blades are about to penetrate the belly at higher speeds, requiring higher velocity and acceleration.

As shown in these three figures, the maximum angular velocity, acceleration, and

energy consumption are related to 10 fish per minute. Due to the sufficient time interval between the fish grippers, there is enough time to return to its initial position.

6.3.2. Selecting the pneumatic jack of the head cutting subsystem

The results for the Adams software output are shown in Figure 6-23 to Figure 6-25. In order to have a successful head cutting, it is necessary to synchronize the fish feeding rate and cutter penetration. In fact, the faster the jack penetrates and the slower the fish moves, the better the cut is done. It should be noted that, although the lower transfer speeds result in a proper head cut, it results in low system operation capacity.

By comparing the final velocity of the free fall for the head-cutting jack at the end of the cut path, it is obvious that the air jack prevents the moving parts from free-falling. The maximum required force in three capacities resulted in 149.83, 164.33, and 221.63 N, respectively. As shown in Figure 6-23, the amount of required force for the jack in the stop mode is between 127.5-130 N to compensate for the subset weight.

When the fish reaches the head-cutting position, the jack is activated and moves downward. As moving downwards, the required force decreases, and by reaching the end of the cutting path, the force increases to the maximum amount of 149.83 N. This force value resulted in a feeding rate of four fish per minute and the jack penetration speed of 200 m/s. Besides the required force and speed of the pneumatic jack, the acceleration, and energy consumption in the simulation time interval in the three working capacities are shown in Figure 6-23c and Figure 6-23d. Similarly, the amount of required force in seven and ten fish per minute at blade penetration speeds of 350 mm/s and 500 mm/s resulted in 164.33 and 212.63, respectively.

Similar results for the two penetration velocities of 350 mm/s and 500 mm/s are shown in Figure 6-24 and Figure 6-25. The maximum required force to provide a speed of 500 mm/s resulted in 2221.63 N. By multiplying this force by 1.5 as the design coefficient, the final force size on which the jack resulted in 332.45 N. By referring to the diagram presented in Figure 6-25 based on the operational position of the jack (vertical or horizontal) and air pressure, the size of the air jack was determined based on the maximum force required to move the head cutting subset (332.332 N). Since the supplied force in

extraction mode is more than the retraction, the pneumatic jack was selected based on the amount of the force that the jack can supply in retraction mode so that it can supply the required force while the jack ascends toward the initial position. On the other hand, it should be considered that the operating speed of the jack is one of the most important characteristics for determining the size of the jack. By following the line obtained from the intersection of the axis related to the vertical operating coefficient of 0.5 and the axis of air pressure, 0.4 MPa vertical line is determined.

By contacting this line with the force axis equal to 332.45, a cylinder with an internal diameter of 50 mm was selected. The minimum displacement of 180 mm was considered to have successful head cutting and avoiding any contact with the moving grippers, but to ensure any contact, among two different courses of 200 mm and 250 mm, the larger size was installed in the system. Therefore, the penetration rate of 500 mm/s was considered as the final penetration rate of the cutting blades. This condition will be the desired condition for head cutting in lower feeding rates. On the other hand, choosing this speed can result in an acceptable head cutting without any considerable fillet loss.

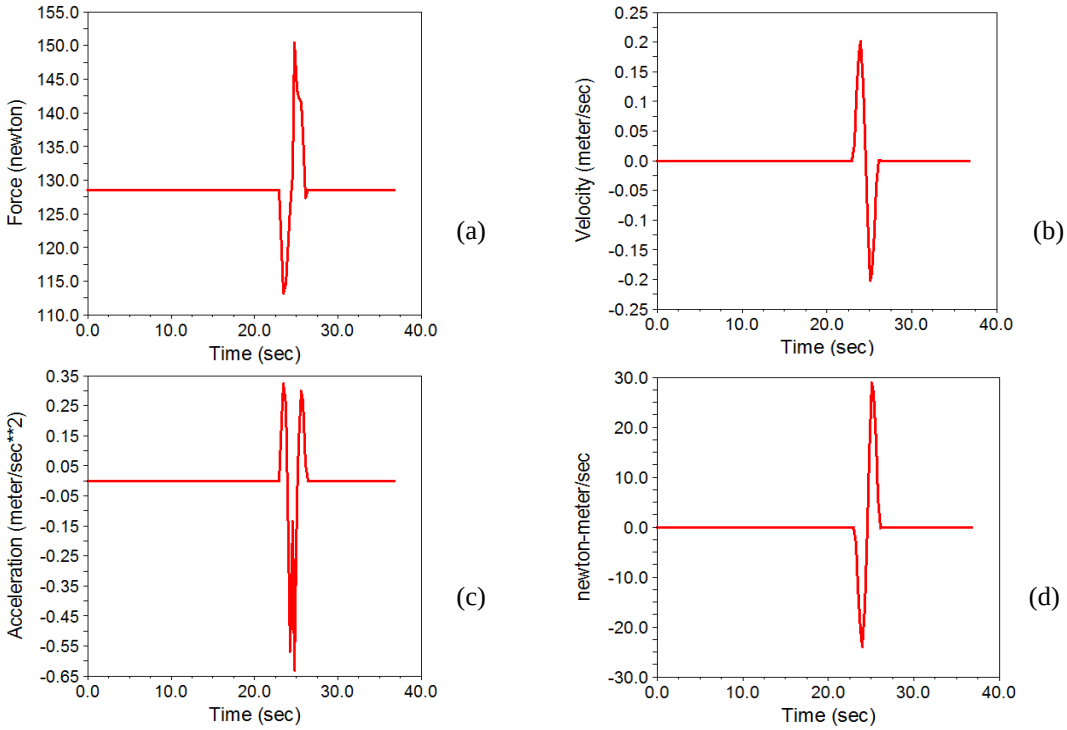

Figure 6-23. Results of simulation for the jack of the head cutting subset (4 fish per minute).

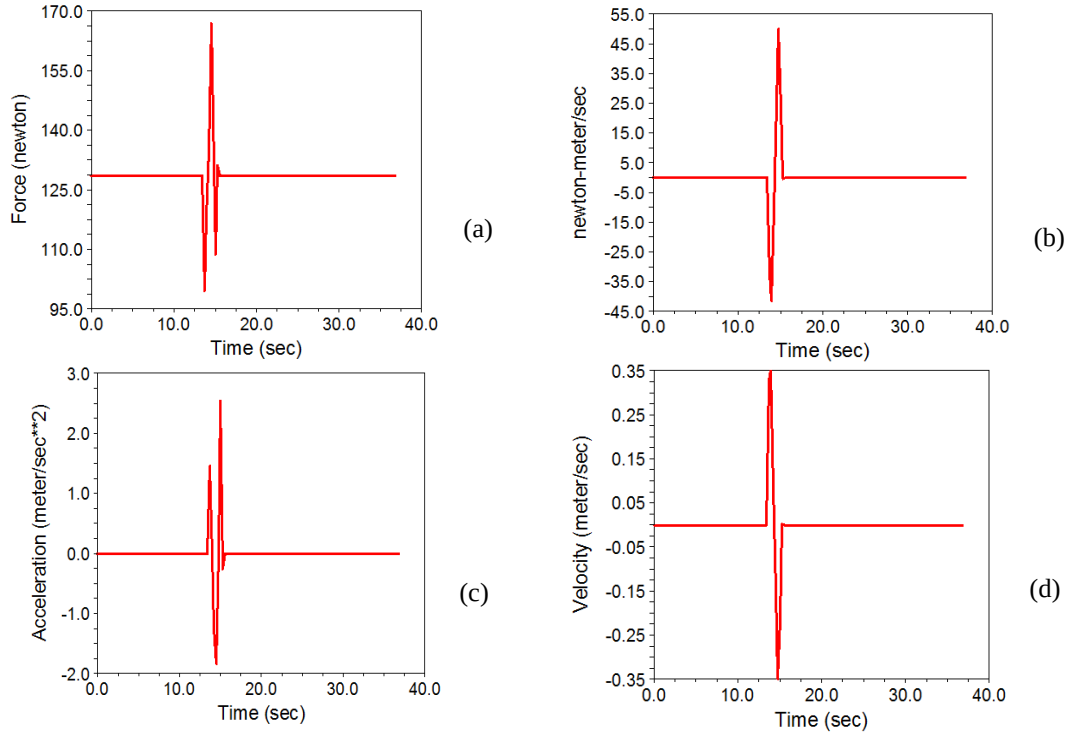

Figure 6-24. Results of simulation for the motor characteristics of the head cutting subset (7 fish per minute).

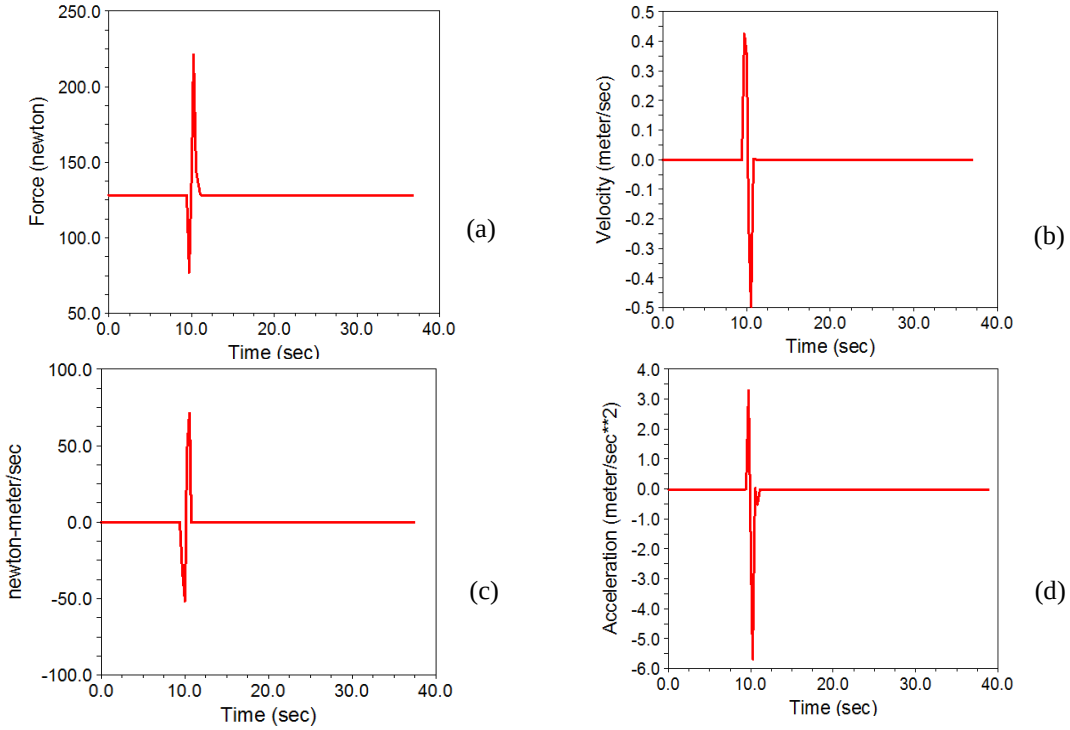

Figure 6-25. Results of simulation for the head cutting subset jack (10 fish per minute).

6.3.3. Selecting the stepper motor of the gutting subsystem

The results of motion simulation for selecting the motor characteristics in three feeding rates are presented in Figure 6-26 to Figure 6-28, respectively. In all the figures, the required torque, angular velocity, angular acceleration, and energy consumption are presented for each of the feeding rates. The diagrams present both clockwise and counterclockwise motions.

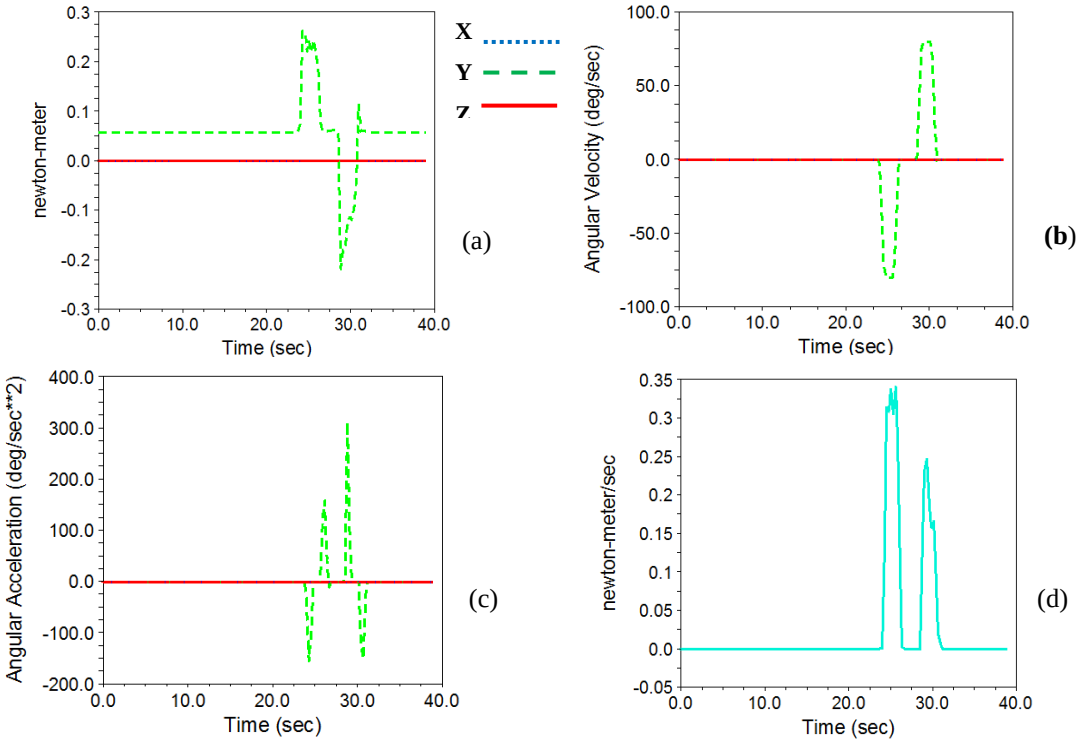

Figure 6-26. Results of Adams software simulation to determine the motor characteristics of the gutting subset (4 fish per minute).

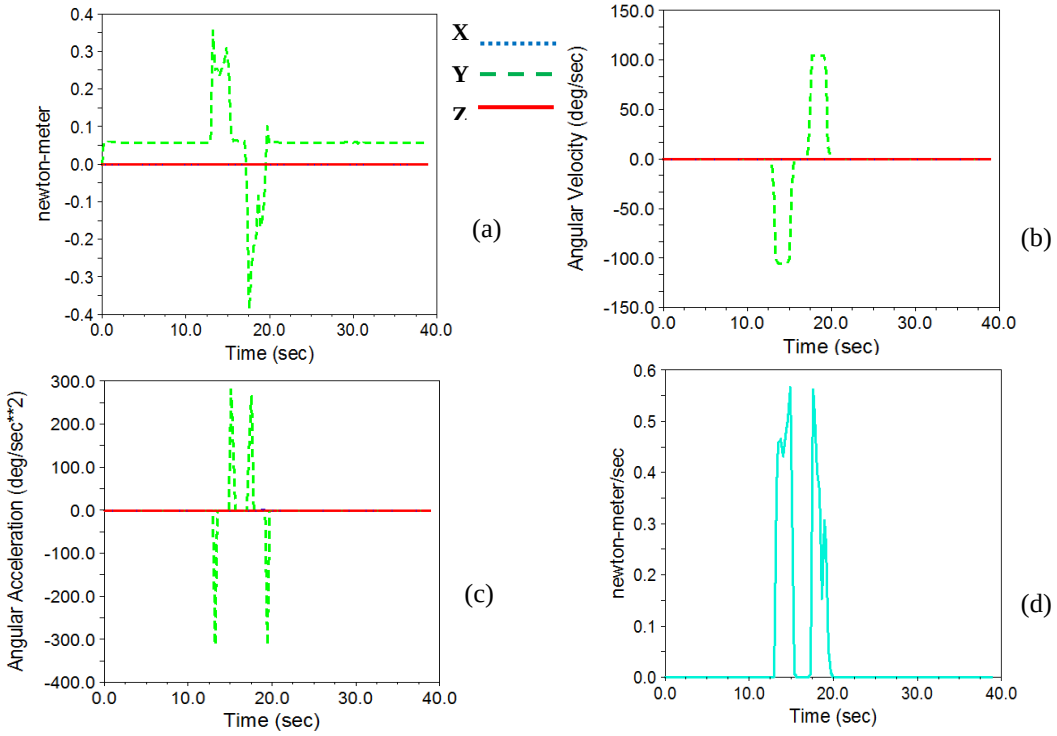

Figure 6-27. Results of simulation for the motor characteristics of the gutting subset (7 fish per minute).

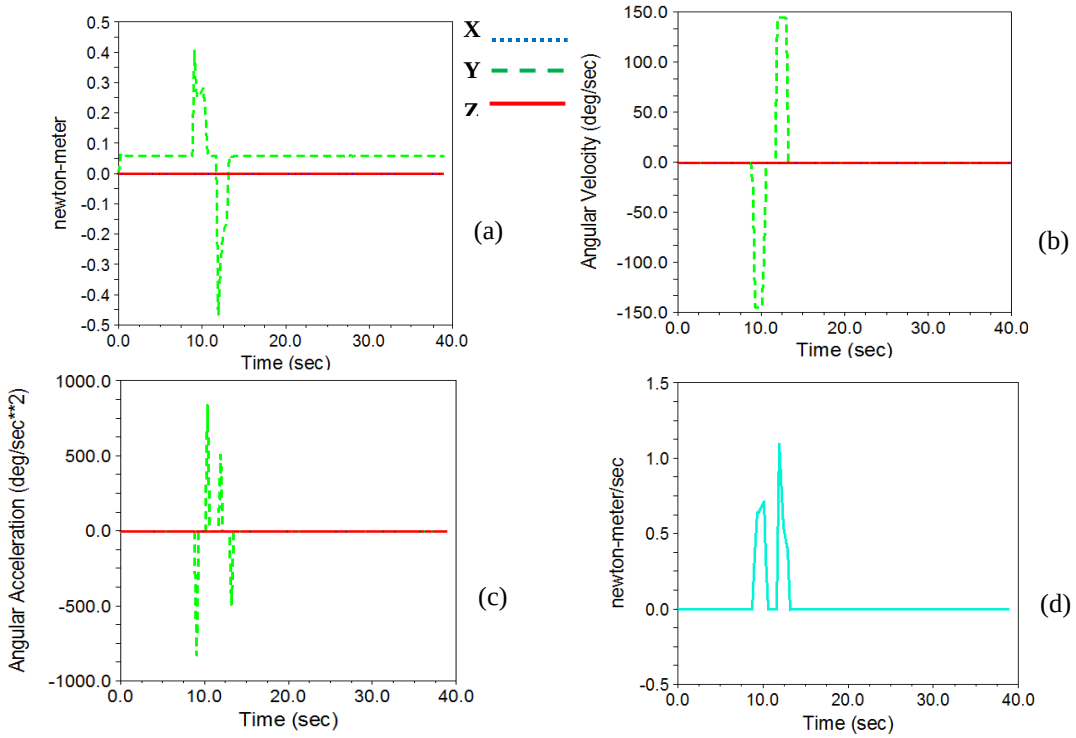

Figure 6-28. Results of simulation to determine the motor of the gutting subset (10 fish per minute).

As shown in these figures, the maximum required torque to move the suction pipes in a vertical direction resulted in the highest working capacity. In this section, when the fish reaches the suction position, the stepper motor rotates in clockwise and counterclockwise directions depending on the fish dimension. As soon as the tubes open, the material inside the trout belly is evacuated. Due to using two discharge pipes, the required torque for lifting two pipes is less than the condition at which the stepper motor controls one suction tube.

The required torque increases by increasing the angular velocity; whereas, in the maximum angular velocity, the maximum amount of required torque in the three input velocities was 0.226, 0.386, and 0.465 Nm, respectively. Since the maximum required torque resulted in 0.465 Nm, the required torque was estimated to be 0.698 Nm by considering the design coefficient of 1.5. As the pinion is connected directly to the rack gear, a gearbox mounted stepper motor was applied to move the suction pipes. Therefore, a stepper motor with a reduction ratio of 1:18 with a total maximum torque of 0.8 Nm was applied.

6.3.4. Selecting the pneumatic jack of the cleaning subsystem

After evacuating the belly content, it is necessary to clean any sticky materials attached to the spinal cord and belly cavity. A rotary brush with a ferry-ribbed edge was driven with an AC electromotor. In order to move the belly cleaner set, it was necessary to use a jack to raise and lower the rotating brush to avoid hitting the fish grippers.

The final stage of the fish processing in this system is to clean the belly content. As long as the clamp reaches the cleaning subsystem, the cutter descends to clean the belly. As long as the fish is moving towards the end of the machine, depending on the size of the fish, the arm is in an operating position based on the fish length. As soon as the fish cleans, the arm returns to the initial position. The results for the output of Adams software in three capacities are presented in Figure 6-29 to Figure 6-31.

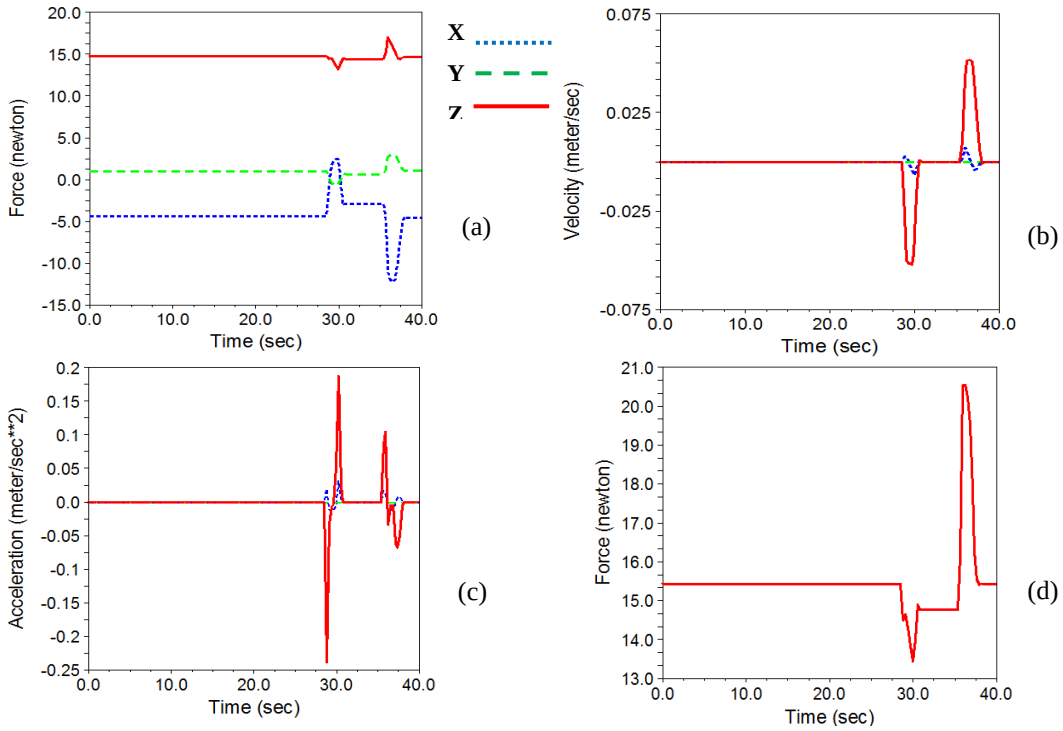

Figure 6-29. Results of Adams software simulation to determine the characteristics of the pneumatic jack of the cleaning subsystem (4 fish per minute).

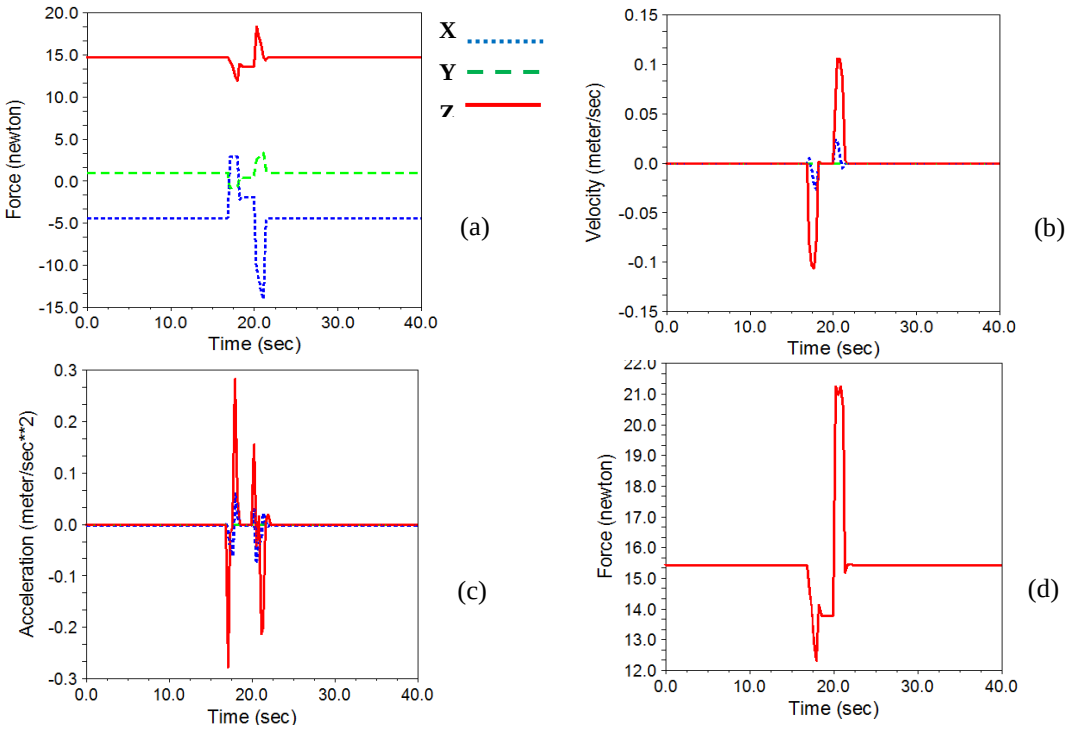

Figure 6-30. Results of simulation of the pneumatic jack of the cleaning subsystem (7 fish per minute).

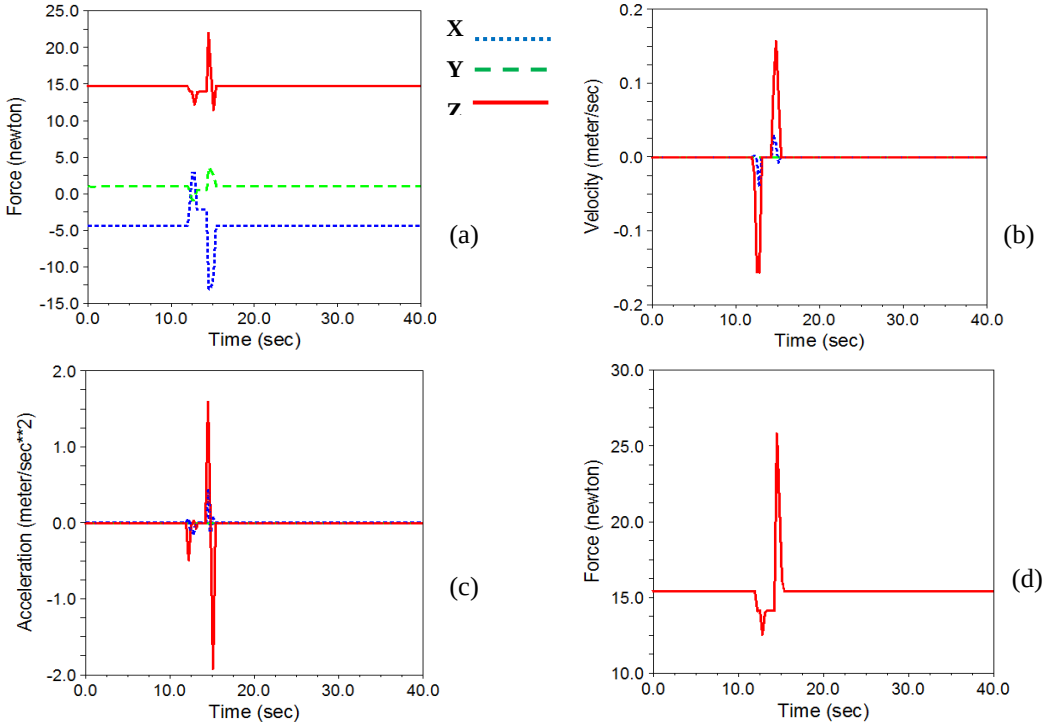

Figure 6-31. Results of Adams software simulation to determine the characteristics of the pneumatic jack of the cleaning subsystem (10 fish per minute).

In these diagrams, the force diagram in three directions of x, y, and z (diagram a), the velocity and acceleration (diagrams b and c), and the total force values (diagram d) are presented. As shown in these figures, unlike the jack used in the head-cutting subset, in addition to applying force along the z-axis, force components are also observed in both the x and y directions. The maximum required force to move the arm at the capacity of four, seven, and ten fish per minute was 20.55, 21.26, and 25.84, respectively. Multiplying the maximum force by 1.5 as the design coefficient, the final force results in 38.76 N. By referring to the diagram presented in Figure 6-31, the size of the jack was determined based on working position and air pressure by referring to the calculated force (38.76 N). Like the pneumatic jack of the head cutting subsystem, the retraction mode was selected as the criteria to select the jack. Since the arm operates at a considerable angle to the horizontal line, the vertical operation coefficient was 0.5.

By pursuing the intersection line of vertical operation coefficient and air pressure of 4 bar and contacting the required force value (37.86 N), it falls between the possible standard

bore sizes of the 16 and 20 mm. Finally, a jack with 20 mm was selected. The method of selecting the jack is such that by following the line obtained from the intersection of the axis related to the vertical operating coefficient of 0.5 and the air pressure of 4 bar, the upper limit bore size (20 mm) was selected. To avoid any contact of rotary brush with the moving grippers, the minimum vertical displacement length was 100 mm, so a pneumatic jack with the course of 150 mm was selected.

Machine vision analysis

Machine vision analysis

In order to extract the necessary dimensions and trout cutting points, the images were analyzed in both offline and online stages.

7.1. Offline processing

7.1.1. Image processing setup

A digital camera (Samsung EC-SH100 Wi-Fi Digital Camera with 14 MP, 5x Optical Zoom) was used to capture the images. The imaging system consisted of a stainless steel case with six rows of the lights. Each row contains 72 light-Emitting Diodes (LED) installed inside the case. The images were captured under controlled conditions. Both sides of the chamber were considered as low as possible to reduce the effect of ambient light. Based on the required power, an AC to DC power supply (S-180-12, input 220V-output 12V, 15A) was applied to illuminate the case. The image acquisition setup is presented in Figure 7-1. The image processing algorithm was developed using MATLAB 2013a software running in a Hewlett-Packard S4530 laptop computer with an Intel(R) i5-2410M CPU@2.3 GHz with 8 GB RAM. The image processing system is presented in Figure 7-1. Some sample images of the trout from the back and bottom view are presented in Figure 7-2.

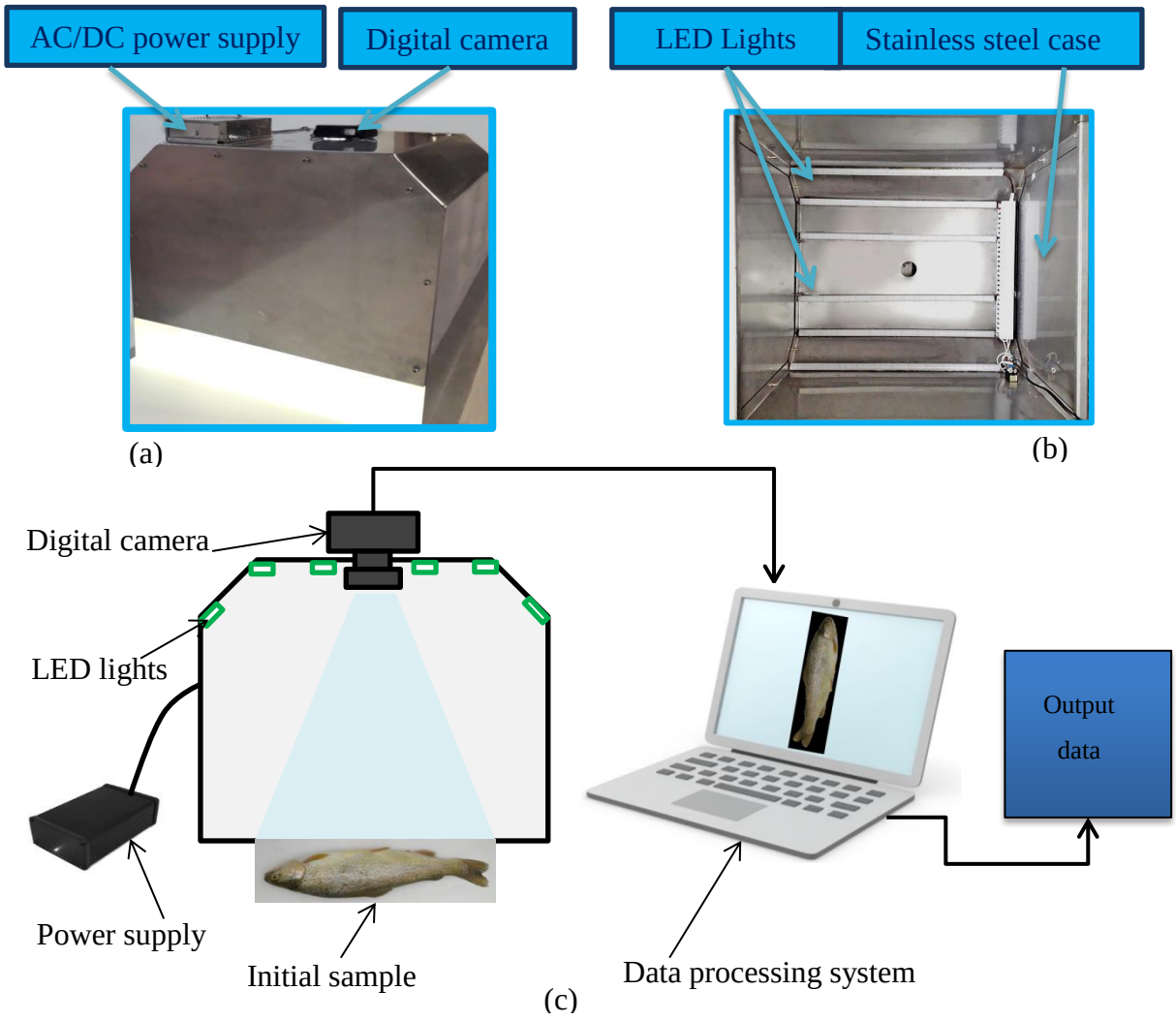

Figure 7-1. Image acquisition setup: (a) imaging case, digital camera, and AC/DC power supply, (b) inside of the imaging case with LED lights installed inside s the case, and (c) data acquisition setup.

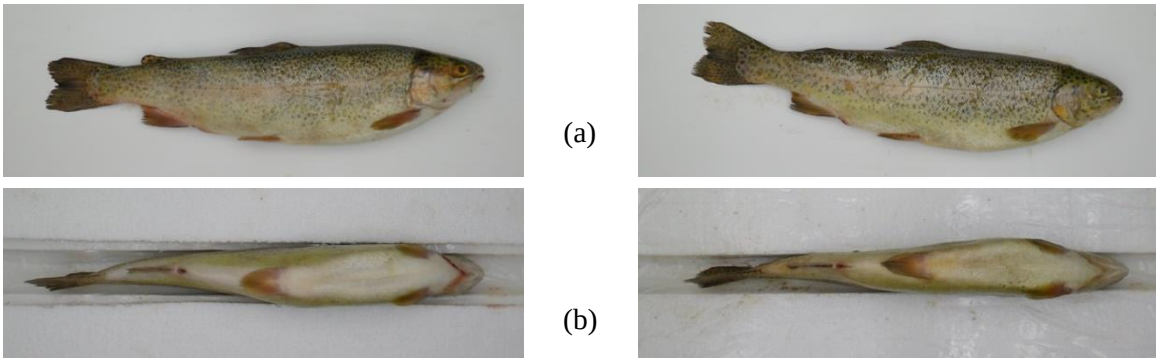

Figure 7-2. Sample trout images captured by the dihital camera: a) side view, and b) botom view

In order to conduct further assessment and observe the position of the trout head,

evacuated belly, and its spinal cord, an X-ray image was also provided by an X-ray setup (X-ray SEDECAL, APR-VET - Tube Support S2). A sample image is presented in Figure 7-3.

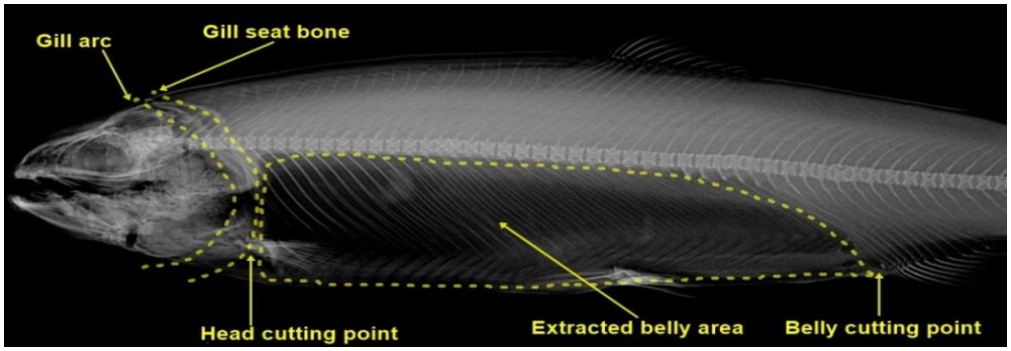

Figure 7-3. Image captured by X-ray setup with evacuated belly.

7.1.2. Trout segmentation from the background

Image segmentation is one of the significant steps of image processing that directly influences other post-segmentation processes (Teimouri et al., 2014). In order to meet the food processing sanitary safety regulations, the conveyor belt must be considered from white food-grade materials. This fact imposes a specific image processing procedure; otherwise, the fish will be inappropriately segmented from the white background.

In general, a fast and automatic thresholding method is desired (Lin 2005). Like most typical image processing studies, we applied the Otsu (1979) thresholding algorithm at the first step. Since, in some cases, the area near the trout chest and belly had similar pixel intensity values to those of the white background, the trout region was not completely segmented using this method. In order to improve the method, we noticed that the region of interest depends on the contrast between the fish sample and the background (Mendoza et al., 2006), then, all channels of 'RGB', 'HSV', and 'L*a*b*' color spaces were tested on the image (Figure 7-4). Finally, the channel 'B' of the 'RGB' color space showed a high contrast between the pixel intensity values of the trout and the background providing the best results. Finally, a threshold intensity value of 150 was selected as the initial step in the segmentation process.

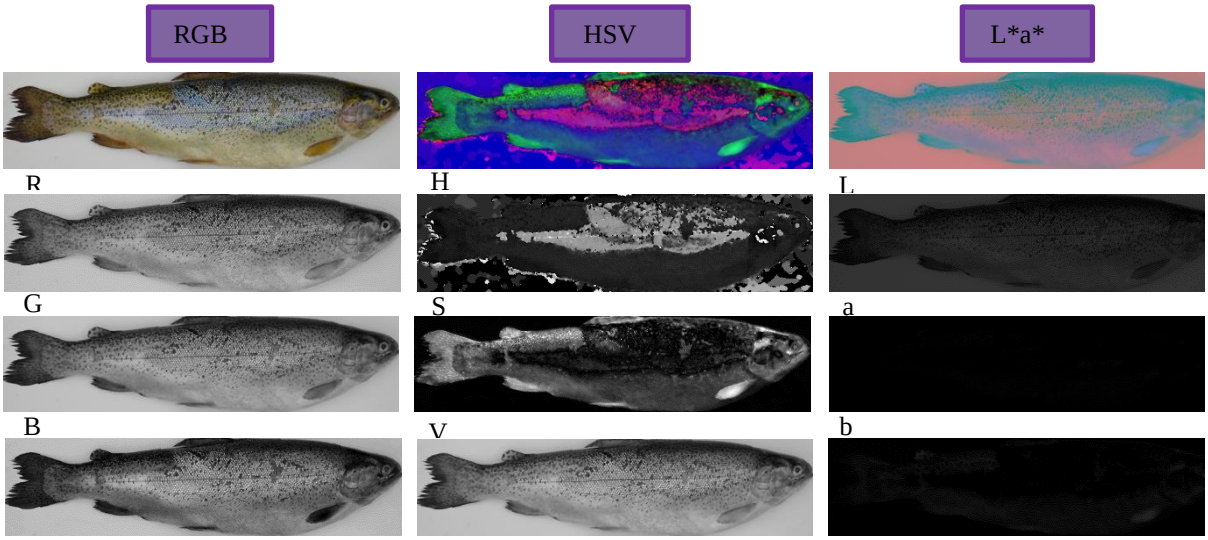

Figure 7-4. RGB, HSV, and L*a*b* color spaces with related color channels examined in trout segmentation.

The initial image was captured in the dimension of 3240×4320 in rows and columns, respectively. This image was converted to a 736×351 matrix after resizing and cropping, considering a trade-off between the image quality and processing time. As the dimension of the initial image matrix is large, we resized the images to an optimized size regarding the balance between acceptable reduced image quality (preserve any required small objects like pelvic fins and their color features) and the computation time gets more significant in fast real-time systems. In the next step, the resized images were converted into binary images (black and white): the pixels with intensity values lower than 150 were considered as '1' (white), and the rest were considered as '0' (black). Afterward, some smaller areas apart from the target (trout sample) still appeared in the background. On the other hand, some pixels inside the trout region were omitted (Figure 7-5c). Thus, a 4x4 structure element was defined to remove the isolated pixels in the binary image, and on the other hand, any possible holes in the trout region were filled (Figure 7-5d). Finally, the samples were completely segmented from the background and a bounding box with the final dimension was assigned (Figure 7-5e). In this study, two different segmentation stages (sample-background and fish-fin) were performed.

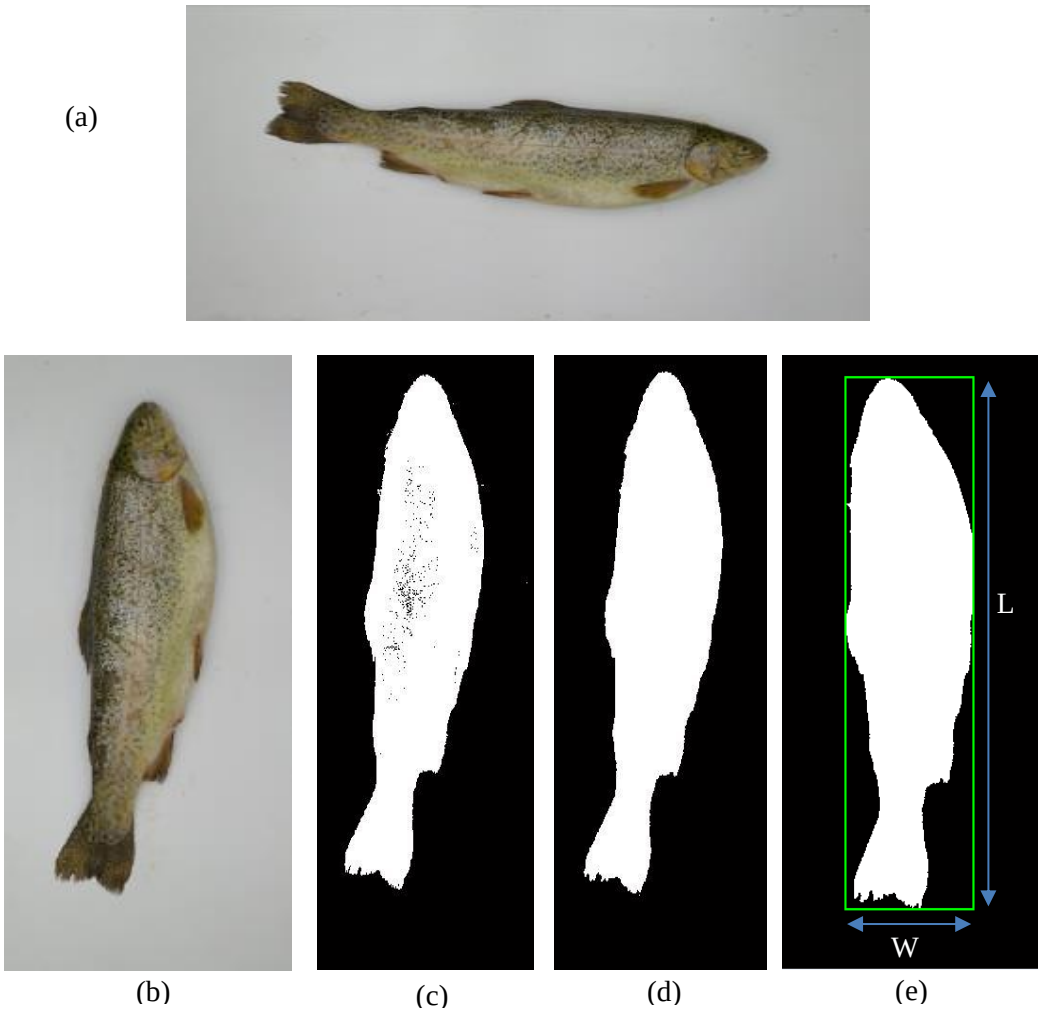

Figure 7-5. Trout segmentation, bounding box correction and dimension extraction: a) initial image, b) cropping the image, (c) binary image of fish generated by the applied threshold, (d) optimized image by removing any extra objects and filling the holes in the fish target, (e) the oriented fish image and corrected bounding box.

7.1.3. Fish dimension determination

The extracted dimensions (length and width) are applied in the image processing algorithm as stated in the following:

(1) The image was cropped in two different steps to reduce the computational load. In the first step, the initial image was resized, and a wide margin of the image was cropped to remove a significant part of the background. In the next step, the image was cropped based on the second bounding box area with the length of 'L' and the width of 'W'.

(2) Defining two lines from 10% of the length on both sides and further seven lines

between these two lines.

(3) Defining two lines from 1/15 of the length of the fish from both sides along its length and further 45 lines between these lines.

(4) Defining structure element as equal to the 0.001% of trout bounding box area.

After trout segmentation, defining the proper bounding box, and extracting the length and width, trout back and belly sides are determined in the following. The two-dimensional (2D) intensity histogram of trout image in channel 'B' is represented in Figure 7-6. The values of the fin pixels were less than 90 in most of the samples (dark blue pixels). As shown in this figure, the pixel values in back-left (BC-L) and back-right (BC-R) have similar intensity values as trout fins, which makes the fin segmentation process difficult.

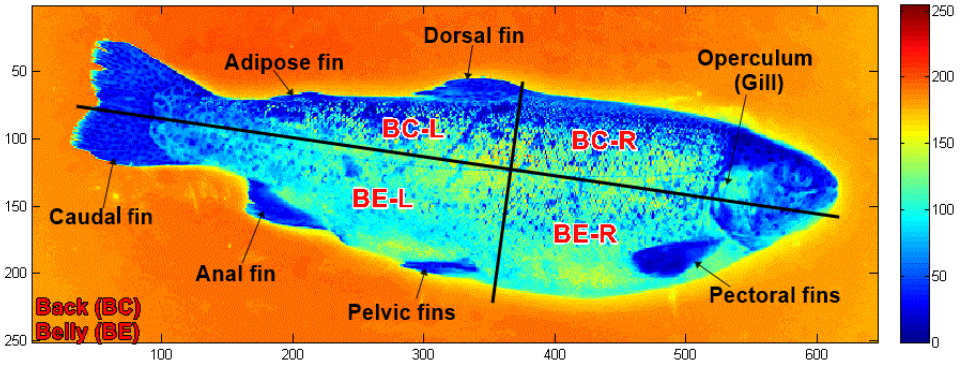

Figure 7-6. The (2D) intensity histogram of trout in the range of [0-255]. This figure shows the difference between the trout and background. It also illustrates the difference between the intensity values of trout and its fins. (BC-L: back left; BC-R: back right; BE-L: belly left and BE-R: belly right).

7.1.4. Back-belly side determination

As shown in Figure 7-7, two horizontal lines passing from 10% of the total length from the top and the bottom of the segmented trout were determined. Additionally, seven horizontal parallel lines were drawn between them, and their midpoints were connected to extract the central line. The horizontal lines and the obtained central line are shown in Figure 7-7. By determining the central line, the images are divided into two parts (P and Q) as shown in Figure 7-7b and Figure 7-7c. These parts were analyzed to identify the belly and back sides by comparing the gray intensity values of both parts (Strachan 1994; White

et al., 2006). Since the color near the trout belly is lighter than its back, the part with greater mean gray intensity value is considered the belly side.

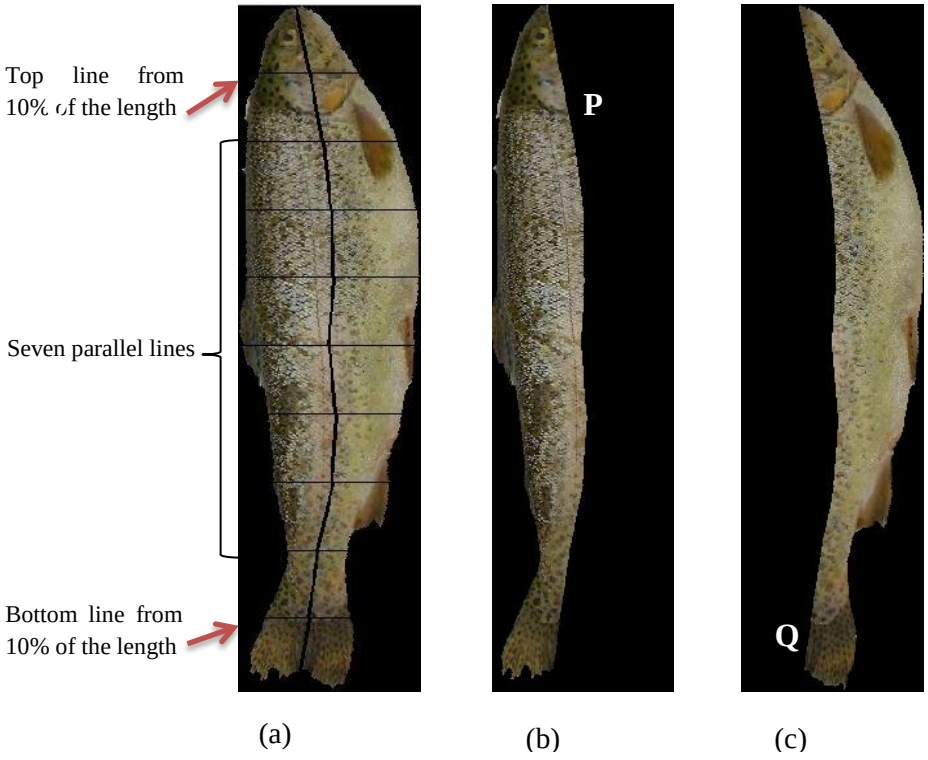

Figure 7-7. Centerline determination for back-belly detection: (a) two lines from 10% of the width with seven parallel horizontal lines defines the centerline by connecting the midpoints, (b) extracted image for back-side 'P', and (c) extracted image for the belly-side 'Q'.

In order to have successful fin segmentation, part Q shown in Figure 7-7c was divided into two other parts (Q-1 and Q-2) with a secondary centerline (Figure 7-9b) This was done by determining the horizontal lines and connecting their center points (Figure 7-9a) similar to the initial line determination process. Since part 'Q-2' is now a narrow area, it is necessary to define more horizontal lines compared to the initial line. On the other hand, increasing the number of lines leads to inappropriate centerline, which is not the desired one. By testing different number of the lines, a range of lines between 35 to 55 resulted in the most appropriate line. Finally, 45 horizontal lines were selected and drawn between two other lines, which were considered from $\frac{1}{15}$ of the trout length from the top and the bottom. These lines are shown in red color in Figure 7-9a.

After separating the fish into the back and belly sections, the result of gray color intensity of 97 samples examined in the offline mode is presented in

Figure 7-8. The values for the back and belly sides are shown in yellow and red colors, respectively. As the back of the trout is darker than the belly side, the backside showed a mean value of 92.83 with 5.82 of standard deviation while the mean value of the belly side was 106.93 with 5.29 of standard deviation, which showed successful back-belly side identification in all of the tested samples.

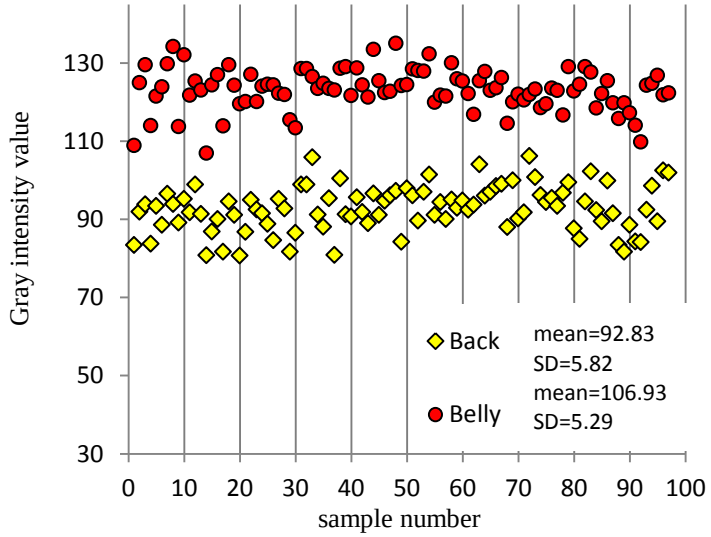

Figure 7-8. The intensity values of the gray image for both the back and belly sides of trout**.**

7.1.5. Belly crest defining and fin segmentation process

The object labeling process in Matlab software starts from the top left to the bottom right in the image matrix. So, the region ‘Q-1’ on the left side of the center line will be labeled as ‘1’ and the region ‘Q-2’ on the right side will be labeled as ‘2’ (Figure 7-9c). Afterwards, ‘Q-1’ was discarded since the fins are always located in ‘Q-2’. Back and belly identification guarantees the fins are in ‘Q-2’ even if the head of the trout is downward.

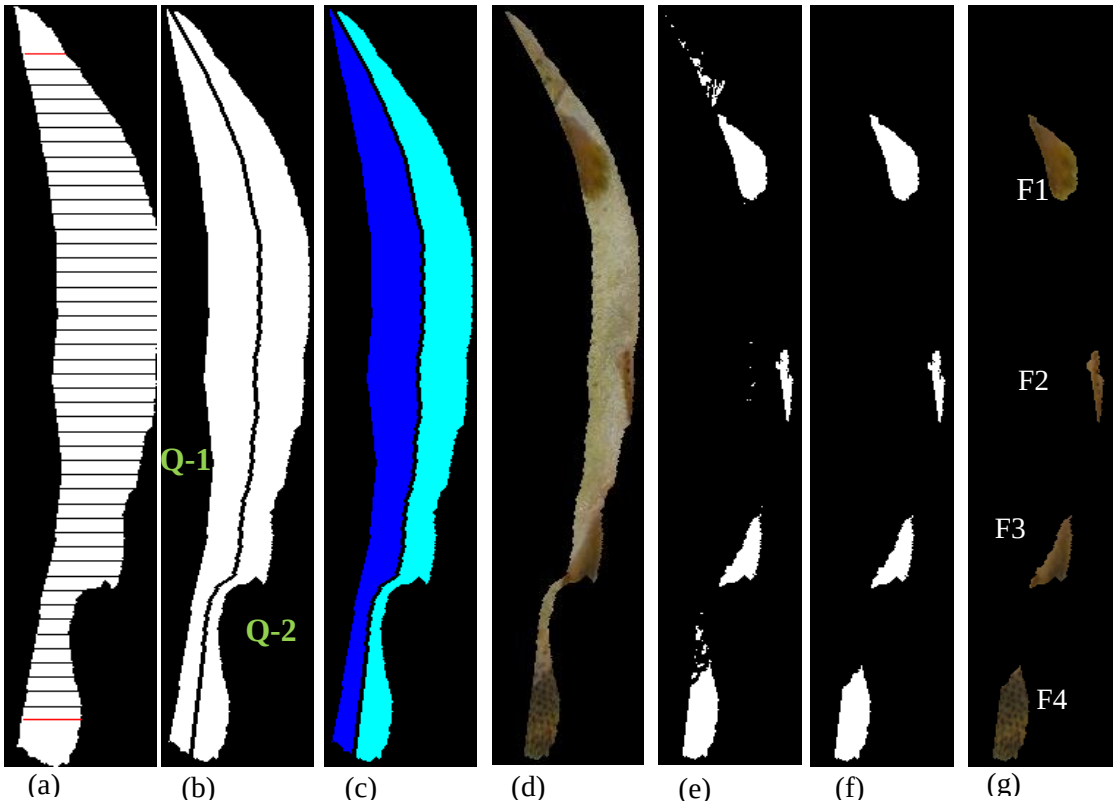

Figure 7-9. Trout fin segmentation process: (a) defining 45 horizontal lines between two red lines from 1/15 of the length from the top and the bottom of trout, (b) drawing a center line in the binary image, (c) labeling the left side as '1' (dark blue) and the right side as '2' (light blue), (d) applying a mask to get the color image in part 'Q-2', (e) applying fin segmentation threshold, (f) removing the extra object and filling any possible holes, and (g) final segmented fins (F1, F2, F3, and F4).

The next step is to segment pectoral (F1), pelvic (F2), anal (F3), and caudal (F4) fins. The position of F1, F2, and F3 will be used in the trout cutting process. The caudal fin is used to identify the head and tail sides. Alike initial trout segmentation step, channels of 'RGB', 'HSV' and 'L*a*b*'color spaces were tested for fin segmentation. Among them, channel 'B' was again considered the best one since it showed a better distinction between the fins and non-fin regions. The fins and non-fin regions are shown in Figure 7-12a for all tested channels. In this case, the pixels with intensity values less than 65 were considered the fins and the rest were considered the background (non-fin region).

In the segmentation process, some small objects and spots appeared in the binary image (Figure 7-9e). As these objects were redundant, they were removed by considering an appropriate number of pixels in the binary matrix. To avoid removing the fins,

especially the smallest fin (F2), the objects (in pixel) smaller than 0.001% of the bounding box area (W×L) were omitted since the fin area is concerning the trout dimension. To fill any holes inside the fins, a morphological function of MATLAB software was applied in which the connected pixels of background (logical '0') change to foreground pixels (logical '1'), stopping the process as it approaches the object boundaries. Using the filling algorithm of morphological operations (Soille, 2013), the filled binary image can be written as equation (1):

$$J = \text{imfill}\{I, 'holes'\} \tag{3.18}$$

Where 'I' is the binary image matrix, 'J' is the binary image in which the 'holes' are filled. In morphological operations, a hole is defined as a set of background pixels that cannot be reached by filling in the background from the edge of the image (Wang, 2014).

7.1.5.1. Solving belly crest possible errors

The flowchart of the image processing steps is presented in Figure 7-10. All the processing method together with solving any possible errors in belly crest determination

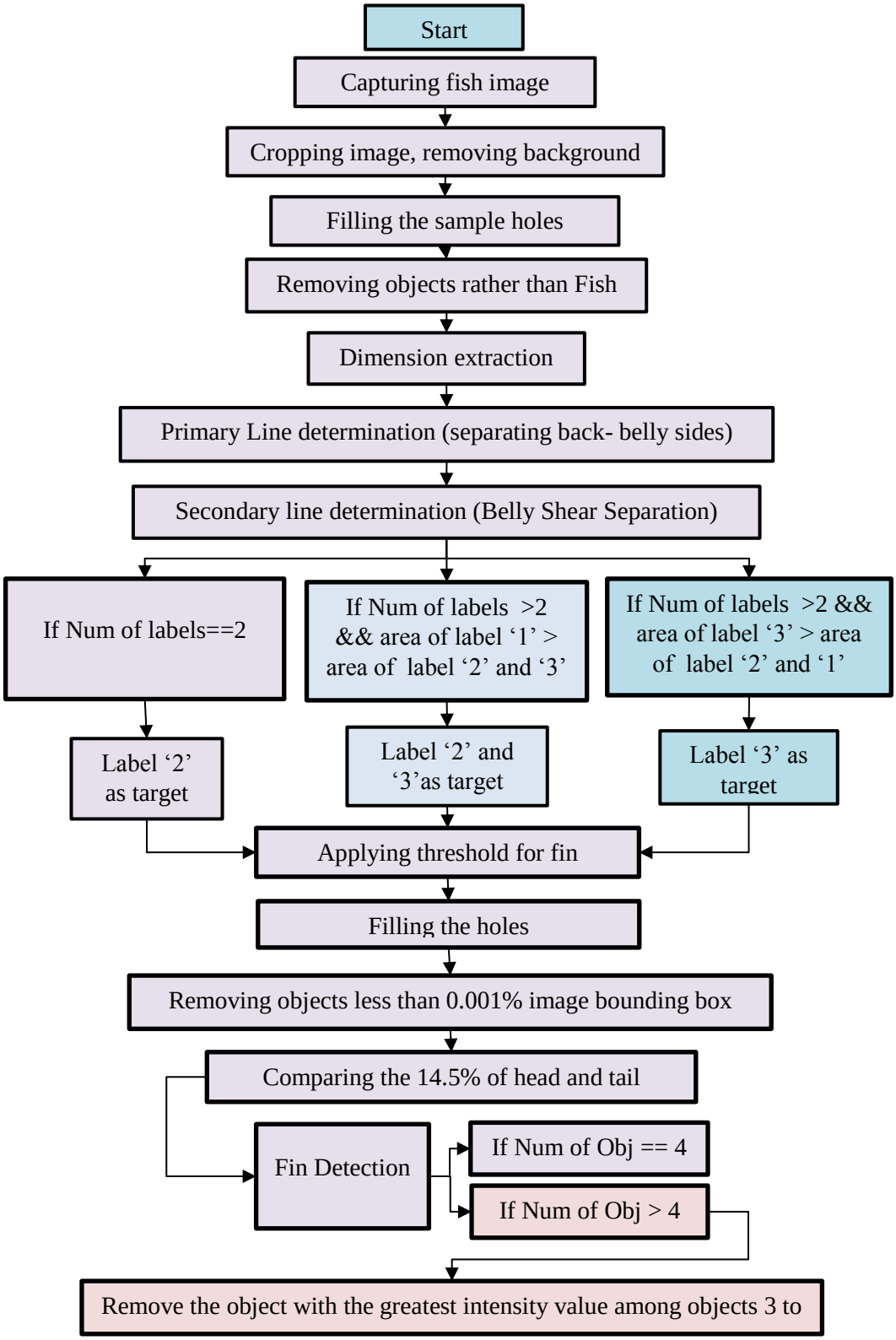

Figure 7-10. Complete flowchart of the trout processing in the offline stage.

As presented in Figure 7-9, considering two labels can satisfy the fin segmentation process, but an improper central line will lead to the incorrect fin segmentation process. In other words, we must separate the belly side into two parts with labels ‘1’ and ‘2’ in which the part with label ‘1’ is omitted. Examples of incorrect labeling (three labels) and the wrong detected fins are shown in Figure 7-11.

In the secondary line determination step, three types of errors, including error type ‘1’ (E1), error type ‘2’ (E2), and error type ‘3’ (E3), were observed. ‘E1’ occurred when we considered more lines. In this case, as the number of horizontal lines increases, the center of a horizontal line comes close to the anal fin (case ‘b’ of ‘E1’), which guides the centerline to fall out of the fish area in distorted anal fins. On the other hand, considering a low number of horizontal lines results in an improper line that is not passing through the center (e.g., ‘E1’), causing problems in the narrowest region of the fish (‘E2’).

The third type of error (E3) occurred when one horizontal line was not properly created. Even though an increased number of lines decreased the errors, in the case of 45 lines, there were seven errors, including four errors of both ‘E1’ and ‘E2’ and three errors of ‘E3’. Table 7-3 presents the secondary line determination errors in detail. In order to solve these errors, two different comparative conditional statements were added to the algorithm. Determining the centerline is critical since the fin detection process depends on this step. As it is shown in Figure 7-11, in cases of ‘E1’ and ‘E2’, the area (in pixels) of blue color with the label ‘1’ is greater than the area of yellow and light blue colors with the corresponding labels ‘3’ and ‘2’. In these cases, both labels ‘2’ and ‘3’ were considered the target for further fin detection process, and the region with label ‘1’ was discarded. In the case of ‘E3’, the area of label ‘3’ with a corresponding yellow color is greater than the area of both labels ‘1’ and ‘2’. In this case, the label ‘3’ was considered the target. This procedure led to appropriate fin segmentation in all 97 trout samples.

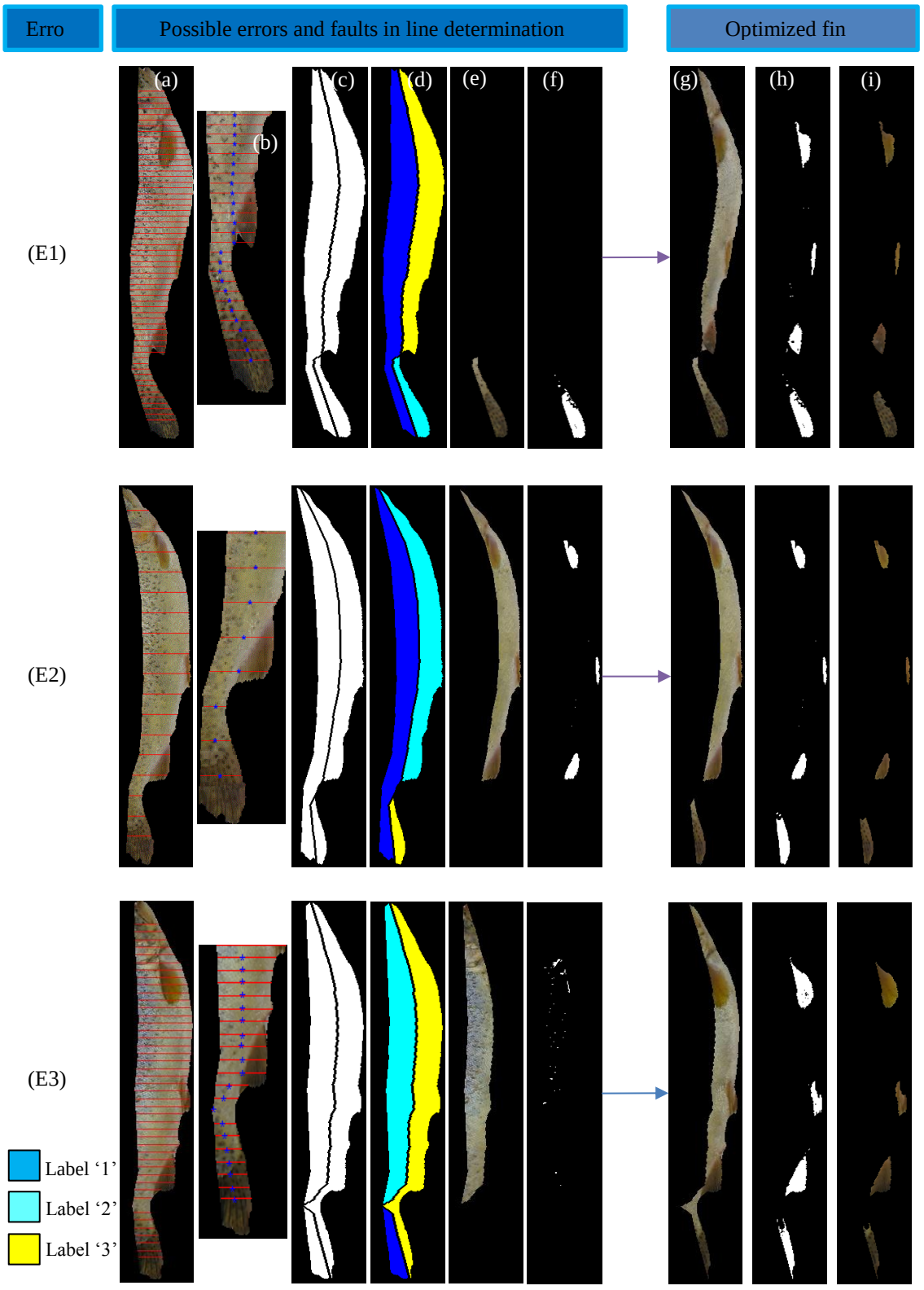

Figure 7-11. Three different errors in the secondary line determination step which leads to an incorrect segmentation: (E1) applying an excessive number of horizontal lines causes incorrect labeling in distorted anal fins, (E2) considering a low number of horizontal lines, and (E3) indexing problem in the start and endpoint.

The initial segmentation (segmenting the trout from the background) and secondary segmentation (fin segmentation from the region Q-2) were done based on manual thresholding. The initially applied method resulted in acceptable trout segmentation. Still, since the whole function of the system is based on the data received from the image analyzing section, it is essential to find the precise cutting points and exact belly cutting length. Any inaccurate or incomplete fin segmentation will lead to improper functioning of the gutting and beheading subsystems. Therefore, the fin segmentation process is as critical as the preprocessing and line determination steps.

7.1.5.2. Visually selecting the proper channel and statistically testifying the selection

The fin shear segmented in the previous section is investigated to select the most proper color channel for the fin segmentation. Based on the visual analysis, the best color channel is the one at which the difference between the fin and non-fin region is the highest. Therefore as shown in Figure 7-12, channel B from RGB color space represents the most distinction among tried channels. To testify the accurate selection, further statistical analysis was conducted. In Figure 7-12, the following sections are presented:

(a) The non-fin region and the fins are considered background and target, respectively

(b) The elements applied in the t-test (non-fin region & fins), and

(c) Elements of ANOVA analysis (fins)

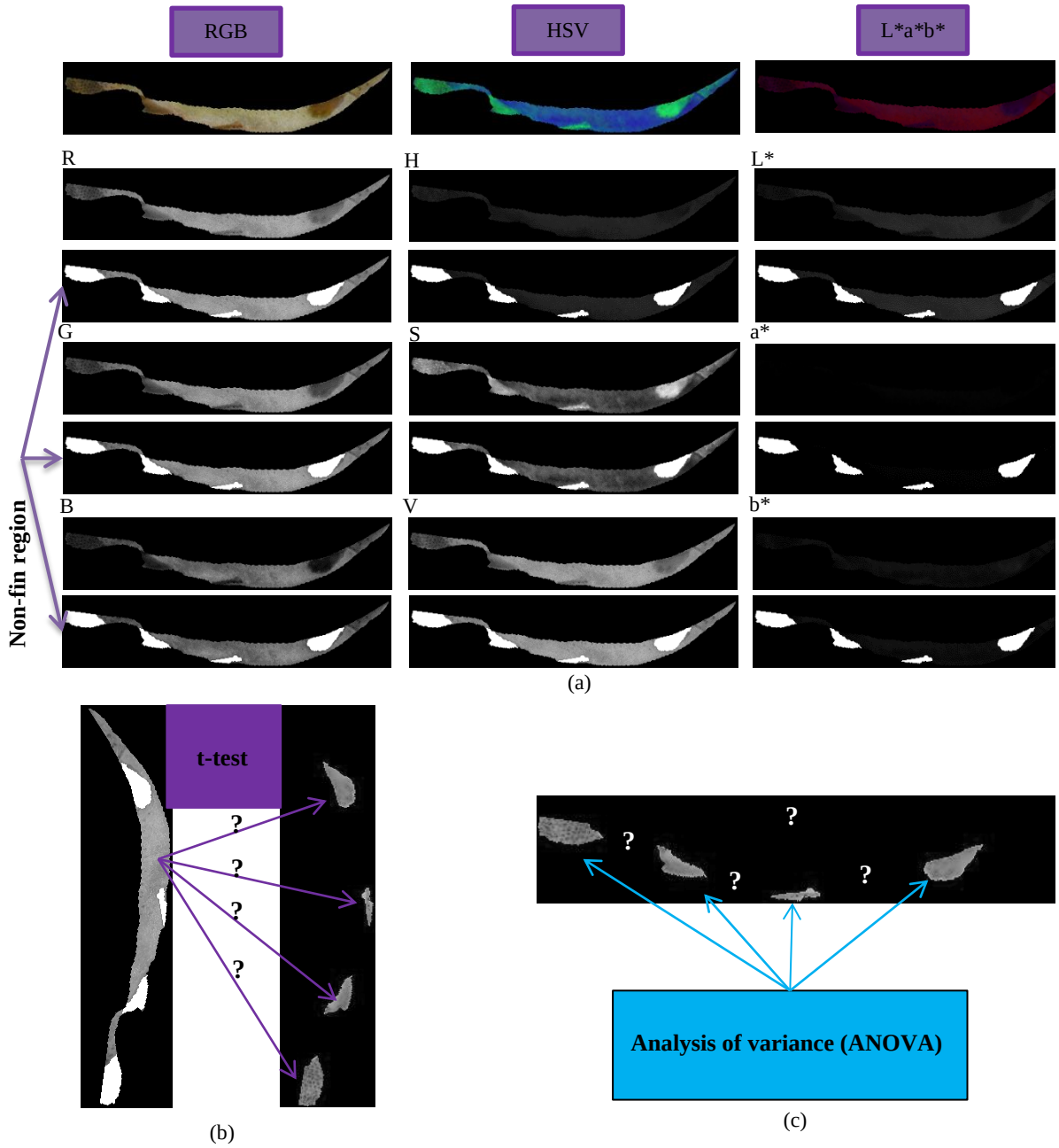

Figure 7-12. Region ‘Q-2’ in RGB, HSV, and L*a*b* color spaces investigated in the fin segmentation process. This figure also shows the non-fin region in which the fins are omitted: (a) The non-fin region and the fins are considered background and target, respectively, (b) the elements applied in the t-test (non-fin region & fins), and (c) elements of ANOVA analysis (fins).

Two further analyses were conducted to testify the channel ‘B’ performance in fin segmentation: t-test and analysis of variance (ANOVA). The t-test is applied to compare

the most significant difference between two groups of data. In this case, it is desired that the difference between the mean intensity values of the fins and the corresponding non-fin area (Figure 7-12b) results in higher t-values. This shows that there is a significant difference between the fin and non-fin region which facilitates fin segmentation. The result of the t-test is presented in Table 7-2. The analysis of variance (ANOVA) is applied among the mean intensity values of the segmented fins (Figure 7-12c) in all the samples. In this method, the least 'F' value shows the least difference between the mean intensity values of the fins.

The result of the ANOVA analysis is presented in Table 7-1. The final result of the proper fin segmentation can be seen in Table 7-3. In this section besides the fin segmentation, the real area of the fins has the most critical role in cutting point extraction. If the visually selected channel was not the proper one, we were not able to rely on the results presented in Table 3, which leads to the extraction of the exact cutting points. The statistical mean intensity values of each object (the fins and corresponding non-fin region) in each color channel were calculated using the following equation:

$$\text{Mean } (\mu) = \frac{\sum_0^i \sum_0^j I(i,j)}{n} \qquad 3.19$$

Where, 'i' and 'j' are the indexes of the pixels in the rows and columns, respectively. 'μ' is the color channel of each color space, 'n' is the number of the pixels of each object and, 'I' is the image matrix with the number of the rows of 'i' and the columns of 'j'.

The standard deviation of the mean intensity values (calculated with equation 2) was calculated using equation (3).

$$\text{Standard Deviation}(\sigma) = \sqrt[2]{\frac{(\mu_s - \bar{\mu}_s)^2}{s}} \qquad 3.20$$

Where '$\boldsymbol{\mu_s}$' is the object mean intensity value and '$\boldsymbol{\bar{\mu}_s}$' is the mean value of $\boldsymbol{\mu_s}$. In this formula, 's' is the number of the samples.

Once the region ‘Q-2’ is properly defined, the fins are segmented using the selected ‘B’ channel. This channel was manually selected according to the trial and error based on the best visual segmentation, but, as this step is crucial in cutting point determination; two further analyses were conducted to testify the channel ‘B’ performance among all other color channels, including the following stages:

(a) Determining the least difference among the fins: To testify the selected channel performance, we performed an analysis of variance (ANOVA). In this case, the F-value is considered a criterion to evaluate the color channel performance (the procedure is shown in Figure 7-12c). In ANOVA analysis, a greater F-value indicates a more statistically significant difference between the mean values of the groups (Lee et al., 2014).

(b) Investigating the most significant difference between the mean intensity values of the fins with the corresponding non-fin region: the more significantly different the mean intensity values are, the higher the t-value will be obtained.

Table 7-1 shows the results of the mean ‘B’ intensity values, together with the other eight tested color channels of RGB, HSV, and L*a*b*. In all the cases, the averages of the mean intensity values are significantly different among the fin groups ($\rho < 0.01$). As stated in the table, the average values of channel ‘B’ for F1, F2, F3, and F4 are 33.78, 43.73, 40.94, and 38.78, respectively. The results show that channel ‘H’ has the least F-value (32.00) among all tested groups. This means that the mean intensity values of the fins are close to each other, which is desired for fin segmentation. Among them, channel ‘B’ has a second-place with an F-value of 64.82.

Although the F-value of channel ‘H’ is less than the value of channel ‘B’, this channel shows a higher visual distinction compared to channel ‘H’ between the fin and non-fin regions. This fact is proofed by conducting a t-test between the fin and non-fin intensity values in all the color channels. The result of the t-test is presented in Table 7-2. As it is shown in this table, the t-values of channel ‘B’ for the paired groups of the non-fin region and each of the fin groups are 90.30, 78.07, 74.28, and 86.01 for F1- non-fin, F2- non-fin, F3- non-fin, and F4- non-fin, respectively. The mean value of the t-test is 82.16, which is the highest value among the tested channels. Thus, these results prove that the visually selected ‘B’ channel is adequate for trout fin segmentation.

Table 7-1. Results of one-way analysis of variance (ANOVA) between the groups of the fins

Color channels	(mean intensity value±SD)					F value
	F1	F2	F3	F4	Total	
R	107.55±10.30	115.23±11.11	88.30±11.81	73.65±10.62	96.19±19.64	171.25
G	80.31±9.53	84.51±9.63	64.43±9.41	59.63±7.86	72.22±13.81	284.90
B	33.78±5.60	43.73±5.31	40.94±5.37	38.78±4.17	39.31±6.29	64.82
H	0.101±0.01	0.095±0.10	0.085±0.02	0.099±0.01	0.096±0.02	32.00
S	0.684±0.06	0.062±0.06	0.531±0.07	0.466±0.08	0.576±0.11	198.59
V	0.422±0.04	0.452±0.04	0.346±0.04	0.289±0.04	0.377±0.08	284.94
L*	22.68±2.41	24.15±2.46	18.59±2.55	16.75±2.18	20.54±3.83	199.98
a*	-0.921±0.69	-0.114±0.26	-0.055±0.07	0.258±0.27	-0.337±0.52	98.28
b*	20.11±3.93	18.26±3.45	11.08±2.95	9.19±2.56	14.66±5.66	258.91

The F-value indicated a significant difference between the mean values of the four tested fin groups at the 99% probability level ($\rho < 0.01$).

Table 7-2. Results of t-test between the groups of the non-fin and the fins in corresponding color channel.

Color Channel	(Non-fin region mean intensity value±SD)	t-value				Mean of t-value
		F1	F2	F3	F4	
R	141.85±6.03	36.42	25.71	43.80	59.94	41.47
G	132.71±6.15	58.19	51.12	65.72	75.85	62.72
B	106.48±7.61	90.30	78.07	74.28	86.01	82.16
H	0.13±0.00	20.81	28.64	19.25	20.92	22.40
S	0.25±0.04	65.00	59.39	35.35	18.01	44.44
V	0.56±0.02	36.46	25.79	43.82	59.94	41.50
L*	36.39±1.65	66.14	49.94	63.24	73.82	63.29
a*	1.52±0.48	23.04	26.83	30.54	29.86	22.18
b*	0.84±0.36	48.43	49.35	35.03	35.03	41.96

The t-value indicated a significant difference between the mean values of the tested paired fin and non-fin groups at the 99% probability level ($\rho < 0.01$).

7.1.5.3. Solving fin segmentation possible errors

Among all the images, there were four samples in which some extra objects were wrongly segmented in the fin detection stage between F2 and F4. Examples of these images are shown in Figure 7-13. These objects will cause system malfunctioning, especially in belly cutting point determination, which is supposed to cut the belly from F3

towards the trout head. To remove the extra objects, a possible solution is to consider a greater structure element, but it results in omitting F3 in some samples because of its small area. Another solution is to eliminate the extra object with label ‘4’ between F3 and F4, but among the mentioned images, there were two images that the extra object was segmented between F2 and F3 (case 2). In such conditions, the anal fin (F3) was wrongly omitted. To avoid such problems, we considered the mean intensity values of channel ‘B’ as a criterion in which the object with the highest mean intensity values (the lighter object) was discarded.

Since the area between F1 and F2 is lighter with fewer dots and other dark spots, no further object was detected in this region. Thus, apart from the intensity value of F1, the intensity values of the other fins, together with the extra objects, were considered for further comparison. Among all of the 97 trout images, four samples were observed with an extra object. These objects had the mean ‘B’ intensity values of 56.92, 96.28, 55.41, and 53.00. These values were significantly different from ‘B’ intensity values of the fins presented in Table 7-1. Therefore, the extra object with the maximum mean ‘B’ intensity value was eliminated among the objects. Finally, in all the trout samples, the fins were successfully detected with 100% accuracy.

The detailed results of fin segmentation in all the samples, including three types of error in secondary line determination step (presented in Figure 7-11) and two different cases of extra object segmentation (Figure 7-13) are presented in Table 7-4. Among the samples, there was not any case with six detected objects, but even in such cases, as the mean intensity values of the channel ‘B’ is determined for the fins and any possible extra object, the first two objects with the least intensity values will be considered F3 and F4.

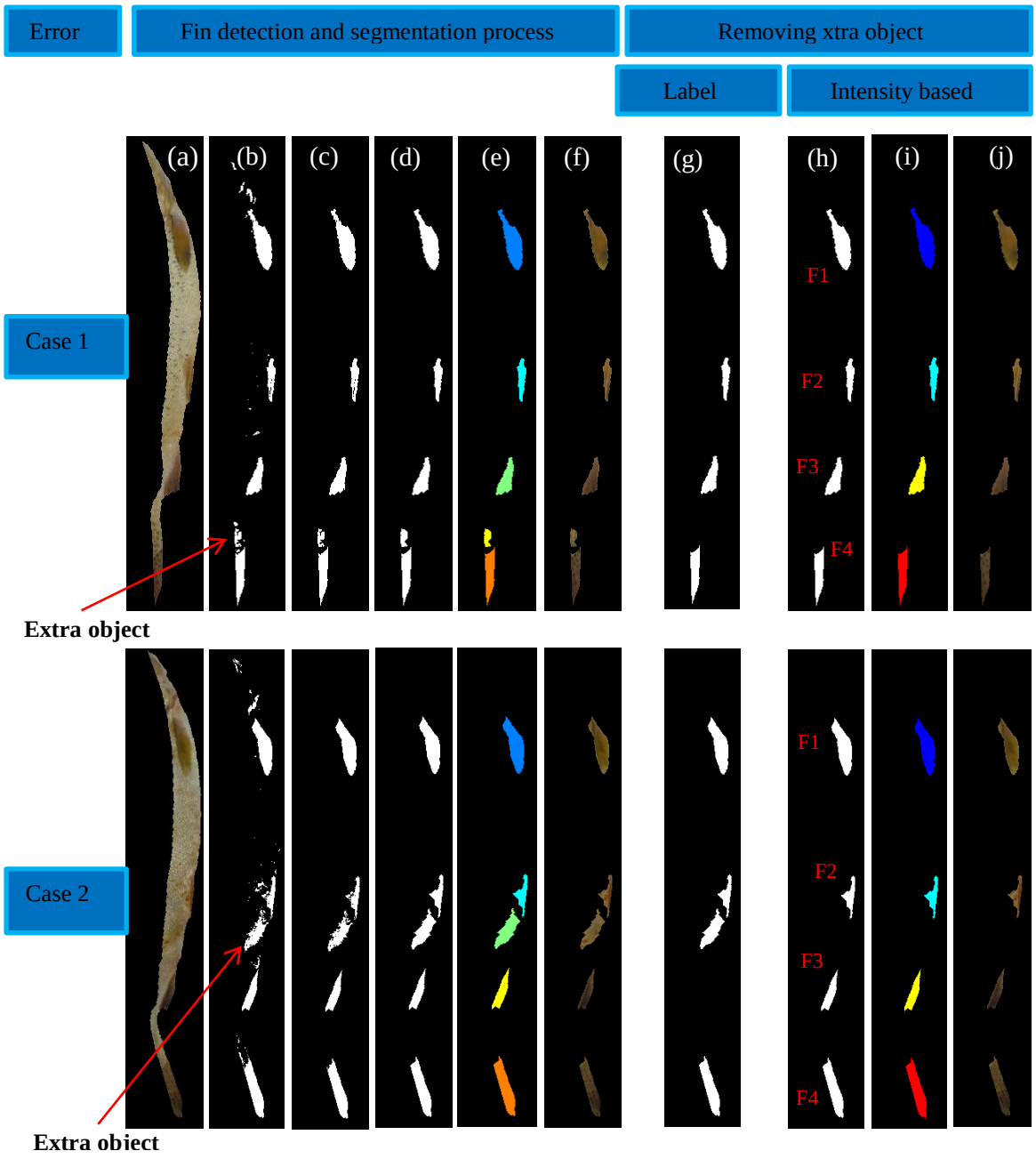

Figure 7-13. Fin segmentation and extra object elimination in fin detection process in the region between F2 to F4: (a- f) fin segmentation procedure, (g) label based non-fin object removing, and (h-i) intensity-based non-fin object removing.

Table 7-3. Detailed fin segmentation results with corresponding errors in line determination and fin identification steps with successful detection and final results.

Total errors of secondary line determination and fin identification (%)					SDWE (%)	FD (%)
12.37						
Line determination error (%)			Fin identification error (%)			
8.24			4.12		87.63	100
E1(%)	E2(%)	E3(%)	Case 1 (%)	Case 2 (%)		
4.12	1.03	3.10	2.06	2.06		

SDWE: Successful detection without errors; FD: Final detection

As shown in this table, among all the samples, 8.24% of the images have the problem of line determination error. The percentage of the error types 'E1', 'E2', and 'E3' were 4.12%, 1.03%, and 3.10%, respectively. As stated above, in 4.12% of images, some extra objects were detected as trout fin. The extra object error was 2.06% for each of the cases. In total, 12.37% of the images had both line determination, and extra object segmentation problem and the rest of the images were properly segmented. By removing both types of errors, the total fin detection value was 100% for all of the 97 trout images.

7.1.5.4. Fin segmentation accuracy

In order to determine the capability of the image processing algorithm for fin determination, 97 fish images (a total of 388 fins) were selected. The position of each fin was manually annotated and compared with the region obtained by the algorithm. Three common statistical parameters including Sensitivity (SE) (probability of a positive test result among those having the target category), Specificity (SP) (probability of a negative test result among those without the target category), and Accuracy (AC) (probability of both positive and negative test results among the target and non-target categories) describe the algorithm performance (Van Stralen et al., 2009), according to equations (4), (5), and (6), respectively (Mjahad et al., 2017). This method is presented in Figure 7-14 for a sample pectoral fin.

In the following equations, the terms True Positive (TP), False Negative (FN), True Negative (TN), and False Positive (FP) indicate the number of pixels which are 'correctly identified as fin pixels', 'incorrectly identified as non-fin pixels', 'correctly identified as non-fin pixels', and 'incorrectly identified as fin pixels', respectively. The related results

are presented in Table 7-4.

$$\text{Sensitivity} = \frac{\mathbf{TP}}{(\mathbf{TP}+\mathbf{FN})} \tag{3.21}$$

$$\text{Specificity} = \frac{\mathbf{TN}}{(\mathbf{TN}+\mathbf{FP})} \tag{3.22}$$

$$\text{Accuracy} = \frac{(\mathbf{TP}+\mathbf{TN})}{(\mathbf{TP}+\mathbf{TN}+\mathbf{FN}+\mathbf{FP})} \tag{3.23}$$

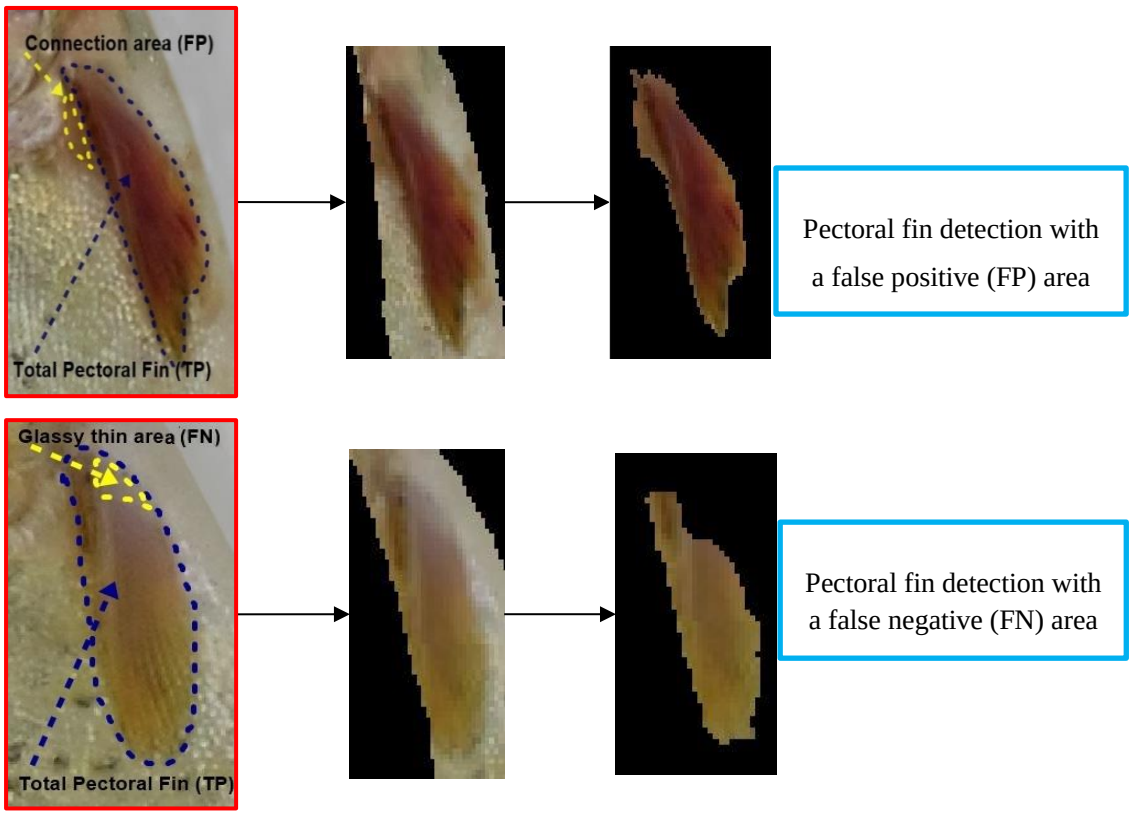

Figure 7-14. Fin detection process in different possible conditions showing the fin segmentation sensitivity, specificity, and accuracy calculations.

Concerning the fin detection results, Table 7-4 presents the percentage of fin detection values, including sensitivity, specificity, and accuracy. The most and the least sensitivity values correspond to F4 and F2, respectively. The reason for the low sensitivity of F2 is its smaller size compared to the other three fins. Since F2 is under the belly, only a small

amount of this fin is visible in this view. The sensitivity value of F1 was lower than F3 and F4. This is due to the thin glassy area of the fin at the joint of the fin and the body, which shows the color of the underneath skin. Since the area of F3 is greater than F1 and F2, and its intensity value is less than both fins, the sensitivity of this fin is more than the other two fins. Finally, the highest sensitivity value was calculated for F4 because of the high thickness and slight change in the pixel intensity.

Table 7-4. Image processing Sensitivity, Specificity and Accuracy values of four trout fins.

	Pectoral Fin (F1)	Pelvic Fin (F2)	Anal Fin (F3)	Caudal Fin(F4)	Overall
Sensitivity%	81.251	75.760	88.546	98.662	86.054
Specificity%	99.964	99.968	99.975	99.951	99.965
Accuracy%	99.774	99.893	99.892	99.938	99.874

Misimi et al., (2017) reported a color-based, pixel-wise, and SVM-based model, developed for accurate segmentation and localization of blood defects in cod fillets with the overall accuracy of 96%. Our results showed an overall accuracy of 99.88% for the fin segmentation. It should be considered that the most significant criterion among these three criteria is the sensitivity since it considers the number of the target pixels (fins) rather than non-target pixels, which is greater than the target pixels in most of the cases. In this research, the overall sensitivity was 85.54% for all the fins.

The desired function of the trout processing system is obtained when the head is properly cut with the least fillet lost. On the other hand, any extra object rather than the fillet, close to trout head, must be removed. Therefore, the cutting process will be performed from the beginning point of F1 in which the removal of the bony area near the fish gill is achieved (Figure 7-15a).

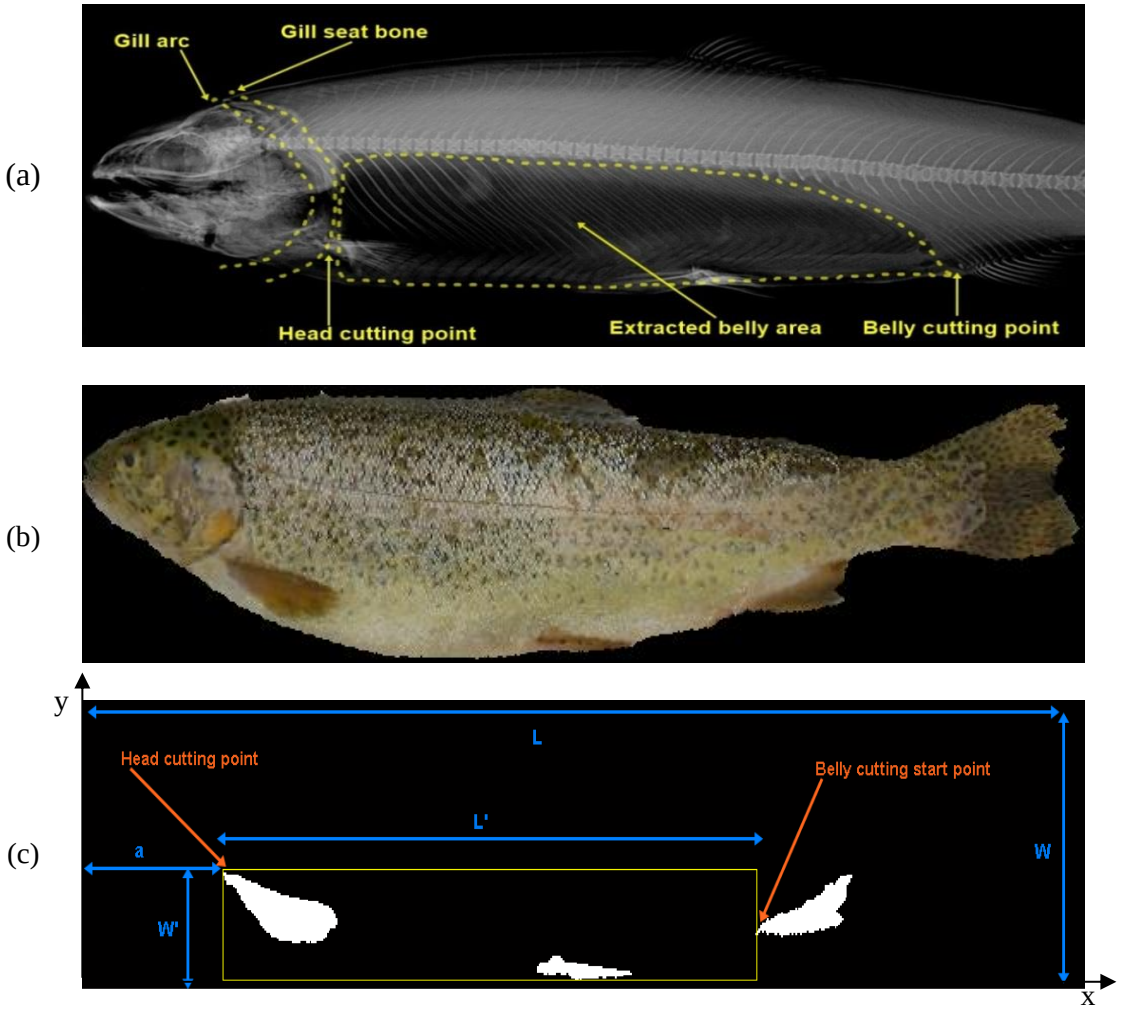

Figure 7-15. (a) Processed area of the belly in X-ray image with yellow dash lines and related cutting points for beheading and gutting, (b) sample fish, and (c) exact cutting position of head and belly after processing the images.

In a trout processing machine, after beheading, the next step is to cut the belly and clean its internal content. In this design, the gutting process will be easily done since, at the end of the fish path, there is no obstacle for the evacuating tools. Figure 7-15a shows the processed area of the belly in an X-ray image with yellow dash lines together with beheading and gutting points. Since the belly intestines are located in the distance between the anal fin and the gill, F3 is chosen as the appropriate place to start the incision in the belly. Afterward, a suction tube with a rotary cleaner brush will clean the abdominal cavity from the anal fin towards the head.

The position of F2 is determined to extract the belly arc and identify the processing rectangle (Figure 7-15c). In this figure, the distance from the head to the start point of F1 is shown with ‘a’, and the rotary cutter movement in X and Y direction is shown by (L′) and (W′), respectively. In this case, after starting the cutting process from F3 and passing through F2, it will reach F1 and complete the abdominal incision and suction processes. This will satisfy the perpendicular movement of the rotary blade that will enter inside the fish body. The entire image processing procedure is illustrated in Figure 7-16. All the details in this figure are described in the detail.

The details of the flowchart are stated in the following:

A-1: Initial image

A-2: Resizing & cropping

A-3: Manual thresholding

A-4: Filling the holes removing objects

B-1: Orientation and Dimension extraction

B-2: Initial line determination for Belly-back side identification

C-1: Labeling segmented binary image

C-2: Three different types of errors in labeling of two different quarters of the trout

C-3: Passible errors in belly shear determination

D: Thresholding to segment the fins

E-1: Two different types of errors in labeling trout fins

E-2: Fin labeling possible errors

F: Defining cutting point and cut length

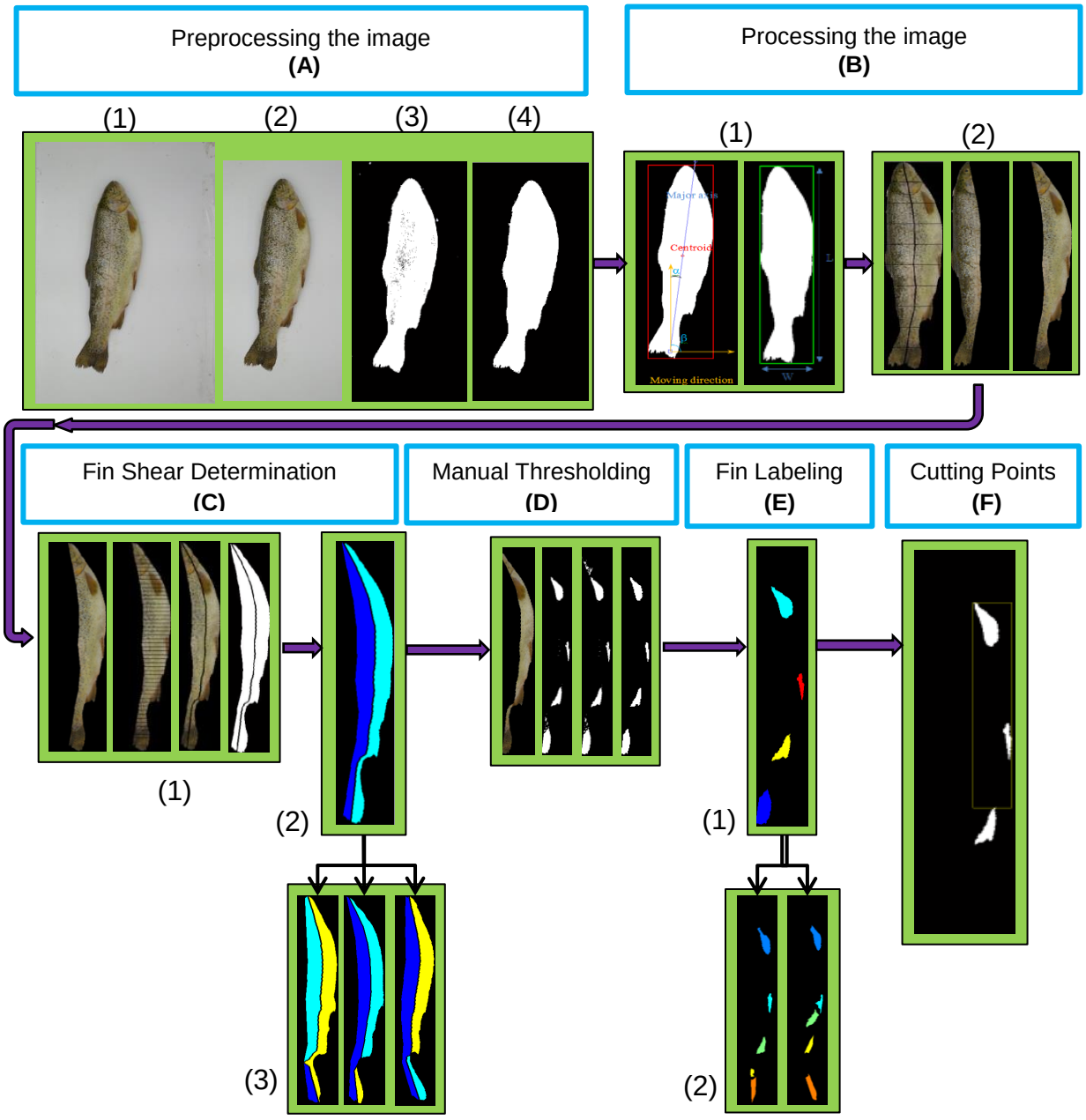

Figure 7-16. Image processing procedure

7.2. Online processing

As described in the offline image processing section, the proper operation of the machine depends on the precise cutting point determination resulting in proper cut with the least fillet loss. At the next step, the images were examined online.

7.2.1. Imaging system

In order to capture the images, an online video camera (Basler, daA1280-54uc, USB3, 1280 × 960, 1.2 MP) was applied. To cover the total fish length considering the distance between the camera and the fish, a wide view lens (Evetar Lens M118B029520W F2.0, f 2.95mm, 1/1.8", S-Mount) was applied. Since this camera will be applied in an online system, we need a higher frame rate to guarantee an explicit image. In order to get the fish images, three frames were saved from each snapshot based on the input number assigned to each fish sample. Afterward, the images were processed for further steps.

The designed imaging case is presented in Figure 7-17. In this figure, all parts of the lighting case are presented in detail. This case is made of stainless steel, and three Plexiglas parts are used as foreground and background light shields. Two blurs white Plexiglas shields (I and II) are used to provide a uniform light diffusion inside the case to avoid any possible glitter from the fish scale in captured images. The blue Plexiglas shield is also illuminated with the backlight to reach a desirable background for fish segmentation.

Since this type of camera is fabricated as an industrial microchip, a polyethylene body was designed to protect the camera from external defects and properly installed inside the imaging case (Figure 7-12b). The fabricated imaging case with the mounted video camera with the LED lights ON and OFF is presented in Figure 7-12c. In order to process the images, MATLAB 2017b software installed in a Hewlett-Packard S4530 laptop computer with the Intel(R) i5-2410M CPU@2.3 GHz with 8 GB RAM was applied.

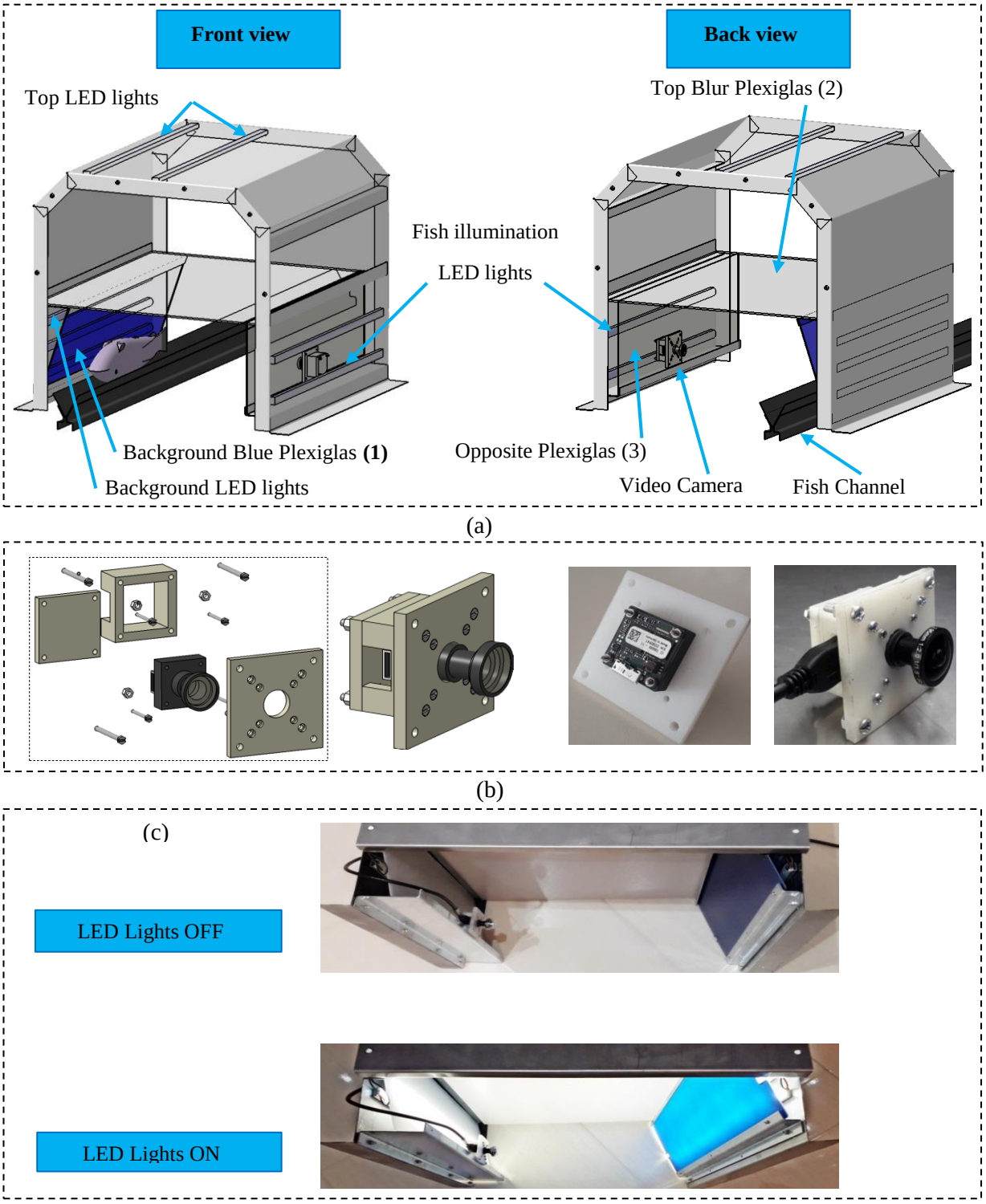

Figure 7-17. The image processing setup: a) front and back view of the imaging case with detailed parts designed in CATIA software; b) designed and fabricated camera case; and c) inside of the imaging case with the lights OFF and ON.

7.2.2. Camera calibration

Since, in this study, a fisheye lens is applied to cover the total length of the biggest tried fish sample, it is necessary to remove any distortion from the initial image. Thus a checkerboard page with a square dimension of 21 mm was applied. In order to calibrate the camera, 17 images were captured from the checkerboard in different positions. A sample image of the fish before and after correction is presented in Figure 7-18. Since the final dimension of the fish will be applied in the fish processing system, the calibration process is of critical importance. By conducting camera calibration, any pixel of the image equals 0.3 mm in the real world. In order to assess the camera distortion calibration accuracy, the dimension of the fish from the head to tail (HT) and the back to belly (BB) were measured. Afterward, these dimensions were compared with the dimensions extracted from the calibrated images.

7.2.3. Fish classification from blue background

One of the most critical steps in image processing is to segment the target (fish) from the background. The segmentation process is more feasible when the contrast between the target and the background is distinct enough to perform with automatic methods like Otsu (1979).

Azarmdel and et al. (2019) applied a constant value as a trout segmentation criterion. Considering the diversities in trout color, they justified that the Otsu method could not segment the fish from the white background (for sanitary restrictions) because of the little nuance between the background and trout belly.

It should be noted that choosing lighter backgrounds facilitates the segmentation process in darker regions (the fins, head, and back part), but segmenting the whole target was performed using manually assigned intensity value. Since, in this study, different species of fish with different colors are processed, it is impossible to segment all the samples in the white background. Therefore, it is essential to select a background in which all species are easily segmented. By proposing a new method for fish transfer, the contact between the fish and any conveyer is resolved, so it is possible to select various colors in the background. After conducting different trial and error, the pure blue color was selected

for fish segmentation.

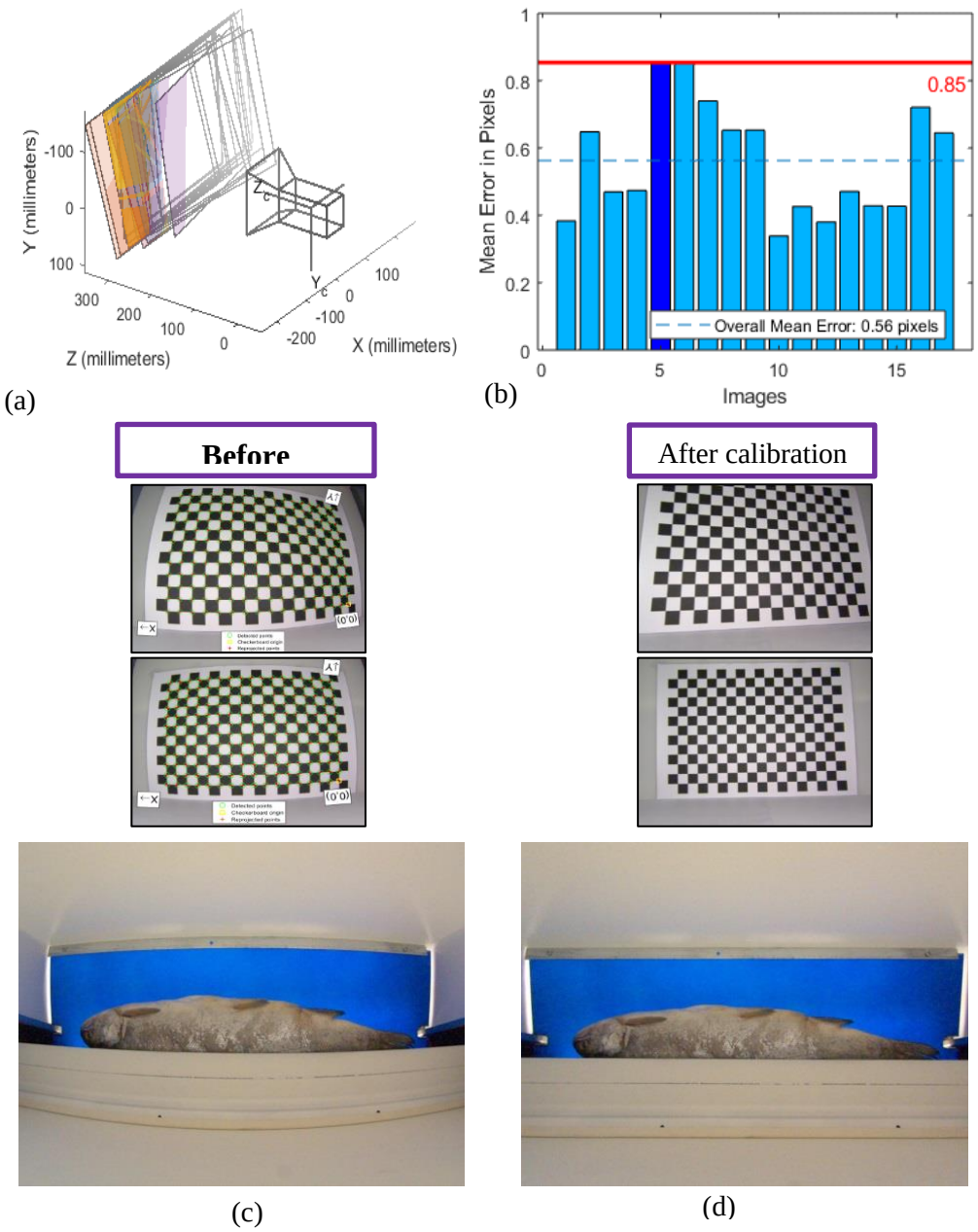

Figure 7-18. Video camera distortion calibration process: a) different checkerboard positions in front of a constant camera; b) mean errors of the calibration tries based on the pixel; c) camera frames before calibration; and d) camera frames after calibration.

Among all fish species, the skin color is so light that the light background is not a proper option. Therefore, choosing a darker background can solve the segmentation process in these species, but it causes the problem in the species with dark skin unless the

darker background intensity is so close or equals to ‘0’. Therefore applying a black background seems to be a proper option. Figure 7-19a shows the black background and the color channels of RGB color space with the intensity values for each channel. It is clear that the pixel intensity values of the black background are distinct enough for lighter fish segmentation, but considering the intensity values of the background and the trout body, especially at the darker parts of its back and the fins, the segmentation process will face a great challenge in numerous fish samples.

Since the mean intensity value of the fins in channel R is higher among the three color channels of RGB color space, by selecting this channel, the most significant difference between the background and the fins is accomplished. The easiest way to create a pure blue background is to use a blue color behind the fish. One of the challenges to reach a pure blue background is changing the background brightness in opposite illumination. The light generated by the opposite LED lights brightens the blue background, which results in an impure color. This was the same in any lighter or darker blue cardboard background (Figure 7-19b). To solve this problem, we applied a blue Plexiglas with a backlight illumination (Figure 7-19c). In order to avoid any glitter of the opposite light on the blue Plexiglas, the plate was inclined at the angle of 72 º. The pure blue color and the converted images in channel R are presented in this figure. In this condition, the pixels with the pure blue color are converted into ‘252’ in channel B representing the white area, while it converts to pure black in channel R with the value ‘0’ (Figure 7-19c). So, this is the ideal condition in which both fish body (lighter area) and the fins (darker areas) are accurately segmented in all species.

Since one frame will be saved for further process in the online system, a snapshot is captured as the tail reaches the end of the imaging case. In this condition, the total length of the fish is exposed in front of the camera vision, and it can ensure a complete image with total body length in all samples. At the next step, the frames are processed for fish segmentation. The fish segmentation process is presented in Figure 7-21. Before segmenting the fish, it is necessary to crop the images based on the defined bounding box to cover the maximum length and width of the fish. Therefore, a 320×320 bounding box was applied to cut the initial image in which the processing task and time decreased.

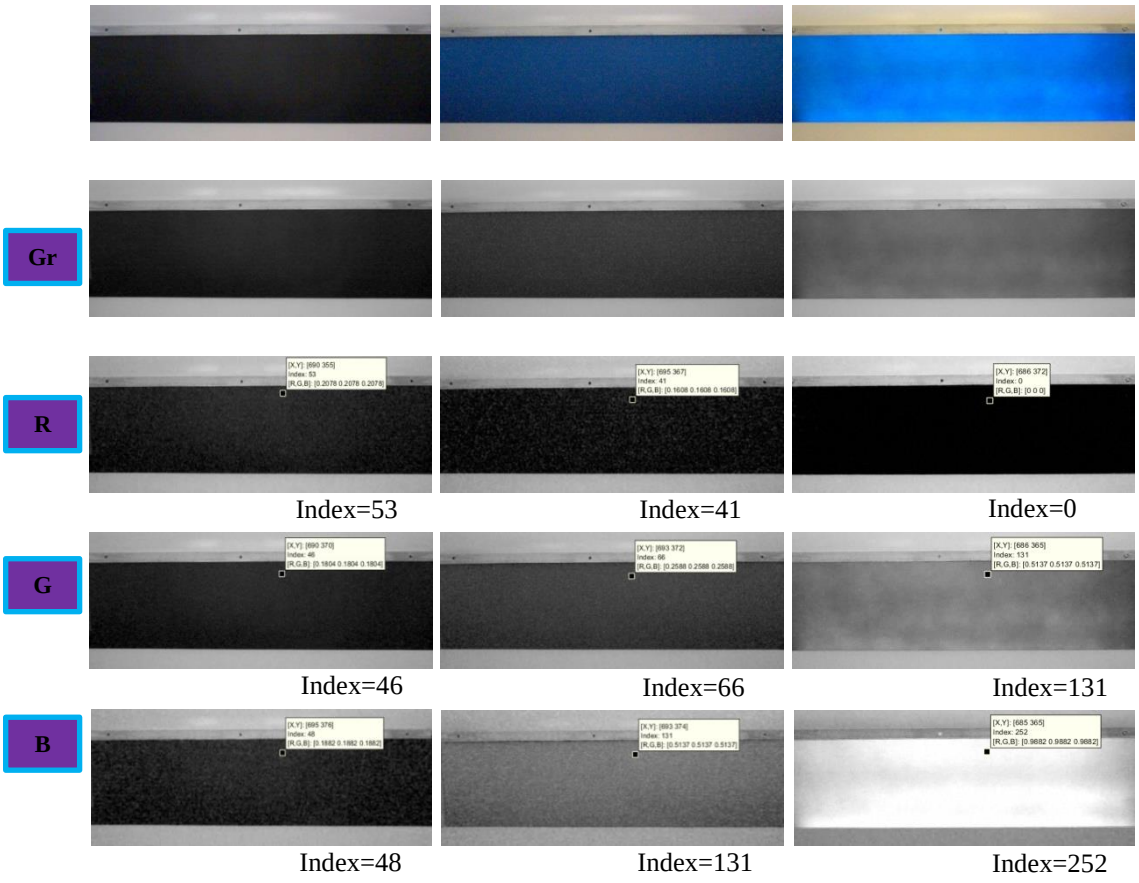

Figure 7-19. Background selection: a) black background, b) blue background, and c) blue illuminated Plexiglas background.

At the next step, channel R of the RGB color space is applied to segment the fish sample from the background. As mentioned above, in this color space, the difference between the fish and the background is distinct enough to segment almost all the fish species from the background properly. Although most of the pixels were assigned the value '0' in the pure blue lighted Plexiglas, some non-zero pixels still existed in the background. By considering a comparative criterion, the pixels with the intensity values of '10' were changed to '0'. To show the amount of the non-zero pixels in the background, we also applied a similar criterion to remove the pixels with the values less than '5'.

It must be considered that for the total intensity values ranging from 0-255, and the least value of the darkest fish species, removing the pixels with the values less than ten, guarantees complete fish segmentation together with avoiding any pixel loss (Figure 7-21a). At the next step to complete background correction, any object smaller

than 300 pixels were removed. By segmenting the fish body, the initial color image is masked to have a color fish sample in the black background in which all color, geometrical and texture features are extracted to further step.

As shown in Figure 7-21, in the first step, the initial image (a) was cut into a fixed size of 1045×260 to reduce the processing operation. In the next step, channel R of the RGB color space was applied to segment the fish sample from the background (c). In the next step, considering the intensity range, pixels with intensity values less than 10 were changed to zero (d). In this case, the fish is properly segmented. Although most pixels are "0", there are still some non-zero pixels in the background. In the next step to complete the fish segmentation process, any small objects with an area fewer than 300 pixels were removed, and a rectangle was drawn on the fish to extract the fish dimension (e).

Finally, to perform the second phase of segmentation (segmentation of fins from fish), a color image was masked on the binary image; so that by matching two images (b) and (f), the pixels of the image matrix (f) with the corresponding indices in an image (b) with the value of “0” is converted to “0” and the rest of the pixels remained constant. Therefore, the color image of trout will be obtained on a black background, which will be used to extract the characteristics of the fins.

Figure 7-20 shows a 2D histogram and the intensity color frequencies in channel R. As shown in this figure, the trout chest pixels are lighter than the other regions like the head and fish back (b). In Figure (c), a large number of pixels are in the range of [0-25] (area 1), which are related to the background (black areas). On the other hand, the pixels related to trout are in the range of [50-175] (Area 2), which has a noticeable difference with background pixels indicating the high capability of the pure blue background for trout segmentation.

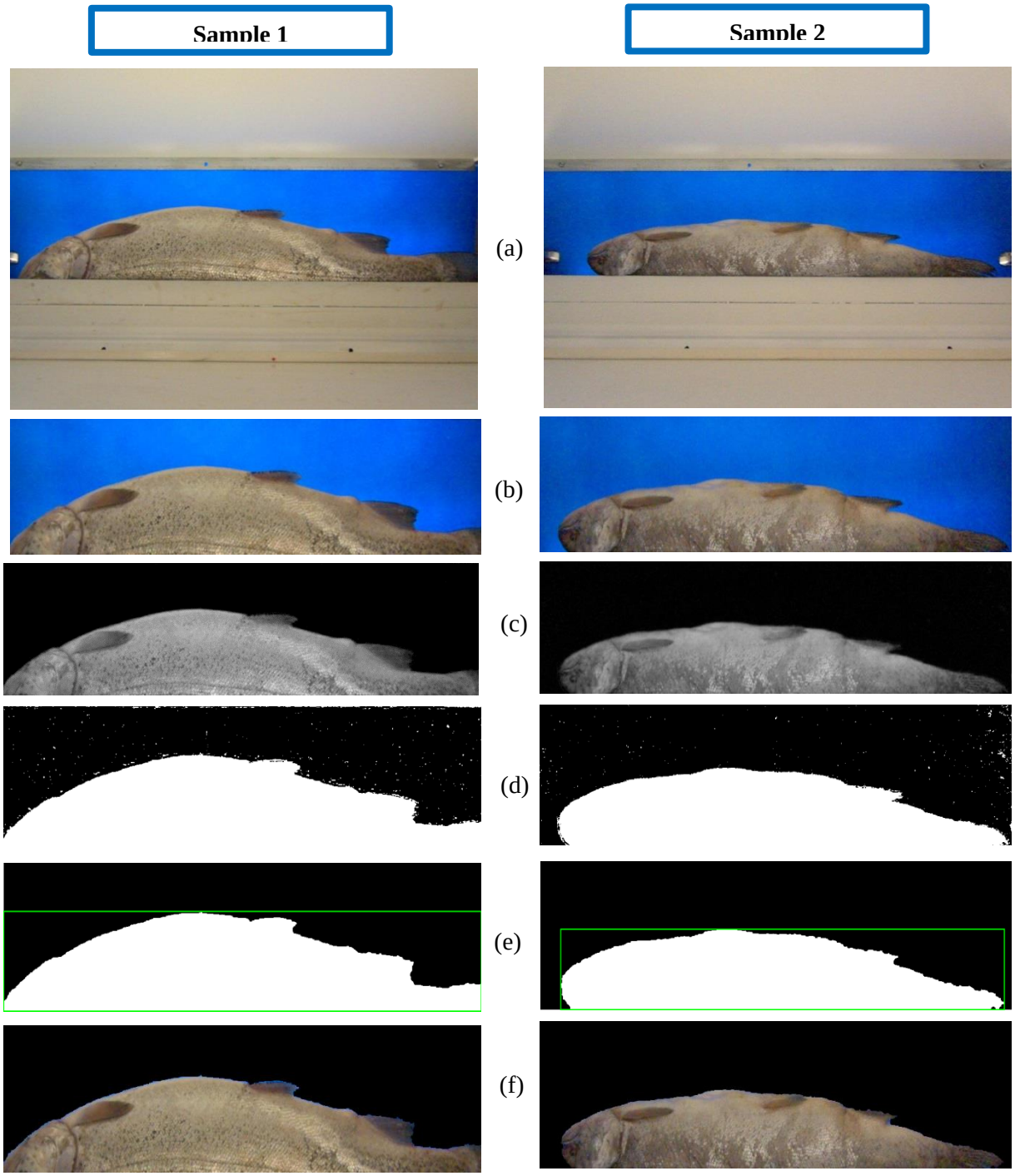

Figure 7-21. Fish segmentation process: a) initial image, b) cropping the image, c) channel R of RGB color space, d & e) making non-zero pixels visile in intensities less than 5 and 10 respectively, f) removing the objects smaller than 250 pixels and assigning a bounding box, and g) final color image.

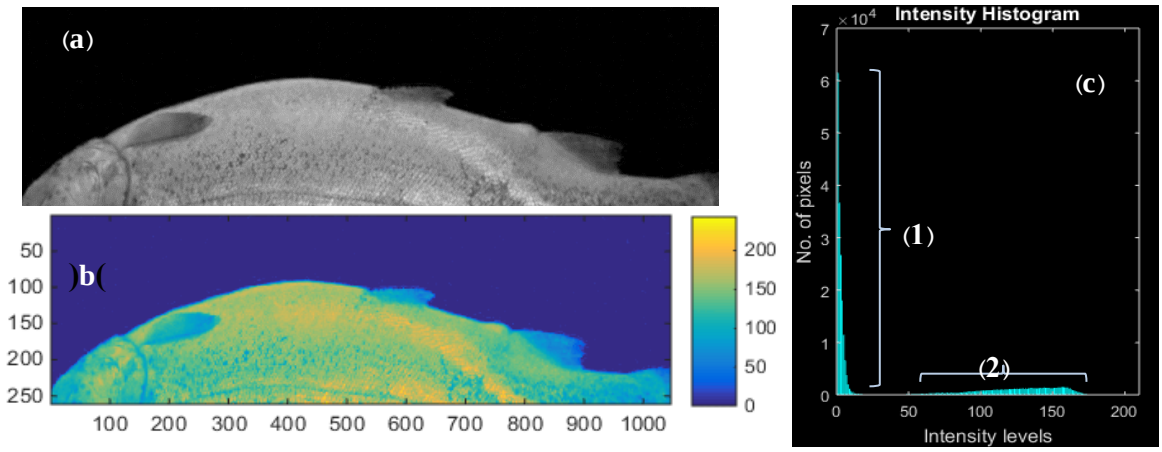

Figure 7-21. Histogram of the pixel intensities in channel R of RGB color space: a) trout image in channel R, b) 2D histogram of the image, and c) color intensity frequences.

7.2.4. Cutting point determination

To find the head cutting point in trout fish, the most significant region is to segment the pelvic fin near the head. The jointing point of the fin with the gill is the exact position to cut the head. The other option is finding the gill arc in trout fish, but since there is no significant intensity difference in this region, the pelvic fin was considered the head cutting point. Therefore, if the pectoral fin is properly segmented, the beginning of this fin will be considered the exact head cutting position. It must be noted that in some fish species, the gill arc has distinct contrast with the body so that it can be easily segmented to identify the head cutting point.

Figure 7-22. Examples of the fish head area including the pectoral fin which considered for head cutting.

One of the main objectives of this study is to extract the belly cutting area, belly cutting length, and the head cutting position. All of these dimensions are extracted by image processing and are be the basis of the trout system operation. The head and belly cutting point determination is presented in Figure 7-23.

In the offline step, since the fish is placed on its side, a line was drawn from the center of the fish to omit the backside of the trout, but in the online stage, as the fish is transferred inside the V-shaped canal, the majority of the dark area in trout back is placed inside the canal and is easily discarded from machine vision process. It should be noted that in this condition the area in trout back is removed and further unnecessary areas are omitted, so the accurate and simple fin segmentation will be achieved. Therefore separating the narrowest shear covering the fins can guarantee an accurate fin segmentation process and subsequently an accurate machine performance.

The method of separating this shear is different from the offline stage. In the offline stage, a primary line is used to separate the fish into two parts, the belly, and the back sides, and in the second stage, the secondary line divides the belly part into two other parts so the final shear serves as a target for fin segmentation, but in the online stage after fish segmentation, the edge along the belly was applied to separate the belly shear. It should be noted that in this case, the lower edge of the fish, which is the straight line, is removed and the upper edge (b) is kept for the next steps. Whereas the fish's pectoral and anal fins are in the range of 10% - 30% and 70% - 90% of the fish length, respectively; a column of the pixels was omitted to remove the beginning and end of the fish edge.

In such a case (creating a shear based on the belly edge), proper division of the pectoral fin and anal fin to determine the incision of the head and abdomen is guaranteed. On the other hand, any unnecessary areas like tail and fish head will be left out. Details of pectoral and anal fin segmentation are presented in Figure 7-23. In fact, In order to segment the fins, if a crest of the fish near the belly with the ratio of the fish width is cropped from the whole body, it can result in an area in which the fins are considered, and the non-relevant area is discarded.

By cutting the belly edge in step (d), the remaining parts of the edges in step (e) were dilated by considering a ‘disk’ structural element with the radius of 30 pixels In this step, after expanding the edges, in step (f), the color image mask of channel R and B were used to identify the anal and pectoral fins, respectively.

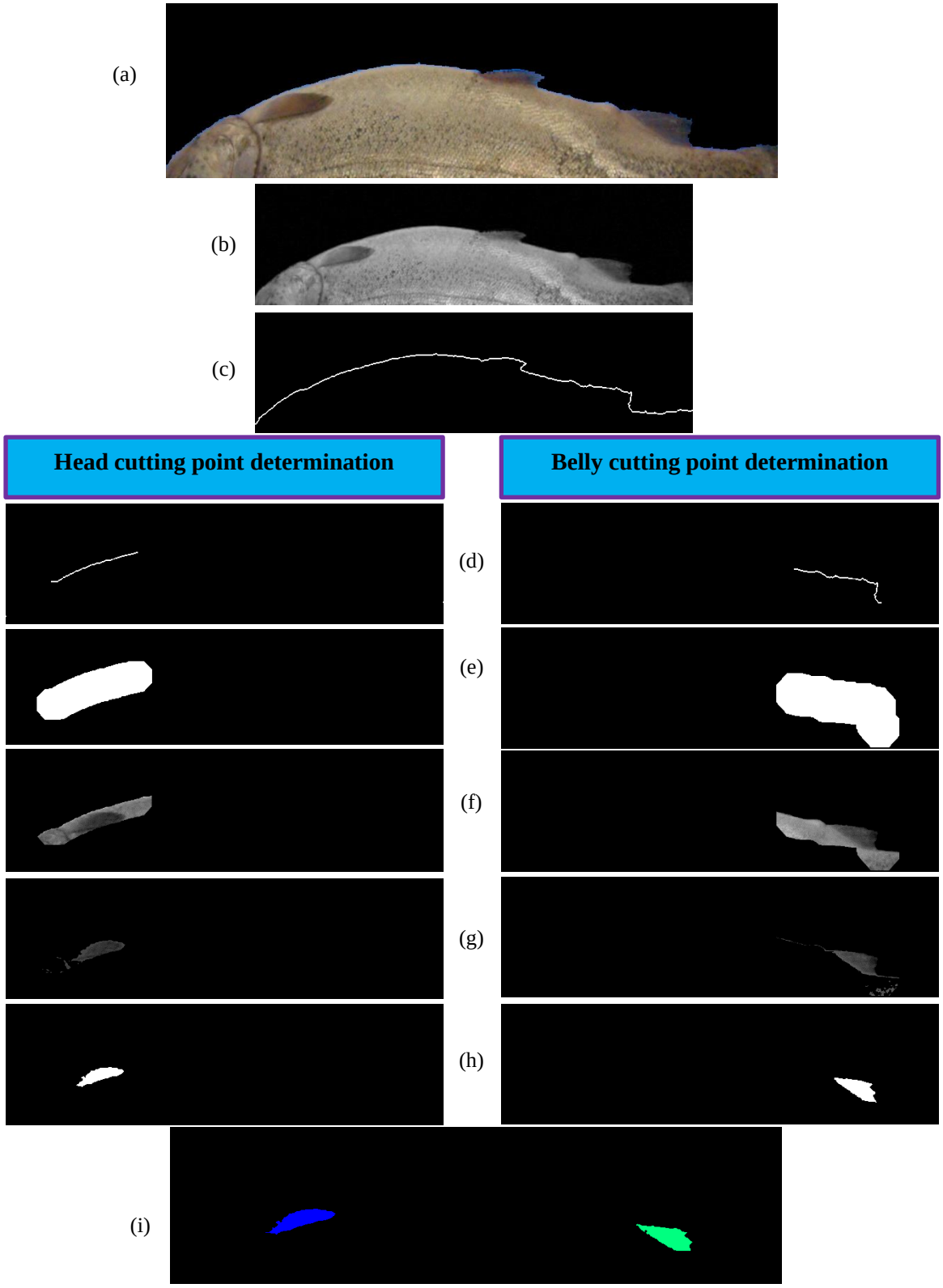

Figure 7-23. Head and belly cutting point segmentation.

The reason for using two different color channels in the online stage is the effect of blue backlight on the anal fin. In this case the amount of blue color in the anal fin color will increase and result in high intensity values. Therefore, the channel R was considered to segmentation the anal fin. This situation is exactly the same as the first stage of segmentation (separating the fish from the blue background). In fact, as the amount of blue color in the anal fin increases, the fin becomes lighter in channel B, while in the color channel R this fin will be darker. In step (g), threshold values of 65 and 85 were used to segment the anal and pectoral fins, respectively. In step (h), all fine and non-target objects were separated from the fin area considering erosive and removal of operators. In some images, some holes appeared in the segmented areas, which were filled using a morphological operator. Finally, two images related to R and B channels were combined, and the final image (i) was extracted to be applied in the controlling unit.

By proper fin extraction, the head and belly cutting points are the beginning of the pectoral and anal fins, respectively. In addition to determining the exact cutting points, the overall performance of the machine will depend on the precise calibration of the system, and the synchronization of the data of the machine vision and the operators.

7.2.5. Online image processing results

As described in the offline Image Processing section, the proper system operation depends on the precise cutting point determination, which results in the least fillet lost.

Therefore, after the initial investigation of the images in the offline section, the images were examined online. In this stage, an industrial digital video camera was used to obtain the necessary frames. Due to the practical operating conditions of the device, at this stage, unlike the offline section, the camera was installed in the wall of the imaging case. As the fish is passing on its back inside the V shape Channel, by installing the camera on the imaging case wall, in addition to the fish length and width, the cut points can be properly identified. These dimensions are the basis of the device's timing and performance.

Figure 7-24 shows the results of the color intensity changes along the indicator lines drawn from left to right. As shown in section (a) of this figure, the color intensity values near the pectoral fin change for all three R, G, and B channels. By moving along the

profile, the intensity values in the fin region decreases, which can be seen as a groove in the diagram. This difference is distinct enough to segment the fin from the fish body. On the other hand, in Figure 7-24b, the intensity change of trout gill is presented. As shown in this section, by moving along the line from left to right, no significant color intensity changes are observed. Therefore, the fish gills area cannot be used to identify the head cutting point.

It should be noted that in some species rather than trout shown in section (c), the difference in gill arch is significant enough to be determined as a head cutting point. The other significant point is the intensity changes in channel R. As seen in these images, the intensity values for this color channel are zero or close to zero in the regions, the profile passes through the background (blue area). It shows the ability of the pure blue background to segment all fish species (white to black species).

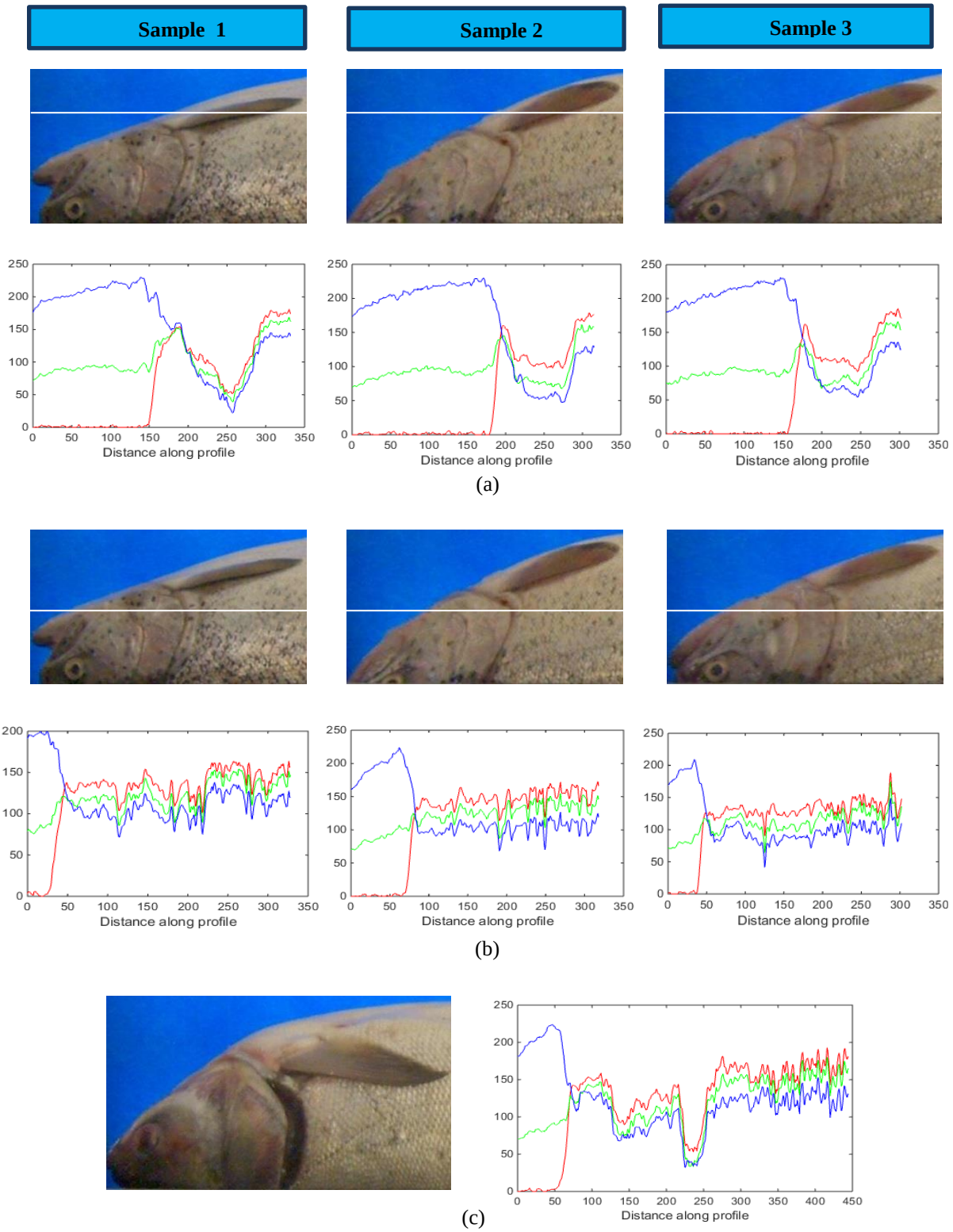

Figure 7-24. Color intensity changes of RGB color space: a) color intensity changes in pectoral fin; color intensity changes of trout gill arc and color intensity changes gill arc of the fish species rather than trout.

Automation system design

Automation system design

8.1. Controlling section

This section includes start/stop switches, emergency disconnect switch, alarm, sensors, computer, and any required control components. Inductive and magnetic sensors were used to control operators and stepper motors movements. Because the movement of the device arms in each of the work steps requires unique control, the device control algorithm was written in three parts: initial setup, manual operation, and online automatic function. To develop the controlling algorithm, Tia Portal software with Ladder logic (LAD) was applied.

At the initial start-up stage it is essential to consider homing route to return the operating arms to the home position. This algorithm is also applied while the main power supply of the device is cut off, or the operator presses the emergency bottom. With the initial setup of the device and returning the arms to their initial position, the machine will be ready to process the fish. In the next step, by pressing the start pushbutton of the motors, the electro motors of the rotary cutter, cleaner brush, and suction pump are turned on. As the blades are in idle condition, the fish gripping section is run by an electromotor with a reduction gearbox of 1:40.

By reaching each gripper to the feeding position, the trout tail is caught by the clamps and transferred along the machine. When the gripper passes in front of the inductive sensor of the machine vision section, one frame is saved and processed in the primary (trout segmentation from background) and secondary (fin segmentation and cutting point extraction) image processing steps.

Since inductive sensors are applied in each of the five subsets (machine Vision, belly cutting, head cutting, gutting, and cleaning subsets), in case there is no fish in the gripper, the dimensions extracted by machine vision will be calculated as “0', and the system operators will perform no function.

Since the maximum number three fish are simultaneously processed in the total machine length, a set of data receiving a block for three different fish were created. In fact,

by reaching the second fish to the machine vision unit, the first fish is still in the middle of the processing stage, so any new data without considering a data logging block will erase the previous sample data. Upon the availability of the data, each fish sample will be cleaned based on the relevant data.

8.2. Applied controller

Different types of controllers can be used for system controlling such as microcontrollers and programmable logic controllers (PLC). Using microcontrollers like Arduino are suitable for controlling stepper motors. These controllers are designed to work with lower voltage ranges. The supply of 5V output voltage and lower prices have broadened using microcontrollers in mechatronic systems but in most industrial systems, PLCs are preferred to microcontrollers. Therefore, while PLCs are applied in the systems it is necessary to adapt the PLC output voltage with the required voltage for the operators like stepper motors and their drives.

Due to the required number of inputs and outputs and the simultaneous control of two stepper motors and solenoid valves, a Siemens controller 6ES7 214-1AG40-0XB0 1214C-DC / DC / DC was selected.

This controller has 14 inputs along with 10 transistor digital outputs. In addition to digital inputs, this controller also has two analog inputs. To power the controller, a 24-volt power supply was applied. The connection and wiring of the Stepper motor, drive, performance specifications with the wiring between controller, stepper motor, and applied drive are shown in Figure 8-1.

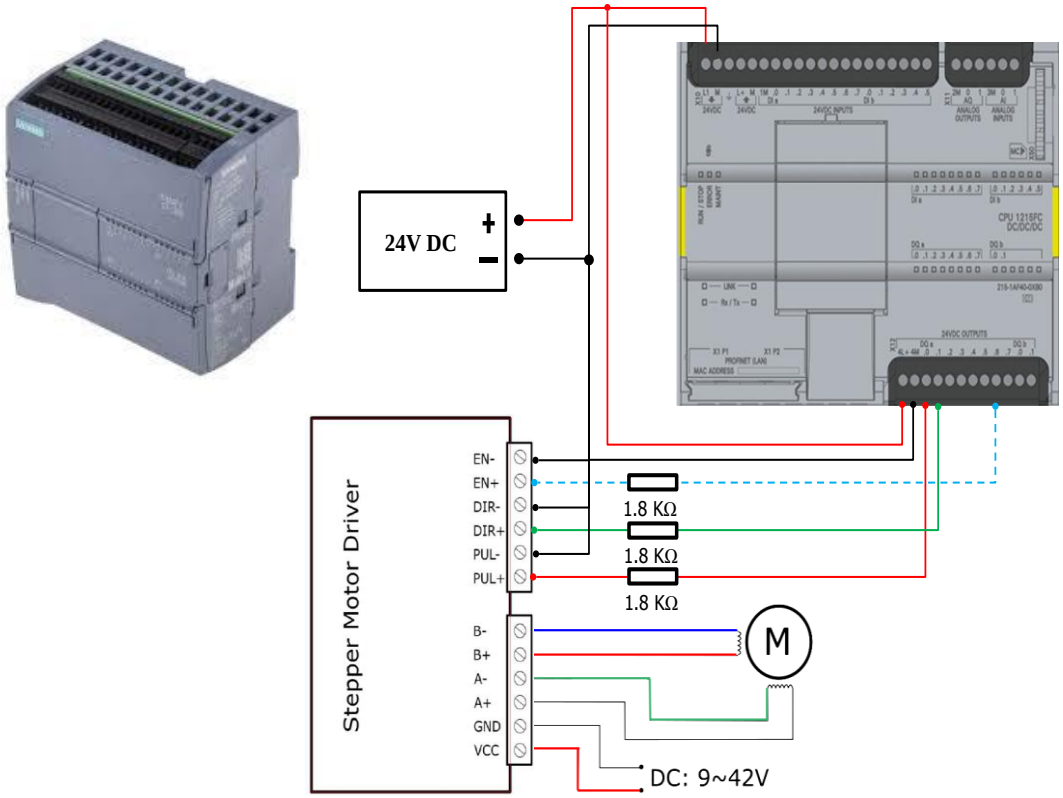

Figure 8-1. Connection of the stepper motor and its drive with the PLC. To reduce the input voltage a 1.8 kΩ resistor was applied before direction and pulse inputs.

8.3. Controlling algorithm of the belly cutting subsystem and applied components

Based on the calculations performed by Adams software, the amount of torque required to move the belly cutting arm resulted in 1.96 N.m. Therefore, a two-phase hybrid stepper motor (57PH20) with a torque of 2 Nm was selected. To start the stepper motor a pulse generator drive (CWD559 - CW MOTOR) was applied. This drive is capable of producing 800-51200 pulses per revolution and can provide a minimum and maximum current range of 2.1-5.6 A. Figure 8-2 shows the applied controlling components in the belly cutting subsystem including the stepper motor its drive, and inductive sensor.

(a) (b) (c)

Figure 8-2. Applied controlling components in belly cutting subsystem: a) stepper motor, b) drive, and c) inductive sensor.

After capturing the image and extracting the required dimensions in the machine vision section, the fish continues the path toward the inductive sensor in the belly cutting subsystem. As soon as the metallic shaft of the gripper reaches the sensor, the start command is sent to the stepper motor. As the stepper motor starts, the belly cutting arm descends towards the fish, and the blade enters the trout belly and penetrates the fish as it rotates counterclockwise (in front view). At the end of the cut, the stepper motor rotates in the reverse direction and returns to its initial position. In the algorithm presented in Figure 8-3 the stepper motor controlling steps are presented for the belly cutting subsystem.

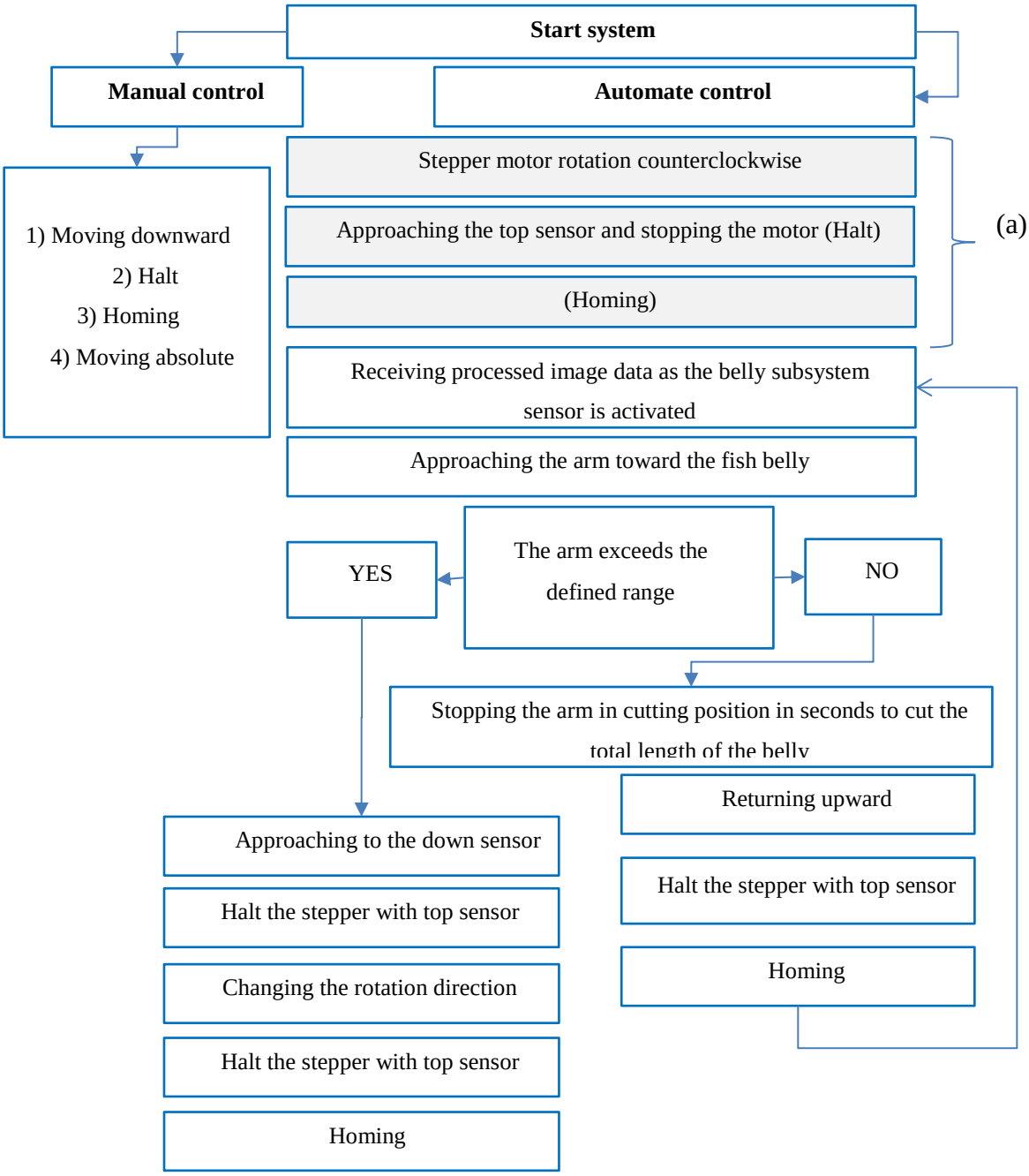

Figure 8-3. Controlling algorithm of belly cutting subsystem: a) initial operation of the system while the system is turned ON, and b) online operation.

As shown in this figure, as soon as the fish arrives at the belly cutting position, the stepper motor starts its rotation. In case there is incorrect data for any fish sample which exceeds a defined range of the arm, the cutting arm reaches the down sensor and returns to the home position. In fact, the expected performance of this section is to create a

longitudinal cut on the fish belly based on the specified length and depth, but if the arm exceeds the specified path, it is necessary to avoid any contact with the channel and grippers. Therefore, by activating the lower sensor, the return command is sent to the stepper motor and returns to the initial position. As the arm moves upward and reaches the upper induction sensor, the arm stops, and the homing process is updated. Figure 8-4 shows the details of the belly cutting subset.

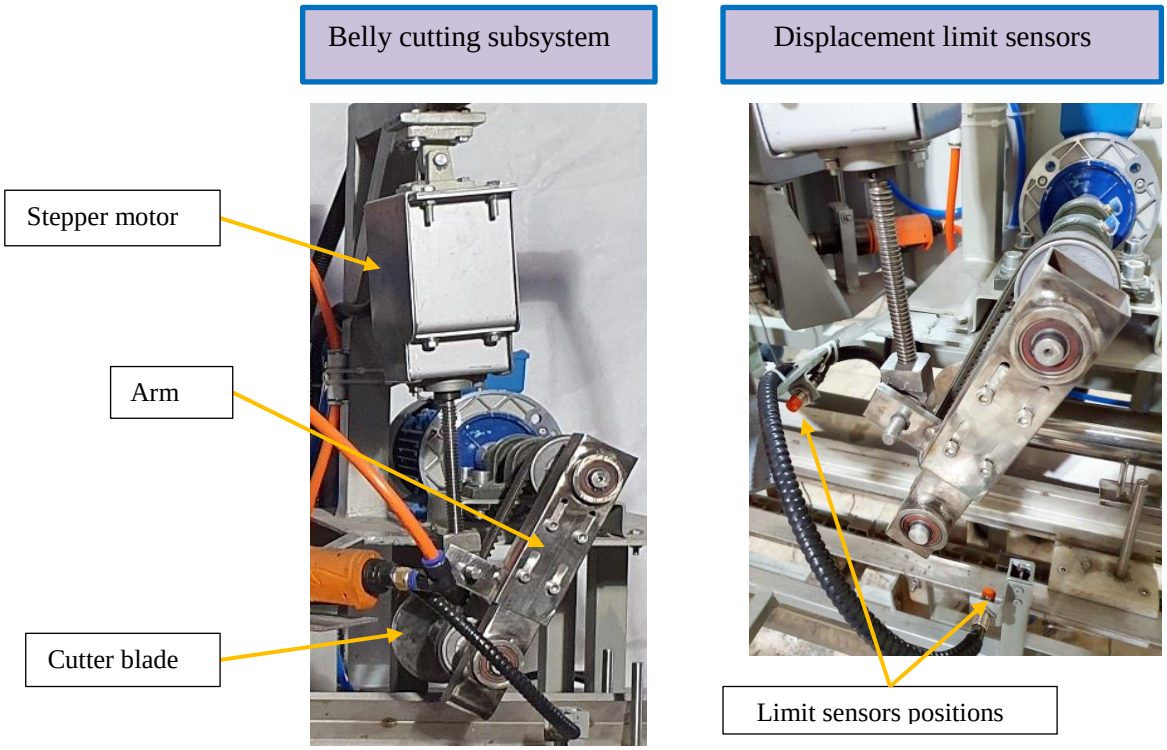

Figure 8-4. Details of the belly cutting subset.

8.4. Controlling algorithm of the head cutting subsystem and applied components

As the head cutting subsystem contain multiple components moving together to cut the head in vertical direction, a pneumatic jack (SC-50 × 250-S) was used to move the head cutting subset. According to calculations based on the speed and displacement of rotary blade, a magnetic sensor (AIRTAC CS1-F) was applied to limit the moving path.

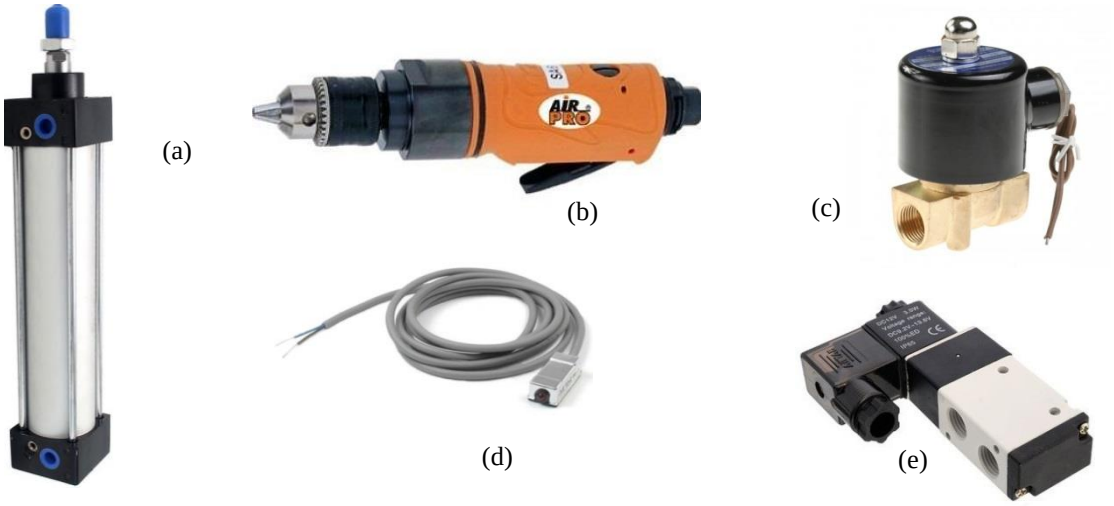

Figure 8-5. Controlling components of the head cutting subsystem: a) pneumatic jack, b) air motors, c) electric valve of the air motors, d)magnetic sensor, and elctric val of the pneumatic jack.

As shown in this figure, this section consists of two air motors, a pneumatic jack, an inductive sensor, a magnetic sensor to control the piston retraction course, two solenoid valves for the pneumatic jack, and air motors.

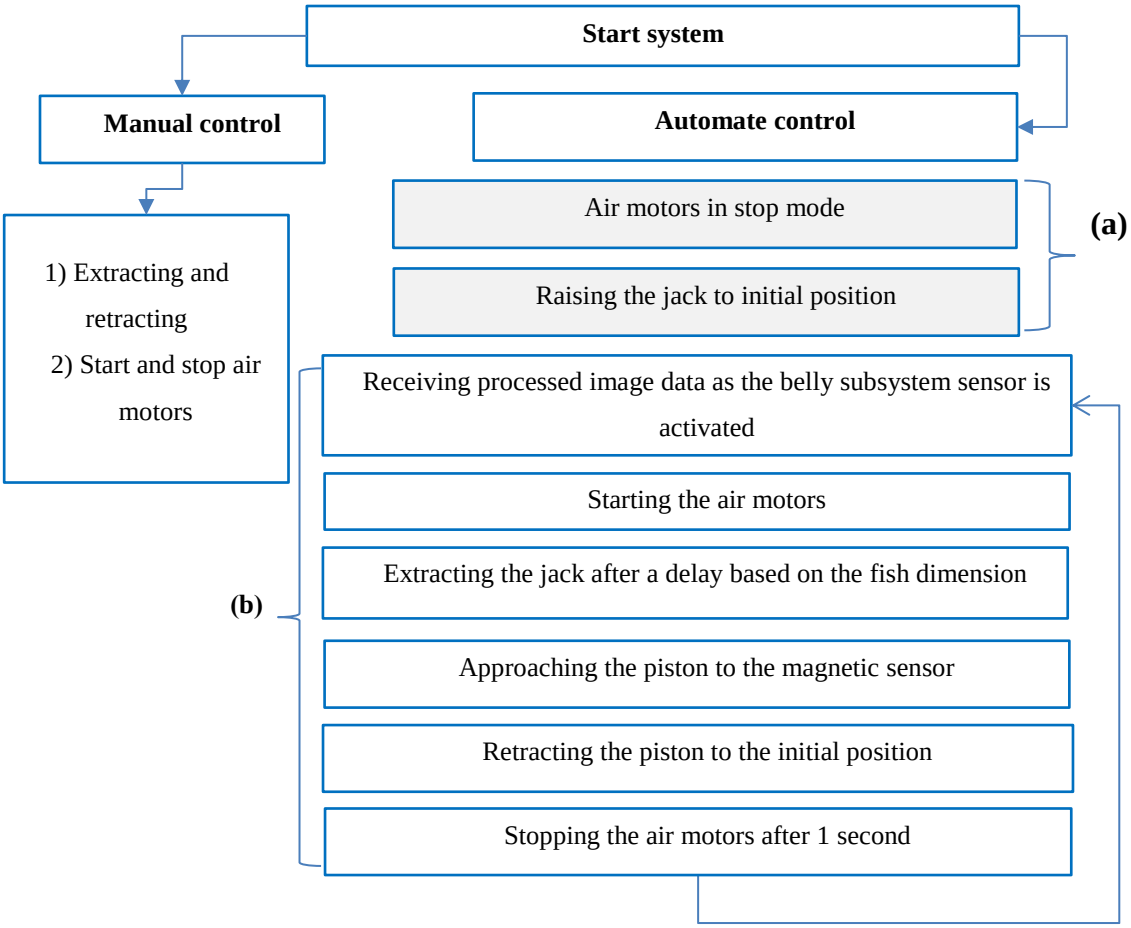

Figure 8-6. Controlling the algorithm of the head cutting subsystem: a) initial operation of the system while the system is turned ON, and b) online operation.

As soon as the inductive sensor is activated by reaching the fish to the head cutting position, the air motors start working and continue spinning until the trout head is completely removed. Meanwhile, after a delay (depending on the size of the fish and the position of the pectoral fin), the piston extract and the rotating blades separate the fish head as moving downwards. As soon as the blade terminates the cutting process, the magnetic sensor sends the termination signal to the control unit, and subsequently, the retracting command is sent to the pneumatic jack and rotary blades. The air motors stop working after 2 seconds to avoid high air consumption by the motors. The head components of the head cutting subsystem and the magnetic sensor is presented in Figure 8-7.

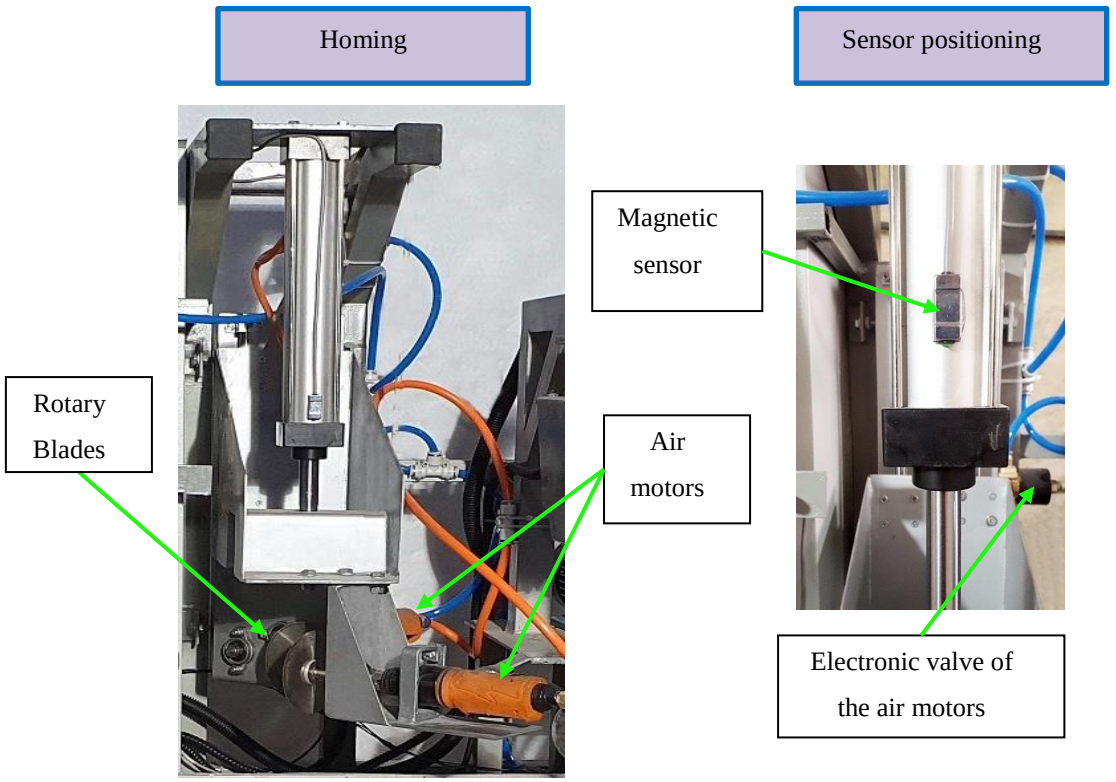

Figure 8-7. The components and applied sensor in the head cutting subsystem.

8.5. Controlling algorithm of the gutting subsystem and applied components

In this section, based on the calculations performed by Adams software, the maximum amount of required torque for the stepper motor is calculated as 7.5 Nm. Since the motor is expected to provide the required torque at low spinning speeds, the stepper motor is equipped with a 1:18 gearbox (Vexta model PK243A1-SG18 Six wires with a torque of 0.8 Nm) was applied.

To run the stepper motor, a TB6600 drive was applied. This drive is capable of producing 200-6400 pulses per revolution, together with supplying a current of 0.7-4 amps. It should be noted that the wiring of the stepper motor applied in the gutting subsystem is the same as the wiring of the belly cutting stepper. The applied stepper motor and its drive is presented in Figure 8-8.

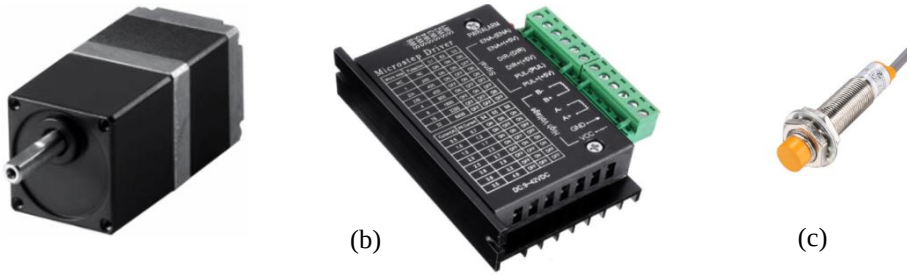

(a) (b) (c)

Figure 8-8. Gearbox mounted stepper motor: a) two-phase stepper motor; b) motor drive, and c) applied inductive sensor in the gutting subsystem.

After cutting the head, the fish reaches the position of the gutting subsystem. At this station, the belly content is evacuated based on the fish dimension. So, two suction pipes have been applied for the small (less than 275) and big fish samples. As the narrow suction tube descends, the bigger pipe rises upward, and the belly content is evacuated.

In this section, an inductive sensor is used to detect the presence of fish. In addition, a stepper motor with a gearbox and two sensors are used to control the displacement of the suction pipes. Figure 8-9 shows the control algorithm developed in Tia Portal software for gutting subsystem.

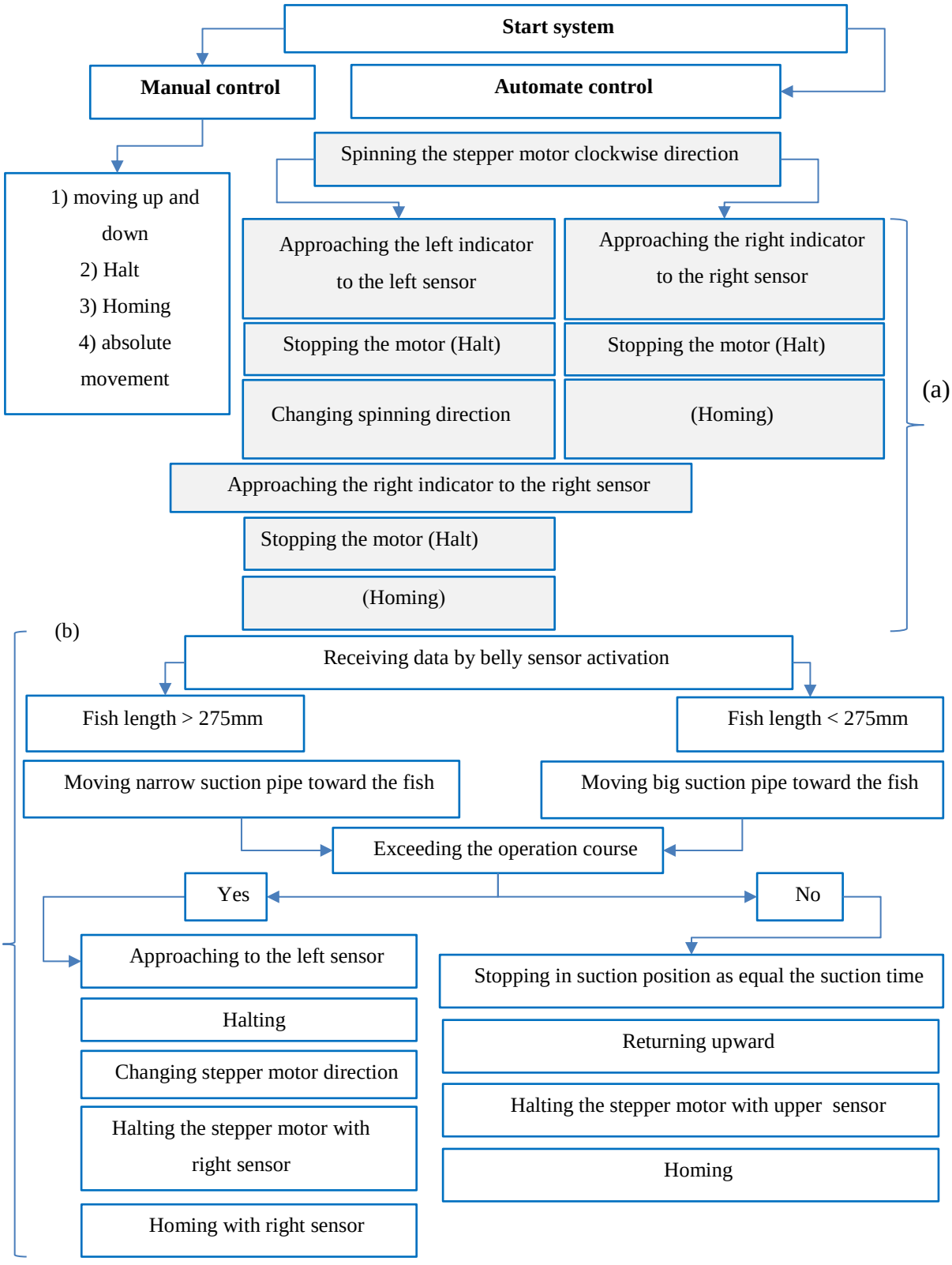

Figure 8-9. Controlling algorithm of the gutting subsystem: a) initial operation of the system while the system is turned ON, and b) online operation.

As shown in this figure, the suction tubes return to the home position by starting the system. This function is the same as the machine emergency stop functioning. Once functioning arms and moving parts are in their home position, the device is ready for use. By passing the fish through the head-cutting subset and reaching the gutting sensor, the suction operation is performed based on the data sent from the control unit. Depending on the calculated data in the machine vision section, the penetration depth will be different. As soon as the sensor sends the signal to the control unit, the time delay and cutting time is assigned to the corresponding fish. When the discharge tube enters the trout belly, all the contents are evacuated while the fish pass in front of the suction tubes. As soon as the fish gutting is performed, the stepper motor spins in the reverse direction and the tubes return to the home position. Although the algorithm is developed properly to have a successful operation, in some cases if the tube exceeds the defined path, the indicator installed in the suction tubes approaches the left sensor. So the stepper motor rotates in the opposite direction and returns to the home position. Besides the course controlling sensors in this subsystem, physical guards were considered to control the moving course. The details of the applied sensors and indicators in gutting subset are presented in Figure 8-10.

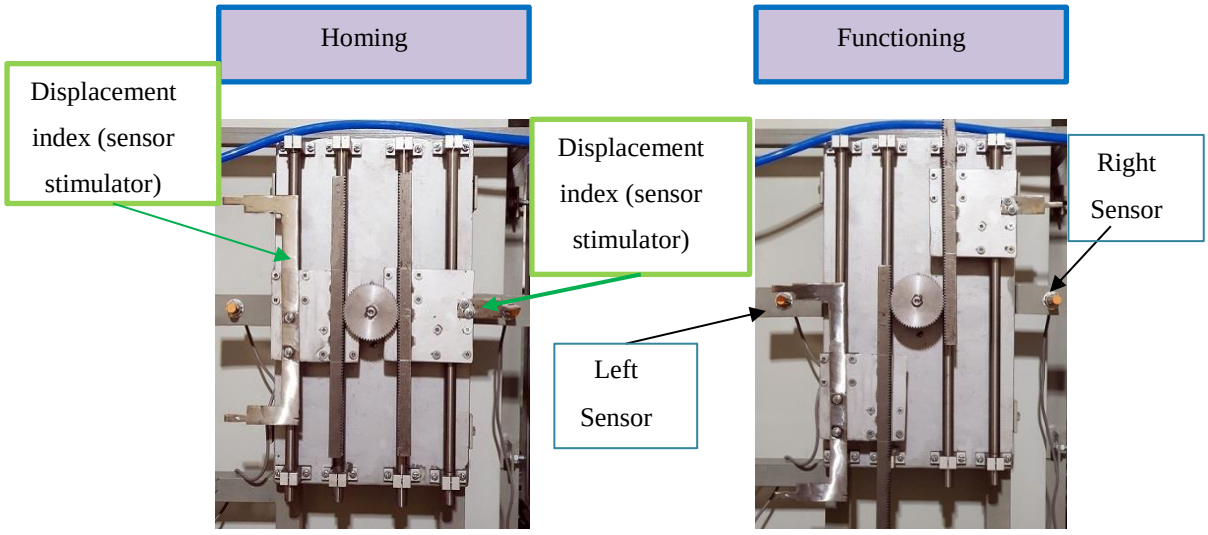

Figure 8-10. Applied sensor in gutting subset and the stimulaters in homing and functioning positions.

8.6. Controlling algorithm of the cleaning subsystem

By continuing the path in the V channel and reaching the end of the machine, the fish

is cleaned using a rotary brush. At this station, as the fish is sensed by the sensor, the cleaner subset is activated and sends the necessary command to the control unit. The applied controlling components in this section are the pneumatic jack, solenoid control valve, and magnetic sensor. Figure 8-11 shows the components used in this subset.

(a) (b) (c)

Figure 8-11. Controlling components of belly cleaning subsystem: a) pneumatic jack, b) electronic valve of the pneumatic jack, and c) magnetic sensor.

Depending on the trout size, the arm descends toward the fish and performs the cleaning operation. The cleaner brush stops as equal to the fish length cleaning time and returns to the home position. The controlling algorithm of the cleaning subsystem is presented in Figure 8-12.

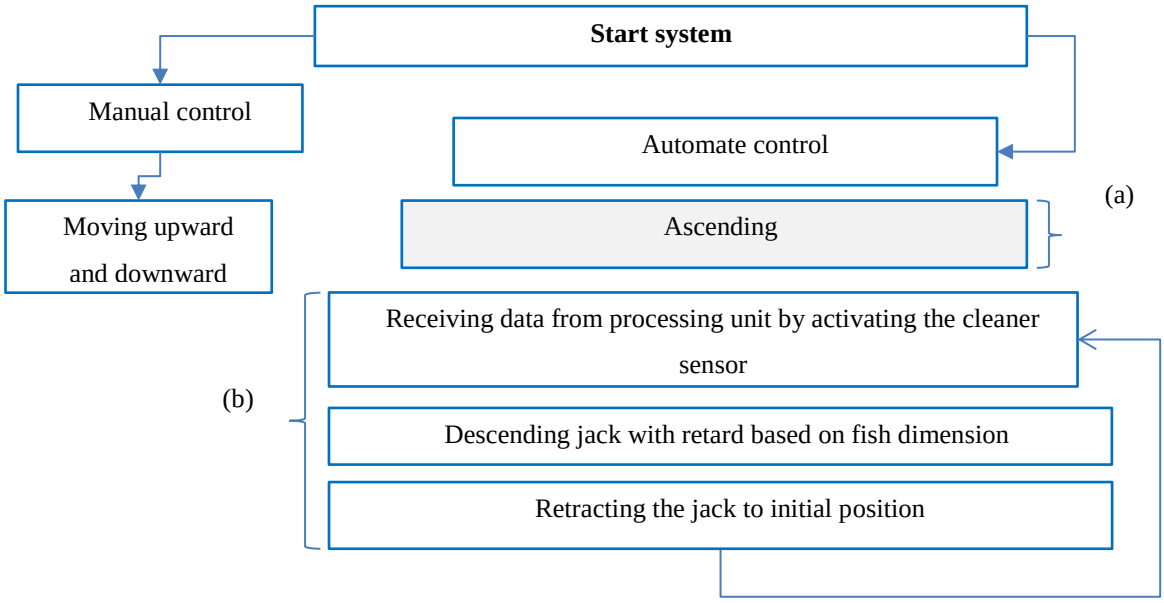

Figure 8-12. Controlling algorithm cleaning subsystem: a) operating system of the machine in automatic mode, and b) online operation.

In Figure 8-13 the cleaning components and the magnetic course sensor is presented. The final designed and fabricated system is presented in Figure 8-14.

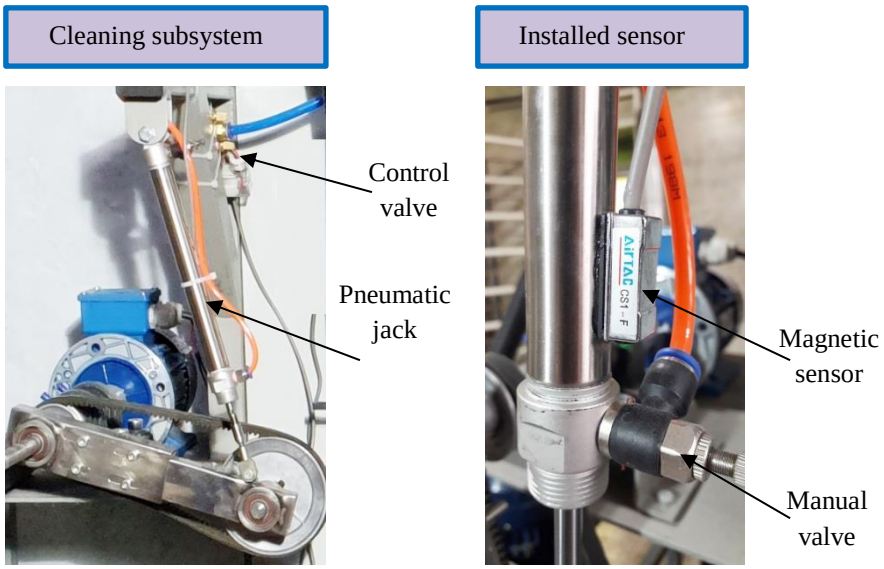

Figure 8-13. The components and applied sensor in cleaning subsystem.

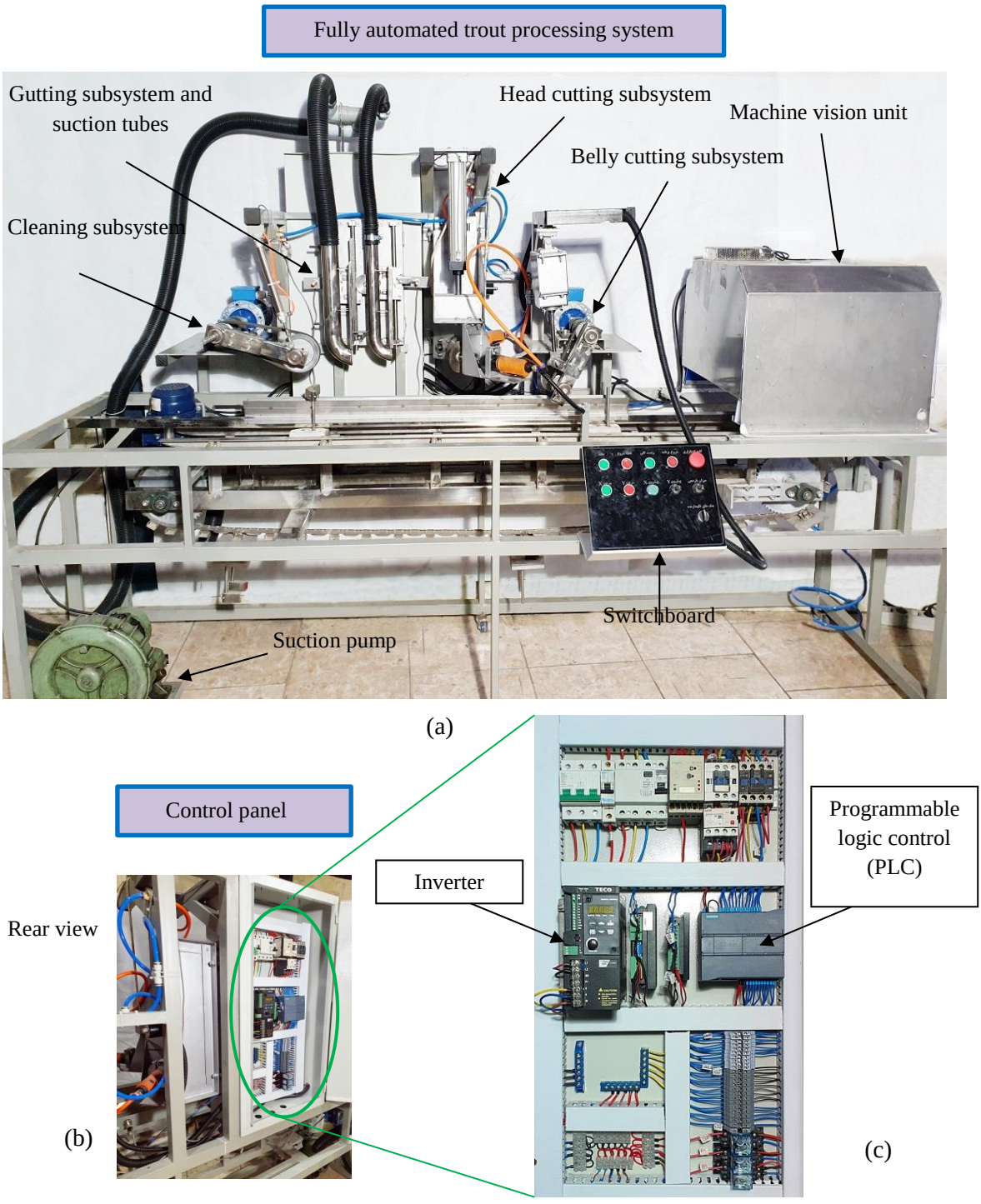

Figure 8-14. Final fabricated trout processing system based on machine vision with electronic control panel.

8.7. Communication protocol

In this thesis, MATLAB 2015 software was applied for image processing and data transmission. In order to increase the speed of image processing and data transmission, only the necessary toolboxes were installed in the software package. To capture the images in the online mode image acquisition package was installed. As the fish gripper reaches the end of the imaging case, the trout is in full vision of the camera at which all the length of the fish can be processed as soon as the frame is captured. In the next step, the trout is segmented, and related dimensions are extracted based on the fins positions.

To transfer the data from the machine vision unit to the control unit, the TCP / IP protocol was selected from the MATLAB software toolbox. In this protocol, MATLAB is considered as the server, and TiaPortal software is considered a slave. To transfer the data, a network cable is applied. When the fish reaches the end of the image processing chamber, the visual sensor is activated and sends the frame capturing command to the control unit. It should be noted that the camera is on and is ready to receive commands from the control unit during the entire operation.

As soon as this signal is received, a frame of the camera is saved, and all processing steps are performed on the images. By terminating the processing and dimension extraction steps, these data are sent to the controlling unit. Since, in this device, it is possible to clean three fish simultaneously along with the device, the data related to each fish are processed with the relevant indexes in MATLAB, and similar indexes are substituted in data reception functions of the TiaPortal software.

The data transferred for the fish sample are:

1- Length of the fish from the gripper to the end of the trout head

2- The distance from the gripper to the anal fin (belly cutting start point).

3-The distance from the gripper to the pectoral fin (head cutting point)

4- Penetration depth (to determine the rotary belly cutting and suction tube penetration depth).

In order to produce the relevant indices, the sensors in the system path were applied. As mentioned, the first sensor of the device is located in the machine vision section, which is used to send the command to take the frame. For each fish sample, four data is extracted; these data were sent in the form of an M1×12 matrix to clean for simultaneous fish processing of three fish along with the machine.

Although the data is sent to Tia Portal software, in order to use it in the next steps, it is necessary to store each of these data in the relevant receive functions. By storing the data and matching the index of each fish sample in the cutting stations with the initial number of fish, the desired fish size for the cutting operation is obtained. This will store the data for each instance in the corresponding function and be used in later steps to avoid data overlapping. In other words, after determining the fish number, new indexes with a sequence of 3 are created and assigned to each of the data receiving functions. As soon as the fish number is equal to any of these numbers, the receive functions are activated, and the number assigned to each sample is stored in the corresponding block.

As the new fish sample arrives, the data is updated older numbers so that data from each sample is available until the end of the fish cleaning path. In fact, one number is assigned to the fish sample as it enters the machine vision section, and another number is assigned by the sensors in each of the fish cleaning subsystems. In these functions, the equal operator is used so that while the number of the fish in the machine vision unit is equal to the number of fish in each of the cleaning stations, the relevant data is allocated to perform the cutting process. In order to control the system operation, especially in manual mode, besides the sensors and physical keys used in the device, the WinCC toolbox of Tia Portal software was used. The designed interface is presented in Figure 8-15.

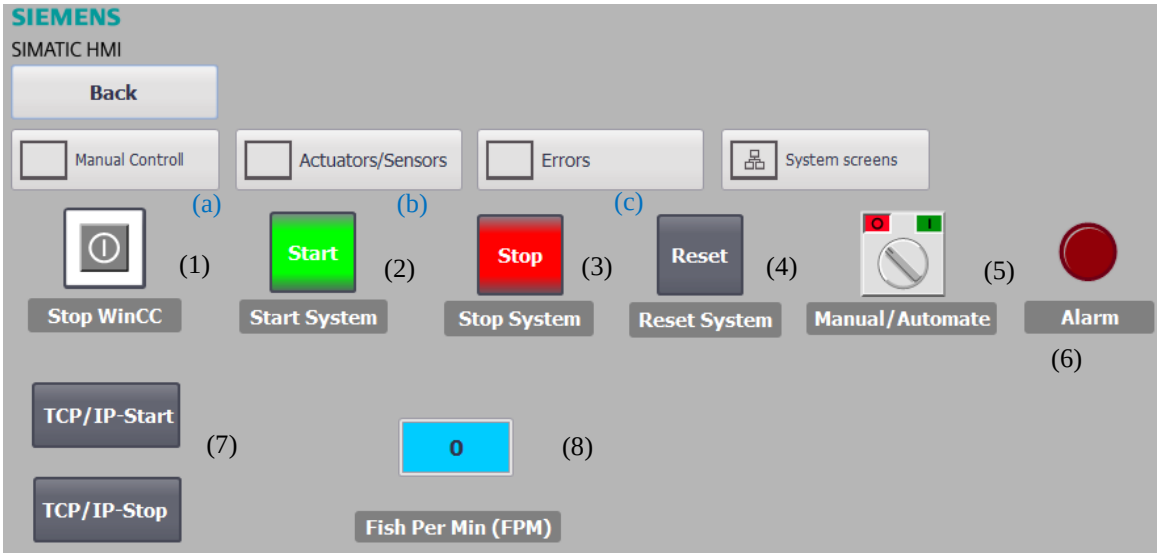

Figure 8-15. Main controlling interface desigend in WinCC toolbox of TiaPortal softwere.

The components of the control system of the system are as follows:

a) Manual control screen

b) Online operating monitoring screen

c) Online error screen

Besides the screen the other components are as follows:

1) WinCC Communication stop button.

2) Start button

3) Stop button

4) Restart button

5) Manual/automate the switch

6) Alarm status in error status

7) TCP/IP communication switch

8) Feeding rate input (fish per minute)

Each of the designed screens includes sections that are used to monitor the device operation. In this figure, the screen (a) is related to the manual movement of the arms of the device. This page is shown in Figure 8-16. This screen includes a manual setting for all four subsystems. Since the stepper motor is applied in two subsets of the belly cutting and gutting subsystems, the manual adjustment in this section includes forward and backward movement, stop, home, and absolute displacement. These keys are shown in Figure 8-16b. In the other two subsystems, on-off switches were used to run the jacks and air motor.

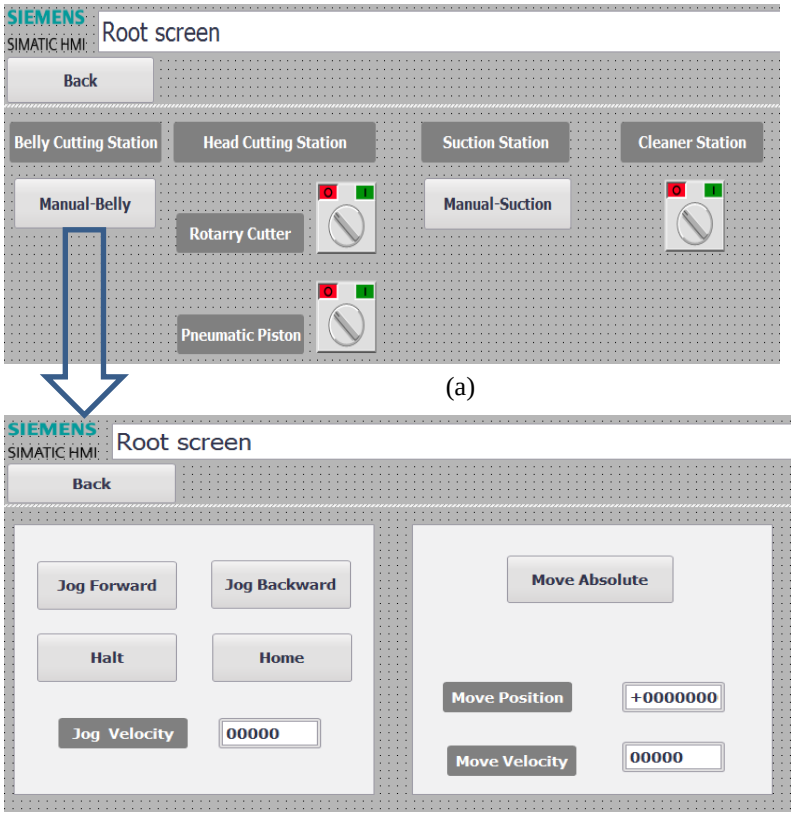

Figure 8-16. A) Menu related to manual control of machine sub-units and b) Manual control sub-menu related to the stepper motor, sub-units of belly cutting, and gutting.

In order to monitor the proper operation of the input and output sensors of the controller during the test and calibration of the device, all physical inputs and outputs were simulated in the WinCC toolbox to trace the controller input and output functioning. The

simulated inputs and outputs of the device controlling section are presented in Figure 8-17.

As shown in this figure, five induction sensors are used to sense the gripper while passing in front of each subsystem. Also, two induction sensors were applied in the belly cutting and gutting subsystems. To control the moving course of the pneumatic jacks, One magnetic sensor was applied in each the head cutting and cleaning subsystems.

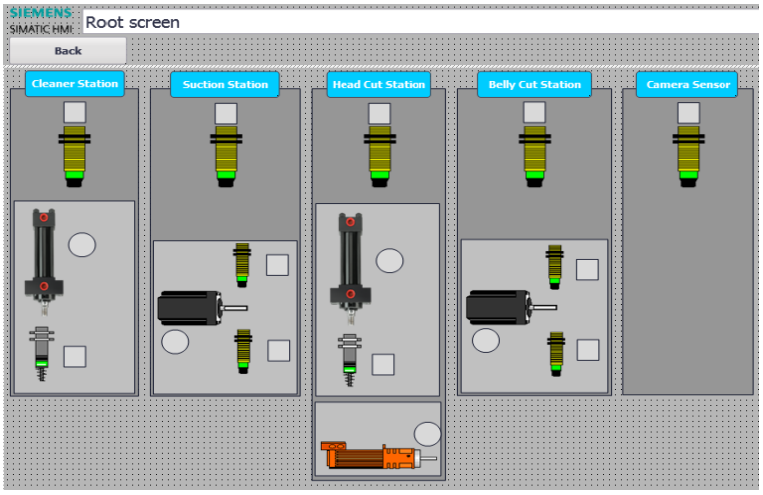

Figure 8-17. Performance monitoring screen of device input and output sensors.

Conclusion

Conclusion

Today, due to the increase of industrial automation in various industries, the need to design and manufacture automated devices with high capabilities in the fish and aquaculture industries is required. Considering the importance of trout consumption in the food basket of people, and the increasing efficiency in production, the quality requires designing and developing systems with higher capabilities compared to previous systems is essential. Due to the slippery skin of the fish and the low friction coefficient, it is so difficult to control the fish. Since the fish processing operation is done step by step, in addition to providing fish stability, the gripper must enable different processing operations along with the system. Therefore, an automatic system with trout belly cutting, beheading, gutting, and cleaning stages on different sizes was designed and manufactured based on the extracted dimension of the image processing section.

Due to the high price of fish cleaners and the limited capabilities of the available systems, a system capable of performing belly cutting steps, beheading, gutting, and cleaning steps were designed and fabricated. Besides, because the choice of fish size is completely in line with customer order, the image processing system was used to measure trout size and extract the precise cutting points. In order to prevent any contact between the grippers and the system operators, and the automated controlling system was designed to control the system operators to process different cleaning operations on fish of different sizes together with providing the system security.

One of the most important points in designing a system that can support different operation is to choose a place at which no interfere occur with cutting and cleaning tools during the various processing steps. Therefore, the fish tail was selected as the roper region, and five grippers were fabricated and installed on the conveyor. By using these clamps, it was possible to perform different cleaning operations in an integrated system. This system is designed in a way that the fish are placed and transferred inside a V-shaped canal. In this system, as the clamp rises, the tail is caught by the gripper fingers and pulled along the machine.

As trout image is capture and processed by machine vision, the necessary dimensions are sent to the controlling unit. In this device, five grippers are considered, in which each

fish is placed independently and pulled on their back along with the machine. As soon as the gripper passes in front of the cutting blades and suction tubes, each of these tools performs the corresponding operation on the fish. After extracting the fish dimensions, the cutting arm descends to create a longitudinal cut along the fish length and returns to its initial position. In the next step, by activating the head cutting jack, the rotary cutters remove the head. As soon as the head is cut, the belly content is evacuated using suction tubes, and the fish is completely cleaned by a rotary brush.

Using this integrated system, it is possible to perform several fish processing steps. In this regard, the use of machine vision as a non-destructive and fast method in fin identification and cutting point determination will increase the system capabilities to process the fish of different types. By designing the system and simulating and analyzing the motion, a system with the highest efficiency was fabricated.

In order to improve the device, the following items are suggested:

1- Using fish identification systems rather than image processing

2- Completing fillet cutting section

3- Increasing the number of fish grippers to increase the processing capacity.

4- Using fish grippers with the possibility of catching fish from the head side and investigating cutting possibilities.

5- Omitting the final cleaning section if the filleting subsystem is added to the machine if the bone separator is designed and built.

References

Reference

Azarmdel, H., Mohtasebi, S. S., Jafari, A., & Muñoz, A. R. (2019). Developing an orientation and cutting point determination algorithm for a trout fish processing system using machine vision. Computers and Electronics in Agriculture, 162, 613-629.

Booman. A. C, Parin. M. A, Zugarramurdi. A (1997). Efficiency of size sorting of fish. International journal of production economics, 48(3), 259-265.

Braeger, H. (2018). U.S. Patent No. 9,888,697. Washington, DC: U.S. Patent and Trademark Office.

Buckingham. R, Graham. A, Arnarson. H, Snaeland. P, Davey. P (2001). Robotics for de-heading fish a case study. Industrial Robot: An International Journal, Vol. 28 Iss 4 pp. 302 – 309.

Budynas, R. G., Nisbett, J. K., & Shigley, J. E. (2011). Shigley's mechanical engineering design. New York: McGraw-Hill.

Costa .C, Antonucci. F, Boglione. C, Menesattia. P, Vandeputte. M, Chatain. B (2013). Automated sorting for size, sex and skeletal anomalies of cultured seabass using external shape analysis. Aquacultural Engineering 52 (2013) 58–64.

De Silva. C. W, Wickramarachchi. N (1997). An innovative machine for automated cutting of fish. IEEE/ASME transactions on mechatronics, 2(2), 86-98.

Dowlati, M., Mohtasebi, S. S., Omid, M., Razavi, S. H., Jamzad, M., & De La Guardia, M. (2013). Freshness assessment of gilthead sea bream (Sparus aurata) by machine vision based on gill and eye color changes. Journal of food engineering, 119(2), 277-287.

Mendoza, F., Dejmek, P., & Aguilera, J. M. (2006). Calibrated color measurements of agricultural foods using image analysis. Postharvest Biology and Technology, 41(3), 285-295.

FAO, 2013. FAOSTAT Database

http://www.fao.org/fishery/culturedspecies/Oncorhynchus_mykiss>

Finke, H., Jurs, M., & Grabau, T. (2018). U.S. Patent Application No. 15/568,395.

Godfrey, D. (1964). Friction of greases and grease components during boundary lubrication. ASLE TRANSACTIONS, 7(1), 24-31.

Gray, D. E. (1964). American institute of physics handbook. American Journal of Physics, 32, 389-389.

Grosseholz, W., & Neumann, R. (2008). U.S. Patent No. 7,427,229. Washington, DC: U.S. Patent and Trademark Office.

Hong, H., Yang, X., You, Z., & Cheng, F. (2014). Visual quality detection of aquatic products using machine vision. Aquacultural Engineering, 63, 62-71.

http://www.smcworld.com/catalog/BEST-Guide-en/pdf/2-m27-49_en.pdf.

Hu, J., Li, D., Duan, Q., Han, Y., Chen, G., & Si, X. (2012). Fish species classification by color, texture and multi-class support vector machine using computer vision. Computers and electronics in agriculture, 88, 133-140.

Ketels, D. (2008). U.S. Patent No. 7,467,995. Washington, DC: U.S. Patent and Trademark Office.

Kowalski, W. (2015). U.S. Patent No. 8,956,205. Washington, DC: U.S. Patent and Trademark Office.

Kragh, H. (2007). U.S. Patent No. 7,252,584. Washington, DC: U.S. Patent and Trademark Office.

Kristensen, I., & Jorgensen, D. B. (2016). U.S. Patent Application No. 15/030,078.

Lang. H, Wang. Y & de Silva. C. W. (2008, September). An automated industrial fish cutting machine: Control, fault diagnosis and remote monitoring. In 2008 IEEE International Conference on Automation and Logistics (pp. 775-780). IEEE.

Lee, W. H., Kim, M. S., Lee, H., Delwiche, S. R., Bae, H., Kim, D. Y., & Cho, B. K. (2014). Hyperspectral near-infrared imaging for the detection of physical damages of pear. Journal of Food Engineering, 130, 1-7.

Mathiassen. J. R, Jansson. S, Veliyulin. E, Njaa. T, Lønseth. M, Bondø. M & Skavhaug. A (2006). Automatic weight and quality grading of whole pelagic fish. In In Proceedings NFTC 2006, the 1st Nor-Fishing Technology Conference, Trondheim, Norway.

Misimi, E., Erikson, U., & Skavhaug, A. (2008). Quality grading of Atlantic salmon (Salmo salar) by computer vision. Journal of food science, 73(5), E211-E217.

Misimi, E., Øye, E. R., Sture, Ø., & Mathiassen, J. R. (2017). Robust classification approach for segmentation of blood defects in cod fillets based on deep convolutional neural networks and support vector machines and calculation of gripper vectors for robotic processing. Computers and Electronics in Agriculture, 139, 138-152.

Mjahad, A., Rosado-Muñoz, A., Bataller-Mompeán, M., Francés-Víllora, J. V., & Guerrero-Martínez, J. F. (2017). Ventricular Fibrillation and Tachycardia detection from surface ECG using time-frequency representation images as input dataset for machine learning. Computer methods and programs in biomedicine, 141, 119-127.

Paulsohn, C., Dann, A., Rüsch, R., & Brandt, M. (2010). U.S. Patent No. 7,828,635. Washington, DC: U.S. Patent and Trademark Office.

Poonnoy, P., Yodkeaw, P., Sriwai, A., Umongkol, P., & Intamoon, S. (2014). Classification of boiled shrimp's shape using image analysis and artificial neural network model. Journal of food process engineering, 37(3), 257-263.

Ryan, R. M. (2013). U.S. Patent No. 8,512,106. Washington, DC: U.S. Patent and Trademark Office.

Ryan, R. M. (2017). U.S. Patent No. 9,839,223. Washington, DC: U.S. Patent and Trademark Office.

Steen Bondø. M, Reidar Mathiassen. J, Aaby Vebenstad. P, Misimi. E, Skjøndal Bar.

E. M, Toldnes. B & Ove Østvik. S (2011). An automated salmonid slaughter line using machine vision. Industrial Robot: An International Journal, 38(4), 399-405.

Storbeck. F & Daan. B (2001). Fish species recognition using computer vision and a neural network. Fisheries Research, 51(1), 11-15.

Strachan .NJC (1993). Length measurement of fish by computer vision. Computers and Electronics in Agriculture, 8 (1993) 93-104.

Taheri-Garavand, A., Fatahi, S., Banan, A., & Makino, Y. (2019). Real-time nondestructive monitoring of Common Carp Fish freshness using robust vision-based intelligent modeling approaches. Computers and Electronics in Agriculture, 159, 16-27.

Teimouri, N., Omid, M., Mollazade, K., & Rajabipour, A. (2014). A novel artificial neural networks assisted segmentation algorithm for discriminating almond nut and shell from background and shadow. Computers and Electronics in Agriculture, 105, 34-43.

Teimouri, N., Omid, M., Mollazade, K., Mousazadeh, H., Alimardani, R., & Karstoft, H. (2018). On-line separation and sorting of chicken portions using a robust vision-based intelligent modelling approach. Biosystems engineering, 167, 8-20.

Urushibara, S., & Yusa, K. (1991). U.S. Patent No. 4,993,116. Washington, DC: U.S. Patent and Trademark Office.

Van Stralen, K. J., Stel, V. S., Reitsma, J. B., Dekker, F. W., Zoccali, C., & Jager, K. J. (2009). Diagnostic methods I: sensitivity, specificity, and other measures of accuracy. Kidney international, 75(12), 1257-1263.

White, D. J., Svellingen, C., & Strachan, N. J. C. (2006). Automated measurement of species and length of fish by computer vision. Fisheries Research, 80(2-3), 203-210.

Soille, P. (2013). Morphological image analysis: principles and applications. Springer Science & Business Media.

Wang, K. F. (2014). Quantitative detection of size and centroid of internal defect based on Radon transform and morphological operation in phase-shifting digital speckle pattern interferometry. NDT & E International, 63, 50-52.